REFRIGERANT FORCED-CONVECTION CONDENSATION INSIDE HORIZONTAL TUBES

Soonhoon Bae

J. S. Maulbetsch

W. M. Rohsenow

Report No. DSR 79760-64

Contract No. ASHRAE RP 63

Department of Mechanical Engineering
Engineering Projects Laboratory
Massachusetts Institute of Technology

November 1, 1969

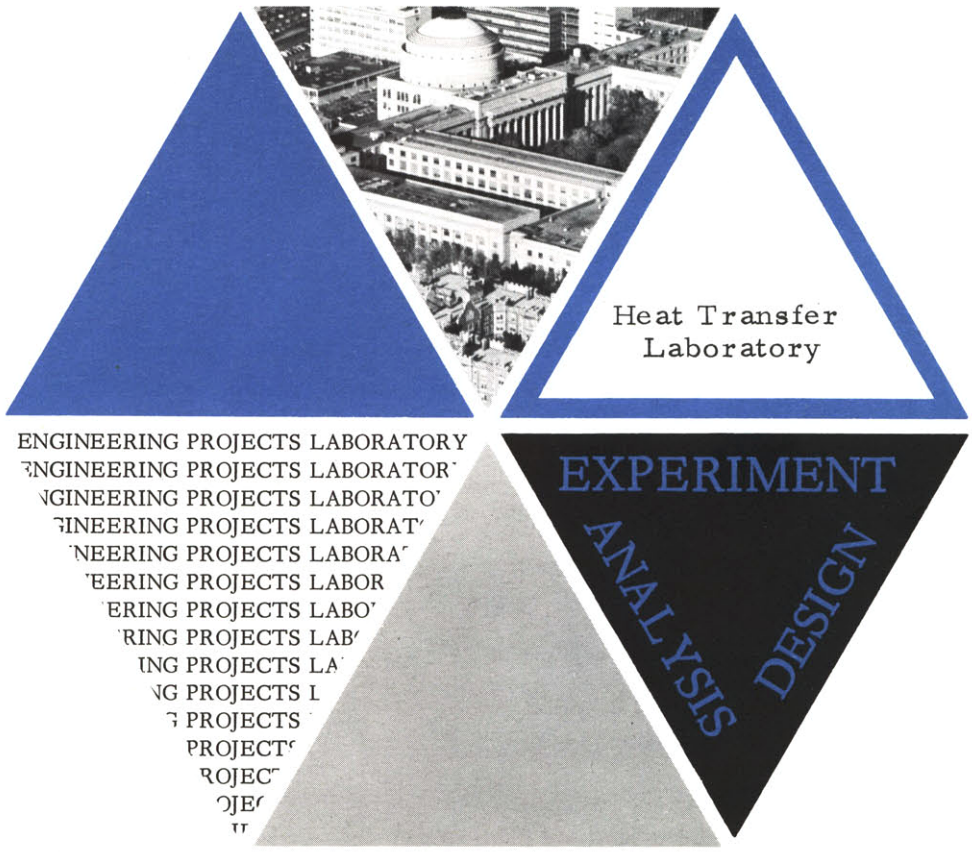

TECHNICAL REPORT NO. 79760-64

REFRIGERANT FORCED-CONVECTION CONDENSATION INSIDE HORIZONTAL TUBES

by

Soonhoon Bae
John S. Maulbetsch
Warren M. Rohsenow

Sponsored by:-

TECHNICAL COMMITTEE 1.3

AMERICAN SOCIETY OF HEATING, REFRIGERATING AND AIR CONDITIONING ENGINEERS

Contract No: ASHRAE RP63

DSR Project NO: 79760

November 1, 1969

Heat Transfer Laboratory
Mechanical Engineering Department
Massachusetts Institute of Technology
Massachusetts Avenue, Cambridge, 02139

REFRIGERANT FORCED-CONVECTION CONDENSATION INSIDE HORIZONTAL TUBES

by

Soonhoon Bae
J. S. Maulbetsch
W. M. Rohsenow
Massachusetts Institute of Technology.

ABSTRACT

High vapor velocity condensation inside a tube was studied theoretically. The heat transfer coefficients were calculated by the momentum and heat transfer analogy. The Von Karman universal velocity distribution was applied to the condensate flow. Pressure drop was calculated by the Lockhart-Martinelli method and the Zivi void fraction equation.

Experimental data was obtained for the flow rate from 240,000 to 485,000 lbm/ft^2 hr. R-22 was condensed in a 0.493" I.D. 18 ft. long test section. The measured heat transfer coefficients agreed with the prediction within 10% except a few points in the very low quality region.

Acknowledgements

This work was supported by the Technical Committee 1.3 of the American Society of Heating, Refrigerating and Air-Conditioning Engineers. Professor A. E. Bergles and Professor A. A. Sonin gave generously of their time for fruitful discussions. The experiment was done in the Environment Control Laboratory directed by Professor A. L. Hesselschwardt, Jr. Miss J. Le Peyre typed the manuscript.

Table of Contents

Appendices

List of Figures

Nomenclature

A	cross section area ft^2
a	actual gravitational acceleration in the axial direction, $g \sin \theta$ ft/hr^2
B	buoyancy modulus, Eq. (37)
C	constants
C_p	specific heat Btu/lbm °F
D	tube inner diameter ft
E	ratio ε_m to ε_h
F_o	defined in Eq. (1) $lbf/ft^2/ft$
F_2	defined in Eq. (22a, b, c)
f_i^*	friction factor at the vapor-liquid interface when condensation occurs, Eq. (C13)
Fr	Froude number, Eq. (36)
g	gravitational acceleration ft/hr^2
g_o	constant, 4.17×10^8 lbm ft/lbf hr^2
G	total mass velocity lbm/ft^2 hr
G_e	mass velocity of the liquid, G(1-x) lbm/ft^2 hr
G_v	mass velocity of the vapor, Gx lbm/ft^2 hr
G_E	equivalent mass velocity, Eq. (C2) lbm/ft^2 hr
h_z	local heat transfer coefficient Btu/hr ft^2 °F
h_m	mean heat transfer coefficient Btu/hr ft^2 °F
h_o	heat transfer coefficient when only liquid flows at the same total mass flow rate Btu/hr ft^2 °F
h_{fg}	latent heat of vaporization Btu/lbm

K	conductivity of the liquid Btu/ft hr °F
L	total length of condensation ft
M	defined in Eq. (18)
Nu	Nusselt number $h_z D/K$
(dP/dz)	Pressure Gradient $lbf/ft^2/ft$
Pr	Prandtl number $\mu_\ell C_p/K$
(q/A)	heat flux Btu/ft^2 hr
Re	total liquid Reynolds number GD/μ_ℓ
Re_ℓ	local liquid Reynolds number $G_\ell D/\mu_\ell$
Re'_v	Reynolds number, Eq. (C6)
S	perimeter ft
T	temperature °F
ΔT	temperature difference between the vapor and the condensing wall °F
ΔT_w	coolant temperature rise °F
v	mean velocity ft/hr
v_z	local velocity in the axial direction ft/hr
v_τ	friction velocity $g_o \tau_o/\rho_\ell$ ft hr
W	total flow rate lbm/hr
W_ℓ	liquid flow rate lbm/hr
W_v	vapor flow rate lbm/hr
x	vapor quality, Eq. (7)
X_{tt}	lockhart-Martinelli parameter, Eq. (D10)
y	radial distance from the wall ft
z	axial distance from the condensation starting point ft

α	void fraction
α_ℓ	thermal diffusivity $K/\rho_\ell C_p$ ft^2/hr
β	defined in Eq. (D35)
δ	thickness of the condensate film ft
ε	eddy diffusivity ft^2/hr
η	defined in the calculation of $(dP/dz)_m$
θ	angle of inclination
μ	viscosity lbm/ft hr
ν	kinematic viscosity ft^2/hr
ρ	density lbm/ft^3
τ	shear stress lbf/ft^2
τ_v	vapor shear stress on the liquid film lbf/ft^2
ϕ_v	Lockhart-Martinelli parameter, Eq. (D8)
Γ	flow rate per unit circumference lbm/ft hr

Subscript

δ	liquid vapor interface
f	friction
g	gravity
h	thermal
i	interface
ℓ	liquid
m	momentum
o	wall
v	vapor
z	local

Superscript

+	non-dimensionalized by $g_o\tau_o/\rho_\ell$
*	non-dimensionalized by $(\mu_\ell\nu_\ell/g_oF_o)^{1/3}$

I INTRODUCTION

Condensation inside tubes is inherently required for some kinds of condensers. When saturated or super-heated vapor flows through a cold tube, the condensation occurs on the cold surface and the condensate liquid film is formed on the tube wall. Depending on the geometry of the surface, the flow rate of condensate and thickness of the liquid film are varied at the same physical conditions. In general, the film condensation heat transfer resistances are divided roughly into two parts. One is the resistance due to inter-phase mass transfer and the other is the conduction resistance through the condensate film, so called "Nusselt resistance". While an inter-phase mass transfer resistance is the predominent resistance in the high conductivity material condensation, it is negligible for the condensation of low conductivity material, such as water and refrigerants, compared with the Nusselt resistance. The purpose of this investigation is to give a clear picture of the fluid mechanics of vapor-liquid flow inside tubes and the predominent heat transfer resistance during condensation of refrigerants.

Since the fluid mechanics of the condensate flow and the heat transfer rate from vapor to the cold tube wall are closely related, the classical Nusselt analysis [49] seems to show a basic approach to this problem.

When the vapor and condensate are convected naturally with low flow rate, laminar flow of uniform thickness liquid film occurs on the wall of a vertical tube, while condensate film is formed on the upper part of the tube and the condensate accumulates at the bottom of the tube inside a horizontal tube. Chaddock [19], Chato [20], and Rufer [57]

gave solutions for the cases of horizontal and inclined tubes. The experimental data show good agreement with those analytical solutions.

In a long vertical tube or in a horizontal tube with high inlet vapor velocity, the condensate flow usually becomes turbulent. It was shown that the transition from laminar flow to turbulent flow does not occur at a particular Reynolds number as it is the case for a single phase flow. The transition occurs at various points depending on not only fluid velocity and viscosity but also local flow conditions such as shear stress distribution in the liquid film [13], [27], [35], [55].

Numerous data and correlations are available for turbulent condensing flow inside tubes. Empirical correlations of non-dimensional group type can be used in practical designing without much involved calculations. However, most of those correlations available to date do not include sufficient variables to describe the condensate flow [1], [2], [16], [21], [51]. A semi-empirical equation by Carpenter and Colburn [17] seemed good to correlate data of some particular fluids. The coefficient and the exponent of the Prandtl number, and the procedure of wall shear stress calculation were modified by later investigators [3], [61]. Since the conduction resistance of the laminar sublayer was assumed to be the only significant resistance, the equation has no general applicability for the wide range of Prandtl number and flow conditions. Another analytical approach appeared in some papers [27], [39], [55]. Using the momentum and heat transfer analogy, assuming that the universal velocity distribution of turbulent flow is applicable to the condensate flow, heat transfer coefficients were solved in rather a complicated form. This analytical approach is the

most helpful, among three approaches, for understanding of the mechanism of condensation flow and heat transfer. This method will be developed for a horizontal tube case and the procedure of utilizing this method for practical designing will be recommended in this paper.

II THEORY

The analysis will be done on the condensation heat transfer inside a horizontal tube for a high inlet velocity (60,000 to 600,000 lbm/hr ft^2). In order to avoid confusing the local value concepts in two-phase flow, the inlet condition will be fixed as 100% vapor quality at saturated states. Details of theoretical derivation and numerical procedure are included in the Appendices. In this section, basic equations and results are presented.

2.1 Flow Model

Annular flow regime with a uniform thickness around the circumference of a tube is assumed to exist in the parameter ranges of interest. In fact for such high vapor velocity, annular flow is the predominant flow pattern and slug flow may appear at very low qualities. Accumulation of the condensate at the bottom of a horizontal tube has a negligible effect when the flow is highly turbulent. Entrainment of liquid droplets in the vapor core will be neglected in the analysis. Analytical theory will be developed for the case of constant temperature difference between wall and vapor along a tube.

2.2 Local Heat Transfer Coefficients

The basic assumptions are as follows:

1. The von Karman equations for universal velocity distribution in turbulent flow are directly applied to the velocity distribution of the liquid film at the wall.
2. The heat conduction in the flow direction and the subcooling of the liquid film are neglected. Because of the turbulence in the liquid film the temperature distribution is nearly uniform and

subcooling enthalpy change is small compared with latent heat. Hence, heat flux is almost uniform in the radial direction.

3. The ratio of eddy viscosity ϵ_m to eddy conductivity ϵ_h is assumed 1.0. Although some experimental data for single phase flow shows the ratio ranging from 1.0 to 1.7, the previous investigations [27], [55] get good results with the assumption of $\epsilon_m = \epsilon_h$.
4. Transition from laminar to turbulent flow occurs at $y^+ = 5$. Since the universal velocity distribution takes account of turbulence as the film thickness increases, no transition theory is necessary [27].
5. A simple flat plate analysis is applied to a tube without a significant error. Even at the down stream of the condenser tube (up to vapor quality 20%), the void fraction for most fluids is larger than 0.8, or the film thickness is smaller than 10% of the tube radius.
6. The vapor temperature is assumed uniform at the saturation temperature. The flow in the vapor core is so highly turbulent that the temperature gradient in the radial direction is negligible. Interface mass transfer resistance is so small that it is neglected. The temperature at the vapor-liquid interface is assumed to be the saturation temperature.

With the above assumptions, consider a control volume as shown in Figure 1.

$$\tau_o = F_o \delta + \tau_v \tag{1}$$

where F_o is the total static pressure plus momentum change in the liquid film and gravity force acting on the film. And from the basic definitions of eddy viscosity and eddy conductivity,

$$\tau = \frac{\rho_\ell}{g_o} (\nu_\ell + \epsilon_m) \frac{dv_z}{dy} \tag{2}$$

$$q/A = \rho_\ell C_p (\alpha + \epsilon_h) \frac{dT}{dy} \tag{3}$$

Local heat transfer coefficients are defined as follows:

$$h_z = \frac{(q/A)_o}{T_v - T_o} \tag{4a}$$

With the assumption (2)

$$h_z = \frac{(q/A)}{T_v - T_o} \tag{4b}$$

The liquid Reynolds number inside a tube is defined as

$$Re_\ell = \frac{G_\ell D}{\mu_\ell} \tag{5}$$

where

$$G_\ell = \frac{W_\ell}{\pi D^2/4} \tag{6}$$

is the superficial mass velocity of liquid. The flow quality x is defined as the ratio of vapor flow weight to the total flow weight in a unit time; that is

$$x = 1 - \frac{W_\ell}{W} \tag{7}$$

From Eq. (6) and (7) with

$$W = G \cdot \frac{\pi D^2}{4} \tag{8}$$

Hence,

$$G_\ell = G (1 - x) \tag{9}$$

The flow rate per unit circumference is

$$\Gamma = \frac{W_\ell}{\pi D} \tag{10}$$

Combining Eq. (6) and (10) gives $G_\ell = \frac{4\Gamma}{D}$ and substituting this

into Eq. (5) yields

$$Re_\ell = \frac{4\Gamma}{\mu} \tag{11}$$

And also

$$\Gamma = \int_0^\delta \rho_\ell v_z \, dy \tag{12}$$

$$Re_\ell = \frac{4}{\mu_\ell}\rho_\ell \int_0^\delta v_z \, dy \tag{13}$$

Von Karman's universal velocity distributions are the following:

$$\delta^+ < 5 \qquad v_z^+ = y^+ \tag{14a}$$

$$5 < \delta^+ < 30 \qquad v_z^+ = -3.05 + 5.0 \ln y^+ \tag{14b}$$

$$\delta^+ > 30 \qquad v_z^+ = 5.5 + 2.5 \ln y^+ \tag{14c}$$

where

$$y^+ \equiv \frac{y}{\nu_\ell}\sqrt{\frac{g_o \tau_o}{\rho_\ell}} \tag{15a}$$

$$\delta^+ \equiv \frac{\delta}{\nu_\ell}\sqrt{\frac{g_o \tau_o}{\rho_\ell}} \tag{15b}$$

$$v_z^+ \equiv v_z\sqrt{\frac{\rho_\ell}{g_o \tau_o}} \tag{15c}$$

Liquid Reynolds number may be expressed in terms of dimensionless variables as follows:

$$Re_\ell = 4\int_0^{\delta^+} v_z^+ \, dy^+$$

Substituting the universal velocity distribution,

for $\delta^+ < 5$

$$Re_\ell = 2(\delta^+)^2 \tag{16a}$$

for $5 < \delta^+ < 30$

$$Re_\ell = 50 - 32.2\delta^+ + 20\delta^+ \ln \delta^+ \tag{16b}$$

for $\delta^+ > 30$

$$Re_\ell = -256 + 12\delta^+ + 10\delta^+ \ln \delta^+ \tag{16c}$$

With the assumption (3), ϵ_h is obtained from Eq. (1), (2) and (14a, b, c) and integration of Eq. (3) leads to the temperature profile. From the definition (4b) heat transfer coefficient is easily derived. The results are the following:

$$h^*_z = \frac{Pr}{F_2} \left(\frac{\delta^+}{M}\right)^{\frac{1}{3}} \tag{17}$$

where

$$M = \frac{1}{1 + (\tau_v^* / \delta^*)} \tag{18}$$

$$h_z^* = \frac{h_z}{K} \left(\frac{\nu_\ell \mu_\ell}{g_o F_o}\right)^{\frac{1}{3}} \tag{19}$$

$$\tau_v^* = \frac{\tau_v}{F_o} \left(\frac{\nu_\ell \mu_\ell}{g_o F_o}\right)^{-\frac{1}{3}} \tag{20}$$

$$\delta^* = \delta \left(\frac{\nu_\ell \mu_\ell}{g_o F_o}\right)^{-\frac{1}{3}} \tag{21}$$

And

(1) For $\delta^+ < 5$

$$F_2 = \delta^+ Pr \tag{22a}$$

(2) For $5 < \delta^+ < 30$

$$F_2 = 5\,Pr + 5 \ln \left[1 + Pr\left(\frac{\delta^+}{5} - 1\right)\right] \tag{22b}$$

(3) For $\delta^+ > 30$

$$F_2 = 5\,Pr + 5\,Pr(1+5Pr) + \frac{2.5}{\sqrt{1+\frac{10M}{Pr\,\delta^+}}} \ln\left[\frac{2M-1+\sqrt{1+\frac{10M}{Pr\delta^+}}}{2M-1-\sqrt{1+\frac{10M}{Pr\delta^+}}} \frac{\frac{60}{\delta^+}M-1-\sqrt{1+\frac{10M}{Pr\delta^+}}}{\frac{60}{\delta^+}M-1+\sqrt{1+\frac{10M}{Pr\delta^+}}}\right] \quad (22c)$$

From Eq. (1), (15b) and (20)

$$\delta^+ = \delta^* \sqrt{\delta^* + \tau_v^*} \quad (23)$$

which is shown graphically in Fig. 2.

2.3 Mean Heat Transfer Coefficients

Although it is clearly preferable to think in terms of local values for a complete understanding of processes involved, the designer is primarily interested in mean values which can be applied directly.

In general, the mean heat transfer coefficient is defined as the average value of local values with respect to the length of a condenser tube. However, for given conditions the above analysis gives only the relation between local heat transfer coefficients and local liquid Reynolds numbers. It is necessary to develop a method of integrating the local values with respect to Reynolds number or quality.

$$Q = \Gamma \pi D h_{fg} = h_m \Delta T \pi D L \quad (24)$$

The differential of Eq. (24) is

$$dQ = \pi D h_{fg}\, d\Gamma = h_z \Delta T \pi D\, dZ \quad (25)$$

From Eq. (25)

$$\frac{d\Gamma}{h_z} = \frac{\Delta T}{h_{fg}} dZ \quad (26)$$

Integration of Eq. (26) from inlet to outlet of a condenser tube gives

for uniform ΔT,

$$\int_0^{\Gamma} \frac{d\Gamma}{h_z} = \frac{\Delta T}{h_{fg}} L \tag{27}$$

Substituting Eq. (24) into Eq. (27),

$$\int_0^{\Gamma} \frac{d\Gamma}{h_z} = \frac{\Gamma}{h_m} \tag{28}$$

$$\frac{1}{h_m} = \frac{1}{\Gamma} \int_0^{\Gamma} \frac{d\Gamma}{h_z} \tag{29}$$

Using Eq. (11),

$$\frac{1}{h_m} = \frac{1}{Re_{\ell_{exit}}} \int_0^{Re_\ell} \frac{dRe_\ell}{h_z} \tag{30}$$

And furthermore from Eq. (9)

$$\frac{1}{h_m} = \frac{1}{\chi_{exit}} \int_{\chi_{exit}}^{1} \frac{d\chi}{h_z} \tag{31}$$

2.4 Local Pressure Drop

In the condenser tube, pressure drop occurs due to the friction between vapor, liquid and tube wall, momentum change of the condensing fluid, and elevation in the gravity field. Total pressure gradients will be obtained by the sum of these three terms.

$$\left(\frac{dP}{dz}\right) = \left(\frac{dP}{dz}\right)_f + \left(\frac{dP}{dz}\right)_m + \left(\frac{dP}{dz}\right)_g \tag{32}$$

Using Lockhart-Martinelli's[43] correlation for friction pressure drop and Zivi's[69] correlation for local void fraction, each term of Eq. (32) may be calculated as follows:

$$\frac{g_o D\left(\frac{dP}{dz}\right)_f}{G^2/\rho_v} = -0.09 \left(\frac{GD}{\mu_v}\right)^{-0.2} \left[\chi^{1.8} + 5.7 \left(\frac{\mu_\ell}{\mu_v}\right)^{0.0523} (1-\chi)^{0.47} \chi^{1.33} \left(\frac{\rho_v}{\rho_\ell}\right)^{0.261} + 8.11 \left(\frac{\mu_\ell}{\mu_v}\right)^{0.105} (1-\chi)^{0.94} \chi^{0.86} \left(\frac{\rho_v}{\rho_\ell}\right)^{0.522}\right] \tag{33}$$

$$\frac{g_o D\left(\frac{dP}{dz}\right)_m}{G^2/\rho_v} = -D\frac{dx}{dz}\left[2x+(1-2x)\left(\frac{\rho_v}{\rho_\ell}\right)^{\frac{1}{3}} + (1-2x)\left(\frac{\rho_v}{\rho_\ell}\right)^{\frac{2}{3}} + 2(1-x)\left(\frac{\rho_v}{\rho_\ell}\right)\right] \quad (34)$$

$$\frac{g_o D\left(\frac{dP}{dz}\right)_g}{G^2/\rho_v} = \frac{1}{Fr}\left[\left(\frac{\rho_\ell}{\rho_v}\right)+B\alpha\right] \quad (35)$$

where

$$Fr = \frac{(G/\rho_v)^2}{aD} \quad (36)$$

$$B = \frac{\rho_\ell - \rho_v}{\rho_v} \quad (37)$$

$$\alpha = \frac{1}{1+\left(\frac{1-x}{x}\right)\left(\frac{\rho_v}{\rho_\ell}\right)^{\frac{2}{3}}} \quad (38)$$

And terms F_o and τ_{wv} in Eq. (1) may be obtained as follows:

$$F_o = -\left(\frac{dP}{dz}\right) + \frac{a}{g_o}\rho_\ell - \frac{G^2}{g_o\rho_v}\frac{dx}{dz}\left[\frac{1-2x}{1-\alpha}\left(\frac{\rho_v}{\rho_\ell}\right)^{\frac{1}{3}} + \left\{\frac{\beta(1-x)}{(1-\alpha)^2} - \frac{2(1-x)}{1-\alpha}\right\}\left(\frac{\rho_v}{\rho_\ell}\right)\right] \quad (39)$$

$$\tau_{wv}\frac{4}{\alpha D} = -\left|\frac{dP}{dz}\right| + \frac{a}{g_o}\rho_v - \frac{G^2}{g_o\rho_v}\frac{dx}{dz}\left[\frac{2x}{\alpha} + \frac{1-2x}{\alpha}\left(\frac{\rho_v}{\rho_\ell}\right)^{\frac{2}{3}} + \frac{\beta(1-x)}{\alpha(1-\alpha)}\left|\frac{\rho_v}{\rho_\ell}\right|\right] \quad (40)$$

where β is the ratio of vapor-liquid interface velocity to the average velocity of liquid film and may be taken 1.2 as a good approximation.

2.5 A Method of Numerical Calculation

With given conditions such as kinds of working refrigerants, saturation temperatures, mass velocities and coolant temperatures, it is required for a condenser designer to know pressure drop, heat transfer rate, and size of condenser tube. Unfortunately, the pressure gradients and the heat transfer rates must be solved simultaneously in a condensation problem. Trial-and-error is inherently involved in the calculation. The following procedure may be used for hand calculations. Known variables: tube diameter, saturation temperature, mass velocity, temperature difference between vapor and wall, and physical properties of fluid.

1. Divide the quality range into several steps. The local value is to be calculated for the average quality of those steps.
2. Calculate the friction pressure drop by Eq. (33) for each step.
3. With an initial trial value of (dx/dz), calculate the momentum term by Eq. (34). In many cases 0.05/ft seemed to be a good initial trial value for the refrigerant.
4. Calculate the gravity term by Eq. (35). This term is zero for a horizontal tube.
5. The sum of those three terms is the total pressure gradient (dP/dz) (Eq. (32)).
6. Obtain F_o and τ_v from the above results and Eq. (39) and (40). τ_v^* can be obtained from Eq. (20), and α from Eq.(38).
7. Calculate Reynolds number Re_ℓ from Eq. (5) and (9).
8. With the Reynolds numbers find δ^+ from Eq. (16a), (16b) or (16c) whichever is appropriate or Fig. 4.
9. Calculate δ^* from the obtained δ^+ and τ_v^* by Eq. (23) or Fig. 2.

10. Using the appropriate equation among Eq. (22a), (22b) or (22c) with Eq. (18) calculate F_2. Substitute the obtained values of δ^+, M and F_2 into Eq. (17) to get h_z^* or Fig. 5-8.

11. Use the definition of h_z^*, Eq. (19), to get the local heat transfer coefficients.

12. From Eq. (6), (7), (8), (10) and (25)

$$\frac{\Delta x}{\Delta z} = 4 \frac{h_z \Delta T}{h_{fg} G D}$$

This should agree with the magnitude of the dx/dz which was assumed in Step 3. If they do not agree, repeat steps 3 through 12 until agreement is reached. Actual repeating this calculation with dx/dz obtained in Step 12 usually requires only the second trial to reach good agreement if the momentum pressure gradient is small. Alternatively this calculation procedure can be set up for computer calculation, Appendix G. A sample calculation is also shown in Appendix H.

III EXPERIMENT

3.1 General Description of Apparatus

The apparatus was designed for a practical range of parameters in the refrigeration industry.

The basic apparatus, schematically shown in Figure 11, consists of a closed-loop refrigerant flow circuit driven by a mechanical-sealed rotor pump. Upstream of the test section, an electrically heated boiler produces vapor, which passes through a flow meter and a throttle valve to the test section. Downstream of the test section, an after-condenser was provided to ensure fully condensed refrigerant at the pump inlet. The pumping power was fixed in test runs and flow rate and pressure level of the test section was controlled by making use of a by-pass loop.

The test section itself is an annular shaped heat exchanger with refrigerant flowing through the inner tube and cooling water running in the outer annulus counter-currently. The test section was divided into six 3 ft-long sections of 0.493 in I.D. straight smooth nickel tube. Each short section has a separate cooling water circuit and those sections are connected smoothly with specially made stainless steel fittings in order not to disturb the condensate flow.

Each of those six sections except the third section from the inlet was separately and identically instrumented to give basic data on the condensing refrigerant. Two thermocouples are placed in the middle of the 3 ft section; one at the outside of the condenser tube and the other one at the center of the tube. Two differential thermocouples are located at the inlet and the outlet of the cooling

water circuit. These thermocouples are located in different radial positions in order to detect any possible non-uniformity in temperature. On the third section, in addition to the above thermocouples, two more thermocouples are placed at the tube wall to measure the circumferential variation of the wall temperature.

All the thermocouples were made of 0.05 in O.D. nylon-sheathed copper and constantan wire.

Seven pressure taps were installed at every connection between the 3 ft sections for measurement of local pressure gradients.

All the loop except the part from the pump to the boiler was insulated with fiberglass. The heat loss from the test section to the atmosphere was not measurable within the accuracy of the potentiometer.

3.2 Test Procedure

In order to eliminate non-condensable gas in the test loop, the loop was evacuated with a vacuum pump (SENCO HYVAC). The pressure of the system went to 28 in Hg vacuum after a two hour operation of the vacuum pump. The loop was charged slowly at the lowest point of the loop with refrigerant 22 by heating the 50 lb-containers of R-22. When the system pressure went up to 5 psia, the charging was stopped and the system was evacuated again. After repeating the process three times, R-22 was charged so that the heating units of the vapor generator were completely submerged under the liquid level. Since the R-22 vapor is much heavier than air, vents at the highest point of the loop were opened until liquid drops of R-22 came out from the valves.

In order to prevent oil contamination, a mechanical sealed rotor pump was used instead of the reciprocating compressors commonly used in refrigeration systems.

Data were taken after steady state had been attained for one hour in the system. The heat flux to the coolant was obtained from the coolant flow rate and the temperature change. The condensing wall temperature was determined from the outside tube wall temperature and the heat flux. All the measurements were done on one 3 ft section at a time from up-stream to down-stream. The coolant flow was regulated such that the wall temperatures were kept almost constant through the test section and the temperature change of the coolant was large enough to give an accurate measurement (1-3°F).

Heat balance was checked with total enthalpy change from the inlet of test section to the outlet of the after-condenser. In most runs, except Run 1, the heat balance error was less than $\pm$ 6%.

IV ERROR ANALYSIS

The cooling water flow rate was determined by weigh-tanks. Time was measured for 200 lbm of water flow. The error is estimated of the order 0.25% of that flow rate. The error in the cooling water temperature rise is within the accuracy of differential thermocouples and is estimated of order 2.75%. Therefore, the error in the heat flux would be around 3%.

The error in the temperature difference between vapor and inside wall temperature comes from the readings as well as the locations of thermocouple junction. Calibration shows that the deviation of thermocouple readings from the standard table is 0.49%. Vapor temperature measurement would be within this accuracy. Inside wall temperature was calculated from the measured value of outside wall temperature. Each thermocouple was soft-soldered to the outside wall and the spot was covered by a small amount of epoxi-resin in order to support the junction in highly turbulent current of cooling water. The temperature rise due to the insulation effect of epoxi-resin is estimated of order 0.01°F by assuming complete insulation. The coolant current distrubance by the support would have small influence on the wall temperature. Therefore, taking account of the capability of K-2 potentiometer, the estimate of the error in the temperature difference between vapor and inside wall is around 2%. The total error in heat transfer coefficient would be the sum of these two or around 5%.

The inherent error in the refrigerant vapor flow meter is stated by the manufacturer to be 2%. Fluctuations in the float reading were of the order of 1%. Therefore, the maximum error in the refrigerant

flow reading would be approximately 3%. This, along with the estimated 3% error in heat flux, would produce an error in the change in quality from the inlet of about 6%. Usually the pressure drop in the whole test section is of the order of 5 psi. The latent heat for the pressure drop is about 0.5 Btu/lb. Hence, the error in the quality due to the pressure drop is negligible compared with other errors.

V Discussion of Results

5.1 Limitation of Analysis

Since the theoretical analysis was based on the annular flow model, the results are applicable only to the case where annular flow is developed. To date no successful investigation has been made of condensation flow regimes. For gas and oil mixtures, a flow regime map was drawn by Baker [9], but it is probably not applicable to two-phase flow with condensation. However, it surely gives an approximate view of the flow regime boundaries of condensation. Quandt [51] analyzed qualitatively the force field of gas-liquid flow. Still a quantitative figure of the flow regime boundaries cannot be obtained from an analysis. Therefore, until more reliable information about flow regimes of vapor-liquid flow with condensation is available, it is recommended that the Baker plot be used for determining probable flow regimes.

In most cases of practical forced-convection flow the regime appears to be annular except at the very low quality region. This analysis is not applicable to the very low quality region because the flow regime may be different and because the condensate film is so thick that the flat plate analysis is no longer valid for a tube. The present method is therefore not suggested for use when the vapor quality is less than 20%. Interpolation between the present correlation at $x = 0.20$ and McAdams equation for single phase flow ($x = 0$) will give useful information for the low quality region.

Entrainment of liquid in the vapor core was neglected in the analysis. Since thermal resistance is mainly offered by the laminar sublayer and the buffer layer, the entrainment effect is not significant when the condensate film thickness is larger than that of the high thermal resistance layers ($\delta^+ > 30$). However, as expected, the effect appears to be significant at the very high vapor quality region where a very thin film exists ($\delta^+ < 5$), as shown in some of the test runs. The theory was somewhat modified implicitly by using the empirical correlations of pressure gradients which were developed for the actual flow. Yet when a considerable amount of entrainment is produced, the theory predicts lower values than actually occur.

In the heat transfer coefficient derivation, no restriction was made on the position of the tube. It is applicable to a horizontal tube as well as to a vertical tube as long as pressure gradients are properly estimated. The suggested equations for pressure gradient were derived for an arbitrarily inclined tube. Since the derivation of the friction pressure drop (Eq. 33) was based on the Lockhart-Martinelli method, which does not explicitly account for the effect of gravity force and momentum changes on the friction pressure drop, it may be applied to a vertical tube without modification. Although there actually exist effects on the friction pressure drop or wall shear stress due to condensation and gravity, these effects were not big enough to appear in experimental data [43], [45].

As the total flow rate decreases, the thickness of the liquid film on the wall of a horizontal tube may be changed significantly.

Even though the flow shape becomes an eccentric annulus, the analysis may give a good prediction because the heat transfer coefficient increases at the top and decreases at the bottom of the tube when this happens. However when the accumulation of the condensate becomes apparent, then another theory should be used.

5.2 Comparison with Data

The data for the 8 test runs are tabulated in Appendix A and plotted in the 8 graphs of Fig. 13 and 14. The prediction curves are also drawn in the figures. In the data reduction, the physical and thermal properties are taken from reference [64]. Because of small temperature differences between vapor and the tube wall, the properties were evaluated at the saturation temperature.

The agreement with the present data is within 10% except a few low quality points. In general predictions are slightly lower than the experimental data within the range of measurement accuracy (Fig. 15). The pressure drop measurement also shows good agreement except for Run 8. It is interesting to note that at the upstream end of the condensing tube the predicted pressure gradient has a negative slope. However, the measurement shows the opposite trend. Except for Runs 5 and 8, the pressure drop of the first section is always higher than that of the other sections.

The data of Altman et al were also compared with the prediction. Again the agreement is within 10% as shown in Fig. 17. Pressure drops are correlated within 10% by the equations suggested in Chapter III (Fig. 16).

The analysis of Kunz et al [39] agreed with the present results. A detailed review is followed in Appendix C.

VI Conclusions

1. The present theory appears to provide good agreement with the present data and the data of Altman et. al.
2. The method of Soliman et. al. [61] was modified in order to get the proper wall shear stress. Still the momentum effect on the total static pressure gradient is negligible compared with the friction pressure gradient.
3. The present theory agrees well with the Kunz [39] result except when the vapor shear stress is small. When the liquid Reynolds numbers become larger than 10,000, the effect of the vapor shear stress on the Stanton number is significant.

VII Recommendations for Future Work

1. The original proposal called for superheated refrigerant vapor at the condenser inlet. The analysis is significantly more complicated for this condition, but should be undertaken to cover the entire expected range of operating conditions. The analysis must be verified by experimental data. The present apparatus would require modification by adding a superheater and changing the pressure measuring technique in the superheated region.
2. Since the entire theoretical analysis is currently based on the shear stress in the tube, a more detailed study should be made of the effect of condensate flow on the effective vapor shear stress at the liquid-vapor interface and also on the wall shear stress.
3. It is generally impractical to make a condenser of straight horizontal tubes. Most commercial units are fabricated with several U-shaped bends in the condensing region. These bends

may have important effects on the development of the internal refrigerant flow patterns. The magnitude of such effects should be investigated.

4. In the high-quality region annular flow is the most probable regime. However at low qualities, it is difficult to predict the flow regime. Since knowledge of the entire quality range is required to determine the overall performance of a condenser tube, a thorough investigation of the possible flow regimes is necessary. A flow regime "map" should be developed for two-phase flow with condensation. Such a map is expected to be different from one prepared for evaporating flows.
5. Slug flow is anticipated for condensation at low-qualities. An analysis of this region, with properly determined flow regime boundaries, should be made and verified by experimental data in order to enable the prediction of overall condenser performance.

REFERENCES

1. Akers, W. W., H. A. Deans and O. K. Crosser, "Condensing Heat Transfer Within Horizontal Tubes", Chemical Engineering Progress, Vol. 54, pp. 89 (1958).

2. Akers, W. W. and H. F. Rosson, "Condensation Inside a Horizontal Tube", Chemical Engineering Progress, Symposium Series, Heat Transfer, Storrs, Vol. 56, No. 30 (1960).

3. Altman, M., F. W. Staub and R. H. Norris, "Local Heat Transfer and Pressure Drop for Refrigerant-22 Condensing in Horizontal Tubes", ASME-AIChE, Heat Transfer Conference, Storrs, Conn. (1959).

4. Altman, M., F. W. Staub and R. H. Norris, "Local Heat Transfer and Pressure Drop for Refrigerants Evaporating in Horizontal Tubes", Trans. ASME, Journal of Heat Transfer, Series C, Vol. 82, No. 3 (1960).

5. Ananiev, E. P., L. D. Boyko and G. N. Kruzhilin, "Heat Transfer in the Presence of Steam Condensation in a Horizontal Tube", International Heat Transfer Conference, Vol. II, pp. 290 (1961).

6. Andeen, G. B. and P. Griffith, "The Momentum Flux in Two-Phase Flow", MIT Report No. 4547-38 and also ASME paper No. 67-HT-32 (1967).

7. ASHRAE Handbook of Fundamentals (1967).

8. Bae, S., J. S. Maulbetsch and W. M. Rohsenow, "Refrigerant Forced Convection Condensation inside Horizontal Tubes", Dept. of Mechanical Engineering, Heat Transfer Lab. Report No. 79760-59, MIT (1968).

9. Baker, O., "Simultaneous Flow of Oil and Gas", The Oil and Gas Journal, Vol. 53, pp. 185-195 (1954).

10. Bankoff, S. G., "A Variable Density Single-Fluid Model for Two-Phase Flow with Particular Reference to Steam-Water Flow", Trans. ASME, Vol. 82, pp. 265 (1960).

11. Baroczy, C. J., "A Systematic Correlation for Two-Phase Pressure Drop", Atomic International, NAA-SR-MEMO-11858 (1966).

12. Bell, K. J., J. Taborek and F. Fenoglio, "Interpretation of Horizontal in-tube Condensation Heat Transfer Correlation Using a Two-Phase Flow Regime Map", 11th National Heat Transfer Conference, Minneapolis, Minn. (1969).

13. Bergelin, O. P., P. K. Kegel, F. G. Carpenter and C. Gayley, "Co-Current Gas-Liquid Flow in Vertical Tubes", Heat Transfer and Fluid Mechanics Inst. Berkeley, Calif. Published by ASME, pp. 19-28 (1949).

14. Borchman, J., "Heat Transfer of High Velocity Vapor Condensing in Annuli", Trans. ASHRAE, No. 2023 (1967).

15. Boyko, L. D. and G. N. Kruzhilin, "Heat Transfer and Hydraulic Resistance during Condensation of Steam in a Horizontal Tube and in a Bundle of Tubes", International Journal of Heat Transfer and Mass Transfer, Vol. 10 pp. 361 (1967).

16. Brauser, S. O., "Turbulent Condensation in a Horizontal Tube", Ph.D. Thesis, Dept. of Mechanical Engineering, Kansas State University (1966).

17. Carpenter, E. F. and A. P. Colburn, "The Effect of Vapor Velocity on Condensation inside Tubes", Proceedings of the General Discussion of Heat Transfer, I. Mech. E. and ASME (1951).

18. Chari, K. S. and B. S. Kulkarni, "Condensation of Saturated Vapor", Journal of Science and Industrial Research, India, Vol. 10a, pp. 199, 144, 326(1951).

19. Chaddock, J. B., "Film Condensation of Vapor in Horizontal Tubes", Sc.D. Thesis, MIT (1955), also Refrigerating Engineering, Vol. 65, No. 4, pp. 36 (1957).

20. Chato, S. C., "Laminar Condensation Inside Horizontal and Inclined Tubes", ASHRAE Journal, Vol. 4, No. 2 (1962).

21. Chen, C. J., "Condensing Heat Transfer in a Horizontal Tube", M. S. Thesis, Dept. of Mechanical Engineering, Kansas State University (1962).

22. Chen, M. M., "Analytical Study of Laminar Film Condensation", Trans. ASME, Journal of Heat Transfer, Vol. 83, Series C, pp. 48 (1961).

23. Colburn, A. P., "Note on the Calculation of Condensation When a Portion of the Condensate Layer is in Turbulent Motion", Trans. AIChE, Vol. 30, pp. 187 (1934).

24. Dickson, A. J. and S. W. Gouse, Jr., "Heat Transfer and Fluid Flow Inside a Horizontal Tube Evaporator. Final Report", Report No. 9649, Dept. of Mechanical Engineering, M.I.T. (1966).

25. Deissler, R. G., "Analysis of Turbulent Heat Transfer, Mass Transfer and Friction in Smooth Tubes at High Prandtl and Schmidt Numbers", NASA, Tech. Notes 3154 (1954).

26. Dormer, T., Jr. and A. E. Bergles, "Pressure Drop with Surface Boiling in Small-Diameter Tubes", Report No. 5767-31, Dept. of Mechanical Engineering, M.I.T. (1964).

27. Dukler, A. E., "Fluid Mechanics and Heat Transfer in Vertical Falling-Film System", Chem. Eng. Symposium Series, Vol. 56, No. 30 (1960).

28. Dukler, A. E. and O. P. Bergelin, "Characteristics of Flow in Falling Liquid Films", Chemical Engineering Progress, Vol. 48, pp. 557 (1952).

29. Gerstmann, J., and P. Griffith, "The Effect of Surface Instabilities on Laminar Film Condensation", Dept. of Mechanical Engineering, Tech. Report No. 5050-36, M.I.T. (1965).

30. Goodykoontz, J. H. and R. G. Dorsch, "Local Heat Transfer Coefficients for Condensation of Steam in Vertical Downflow", NASA TN D-3326 (1966).

31. Goodykoontz, J. H. and R. G. Dorsch, "Local Heat Transfer Coefficients and Static Pressures for Condensation of High-Velocity Steam Within a Tube", NASA TN D-3953 (1967).

32. Goodykoontz, J. H. and W. F. Brown, "Local Heat Transfer and Pressure Distributions for Freon-113 Condensing in Downward Flow in a Vertical Tube", NASA TN D-3952 (1967).

33. Hilding, W. E. and C. H. Coogan, Jr., "Heat Transfer Studies of Vapor Condensing at High Velocity in Small Straight Tubes", NASA CR-124 (1964).

34. Hoogendoorn, C. J., "Gas-Liquid Flow In Horizontal Pipes", Chemical Engineering Science, Vol. 9, No. 1 (1959).

35. Kirkbride, C. G., "Heat Transfer by Condensing Vapor on Vertical Tube", Trans. AIChE, Vol. 30, pp. 170-186 (1933).

36. Koh, J., "Film Condensation in a Forced-Convection Boundary-Layer Flow", International Journal of Heat and Mass Transfer, Vol. 5, pp. 941-954 (1962).

37. Kowalczewski, J., "Heat Transfer to Boiling Refrigerants and Pressure Drop in Evaporators", Australian Refrigeration Air Conditioning and Heating, Vol. 22, No. 1, pp. 14-25 (1968).

38. Kroger, D. G., "Heat Transfer During Film Condensation of Potassium Vapor", International Journal of Heat and Mass Transfer, Vol. 11, pp. 15-26 (1968).

39. Kunz, H. R. and S. Yerazunis, "An Analysis of Film Condensation Film Evaporation, and Single-Phase Heat Transfer for Liquid Prandtl Numbers From 10^{-3} to 10^{4}", Heat Transfer Conference, Seattle, Washington, Paper No. 67-HT-1 (1967).

40. Kutateladze, S. S., "Fundamentals of Heat Transfer", Academic Press, N. Y. (1963).

41. Lehtinen, J. A., "Film Condensation in a Vertical Tube Subject to Varying Vapor Velocity", Sc.D. Thesis, M.I.T. (1957).

42. Lin, C. S., R. W. Moulton and G. L. Putnam, "Mass Transfer Between Solid Wall and Fluid Streams", Industrial Engineering and Chemistry, Vol. 45, pp. 636-640 (1953).

43. Linehan, J. H., "The Interaction of Two-Dimensional, Stratified, Turbulent Air-Water and Steam-Water Flows", Argonne National Laboratory, ANL-7444 (1968).

44. Lockhart, R. W. and R. C. Martinelli, "Proposed Correlation of Data for Isothermal Two-Phase, Two-Component Flow in Pipes", Chemical Engineering Progress, Vol. 45, No. 1, pp. 39 (1949).

45. Martinelli, R. C., "Heat Transferred to Molten Metals", Trans. ASME, Vol. 69, pp. 947-955 (1947).

46. Martinelli, R. C. and D. B. Nelson, "Prediction of Pressure Drop During Forced Circulation Boiling of Water", Trans. ASME, Vol. 70, pp. 652-702 (1948).

47. Misra, B., and C. F. Bonilla, "Heat Transfer in the Condensation of Metal Vapor: Mercury and Sodium up to Atmospheric Pressure", Chemical Engineering Progress Symposium Series, No. 52, pp. 7 (1956).

48. Moor, F. D. and R. B. Mesler, "The Measurement of Rapid Surface Temperature Fluctuation During Nucleate Boiling of Water", AIChE, Journal, Vol. 7, pp. 620 (1961).

49. Nusselt, M., "Die Oberflachen Kondensation Des Wasserdampfes", Seitschrift des Vereines Deutscher Ingenieure, Vol. 60, No. 541 (1916).

50. Page, F., W. H. Corcoran, W. G. Schlinger and B. H. Sage, "Temperature and Velocity Distribution in Uniform Flow Between Parallel Plates", Industrial Engineering and Chemistry, Vol. 44, pp. 411 (1952).

51. Patel, S. P., "Film Coefficient of Heat Transfer of Freon-12 Condensing inside a Single Horizontal Tube", M. S. Thesis, Kansas State University (1956).

52. Quant, E., "Analysis of Gas-Liquid Flow Patterns", AIChE, 6th National Heat Transfer Conference, Preprint 47, (1963).

53. Rohsenow, W. M., "Heat Transfer and Temperature Distribution in Laminar-Film Condensation", Trans. ASME, Vol. 78, pp. 1645 (1956).

54. Rohsenow, W. M. and H. Y. Choi, "Heat, Mass and Momentum Transfer", Prentice-Hall Inc., 3rd Printing (1965).

55. Rohsenow, W. M., J. H. Webber and A. T. Ling, "Effect of Vapor Velocity on Laminar and Turbulent-Film Condensation", Trans. ASME, pp. 1637 (1956).

56. Rosson, H. F. and J. A. Myers, "Point Value of Condensing Film Coefficients inside a Horizontal Pipe", 7th National Heat Transfer Conference, Cleveland, Ohio (1964).

57. Rothfus, R. R. and R. S. Prengle, "Laminar-Turbulent Transition in Smooth Tubes", Industrial Engineering and Chemistry, Vol. 44, pp. 1683 (1952).

58. Rufer, C. and S. P. Kezios, "Analysis of Two-Phase One Component Stratified Flow with Condensation", Journal of Heat Transfer, Trans. ASME, Series C, Vol. 88, No. 3 (1966).

59. Seban, R. A.,"Remarks on Film Condensation with Turbulent Flow", Trans. ASME, Vol. 76, pp. 299 (1954).

60. Silver, R. S., "An Approach to a General Theory of Surface Condensers", The Institution of Mechanical Engineers, London, Advanced Copy, No. P14/64 (1964).

61. Soliman, M., J. R. Schuster and P. J. Berenson, "A General Heat Transfer Correlation for Annur Flow Condensation", Trans. ASME, Journal of Heat Transfer, Series C, Vol. 90, No. 2 (1968).

62. Sparrow, E. M. and J. L. Gregg, "A Boundary Treatment of Laminar Film Condensation", Trans. ASME, Journal of Heat Transfer, Series C, Vol. 81, pp. 13 (1959).

63. Tape, J. P. and A. C. Muller, "Condensation and Subcooling Inside an Inclined Tube", Chemical Engineering Progress, Vol. 43, pp. 267 (1947).

64. "Thermodynamic Properties of Freon-22", Du Pont (1964).

65. Von Karmann, T., "The Analogy Between Fluid Friction and Heat Transfer", ASME, Vol. 61, pp. 705 (1939).

66. Wallis, G. B., "The Transition from Flooding to Upwards Cocurrent Annular Flow in a Vertical Pipe", Atomic Energe Est., Winfrith, AEEW-R142 (1962)

67. Wallis, G. B. and R. S. Silver, "Studies in Pressure Drop with Latheral Mass Extraction", Institute of Mechanical Engineers, Advance Copy PI/66, London, (1965).

68. Webber, J. H., "Effect of Vapor Velocity on Film Condensation", S. M. Thesis, M.I.T. (1955).

69. White, R. E., "Condensation of Refrigerant Vapors -- Apparatus and Film Coefficient for Freon-12", Trans. ASME, Vol. 70 (1948).

70. Wyde, S. S. and H. R. Kunz, "Experimental Condensing Flow Stability Studies", NASA CR-54178 PWA-3215 (1964).

71. Zivi, S. M., "Estimation of Steady-State Steam Void-Fraction by Means of the Principle of Minimum Entropy Production", Journal of Heat Transfer, Trans. ASME, Series C, Vol. 86, pp. 247 (1964).

72. Cavallini, A. and R. Zecchin, "High Velocity Condensation of R-11 Vapor Inside Horizontal Tubes", Quaderno No. 25, Padova, Italy Sept. 1969.

73. Sherkriladze, I. G. and Gomelauri, V. I., Int. J. Heat Mass Transfer 9, pp. 581 (1966).

Appendix A

Tables of Data

Run 1 $G = 250{,}000$ lbm/ft^2 hr $T_{sat} = 86°F$

Measured

Sec No	T_{vapor}	$T_{w_{out}}$	W_{water}	ΔT_w	dP/dz
1	83.17	71.25	2400	1.482	15.3
2	82.97	71.45	2134	1.450	24.7
3	82.40	69.47	2718	1.250	21.2
4	82.31	70.89	1807	1.531	14.1
5	82.04	70.06	1953	1.473	15.3
6	81.88	67.92	2254	1.186	9.4

Calculated

Sec No	Q/A	$T_{w_{in}}$	ΔT	h	x_m
1	9200	72.73	10.44	880	93.8
2	7990	72.74	10.23	780	82.5
3	8450	70.83	11.57	730	72.2
4	7150	71.05	10.26	696	62.4
5	7450	71.26	10.78	692	53.3
6	6820	69.03	12.85	530	44.3

$q_{cond} = 4{,}210 \times 2.6 = 10{,}950$ Btu/hr

$q_{total} = 29{,}200$ Btu/hr

$q_{total} = W(H_{in} - H_{out}) = 402(111.2 - 31.7) = 31{,}900$ Btu/hr

Heat Balance Error -8.5%

Run 2 G = 485,000 lbm/ft^{2}hr T_{sat} = 81°F

Measured

Sec No	T_{vapor}	$T_{w_{out}}$	W_{water}	ΔT_w	dP/dz
1	81.64	72.81	1690	2.61	73.2
2	81.19	70.79	2800	1.58	62.5
3	81.01	70.12	1920	2.29	57.8
4	80.19	68.84	1510	2.85	47.2
5	79.62	68.13	1730	2.50	53.0
6	79.44	67.89	1910	2.20	43.6

Calculated

Sec No	Q/A	$T_{w_{in}}$	ΔT	h	x_m
1	9,440	74.33	7.31	1290	96.4
2	11,400	72.64	7.55	1330	88.3
3	11,350	71.95	9.06	1250	79.4
4	11,100	70.63	9.56	1160	70.6
5	11,200	69.93	9.69	1150	61.8
6	10,850	69.64	9.80	1100	53.3

q_{cond} = 4,280 x 6.3 = 27,000 Btu/hr

q_{total} = 52,310 Btu/hr

$q_{total} = W(H_{in} - H_{out})$ = 645(111.14-31.9) = 51,500 Btu/hr

Heat Balance Error +1.6%

Run 3 G = 250,000 lbm/ft^2 hr T_{sat} = 86°F

Measured

Sec No	T_{vapor}	$T_{w_{out}}$	W_{water}	ΔT_w	dP/dz
1	86.57	70.37	3310	1.27	24.2
2	86.39	71.02	2560	1.47	20.5
3	85.96	70.12	2490	1.37	17.0
4	85.77	69.38	2910	1.07	13.0
5	85.69	69.67	2790	1.02	13.0
6	85.58	71.04	1750	1.36	7.1

Calculated

Sec No	Q/A	$T_{w_{in}}$	ΔT	h	x_m
1	10,850	72.12	14.45	750	91.1
2	9,730	73.09	13.30	730	74.3
3	8,810	71.54	14.42	610	59.6
4	8,050	70.68	15.09	535	46.7
5	7,350	70.85	14.84	495	34.1
6	6,150	72.03	13.55	455	23.0

q_{cond} = 1,180 x 6.35 = 7,500 Btu/hr

q_{total} = 27,210 Btu/hr

$q_{total} = W(H_{in} - H_{out}) = 332(111.4 - 33.2) = 26,000$ Btu/hr

Heat Balance Error +4.65%

Run 4 G = 470,000 lbm/ft^2 hr T_{sat} = 85°F

Measured

Sec No	T_{vapor}	$T_{w_{out}}$	W_{water}	ΔT_w	dP/dz
1	85.53	74.23	2660	1.77	62.3
2	85.01	75.10	1670	2.27	60.9
3	85.00	71.96	3500	1.42	57.0
4	84.54	73.92	1970	1.88	47.4
5	84.19	72.22	2470	1.54	47.2
6	83.64	71.28	3090	1.24	38.5

Calculated

Sec No	Q/A	$T_{w_{in}}$	ΔT	h	x_m
1	12,200	76.19	9.34	1,300	95.1
2	9,700	76.68	8.33	1,160	85.6
3	12,800	74.02	10.98	1,165	76.0
4	9,610	75.47	9.07	1,060	66.9
5	9,840	73.81	10.38	950	59.0
6	9,900	72.87	10.77	920	51.0

q_{cond} = 3,890 x 8.84 = 33,400 Btu/hr

q_{total} = 58,220 Btu/hr

$q_{total} = W(H_{in} - H_{out})$ = 625(111.4 - 33.6) = 54,900 Btu/hr

Heat Balance Error +6.05%

Run 5 G = 270,000 lbm/ft^2 hr T_{sat} = 92°F

Measured

Sec No	T_{vapor}	$T_{w_{out}}$	W_{water}	ΔT_w	dP/dz
1	92.22	74.98	2300	1.87	18.9
2	92.07	75.30	2080	2.02	24.8
3	91.81	71.90	2770	1.69	20.1
4	91.77	71.71	2690	1.54	14.2
5	90.90	73.73	2060	1.67	14.2
6	90.94	72.03	2340	1.35	9.0

Calculated

Sec No	Q/A	$T_{w_{in}}$	ΔT	h	x_m
1	11,100	76.77	15.45	718	92.0
2	10,850	77.05	15.02	721	76.2
3	12,100	73.85	17.94	674	59.7
4	10,700	73.44	18.33	584	43.3
5	8,900	75.16	15.74	566	29.2
6	8,160	73.35	17.59	465	17.0

q_{cond} = 1,720 x 5.22 = 8,980 Btu/hr

q_{total} = 3,290 Btu/hr

$q_{total} = W(H_{in} - H_{out})$ = 359(111.7-33.9) = 31,500 Btu/hr

Heat Balance Error +4.45%

Run 6 G = 240,000 lbm/ft^2 hr T_{sat} = 92°F

Measured

Sec No	T_{vapor}	$T_{w_{out}}$	W_{water}	ΔT_w	dP/dz
1	93.04	80.34	2440	1.16	20.1
2	92.46	80.97	2180	1.26	21.2
3	91.98	79.72	2300	1.19	16.5
4	91.88	79.28	2310	1.15	11.8
5	91.66	78.29	2600	1.04	11.8
6	91.80	77.91	2580	1.01	7.1

Calculated

Sec No	Q/A	$T_{w_{in}}$	ΔT	h	x_m
1	7550	81.52	11.52	655	93.9
2	7100	82.10	10.36	685	82.1
3	7090	80.86	11.12	636	70.6
4	6870	80.39	11.49	599	59.4
5	7000	79.42	12.24	571	48.2
6	6740	79.00	12.80	526	37.1

q_{cond} = 2,340 x 4.73 = 11,100 Btu/hr

q_{total} = 27,480 Btu/hr

$q_{total} = W(H_{in} - H_{out})$ = 319(111.8-34.5) = 27,800 Btu/hr

Heat Balance Error -1.15%

Run 7 G = 308,000 lbm/ft^2 hr T_{sat} = 92°F

Measured

Sec No	T_{vapor}	$T_{w_{out}}$	W_{water}	ΔT_w	dP/dz
1	98.07	80.96	2510	1.83	25.4
2	97.80	82.12	1860	2.13	23.6
3	97.37	80.06	2410	1.72	21.2
4	97.02	79.26	2800	1.69	16.5
5	96.98	78.58	2840	1.39	16.5
6	96.93	77.26	2080	1.58	11.8

Calculated

Sec No	Q/A	$T_{w_{in}}$	ΔT	h	x_m
1	11,850	82.87	15.20	780	92.4
2	10,200	83.77	14.03	726	78.1
3	10,700	81.79	15.58	687	64.6
4	12,200	81.23	15.79	770	49.8
5	10,200	80.23	16.75	610	35.3
6	8,500	78.63	18.80	452	23.2

q_{cond} = 3,450 x 1.8 = 6,210 Btu/hr

q_{total} = 30,880 Btu/hr

$q_{total} = W(H_{in} - H_{out})$ = 410(112 - 37.5) = 30,600 Btu/hr

Heat Balance Error +0.9%

Run 8 G = 316,000 lbm/ft^{2}hr T_{sat} = 103°F

Measured

Sec No	T_{vapor}	$T_{w_{out}}$	W_{water}	ΔT_w	dP/dz
1	103.12	84.63	2530	2.10	15.3
2	102.91	86.73	1390	2.89	28.3
3	101.79	85.33	2480	1.58	27.1
4	101.33	83.72	3000	1.50	20.0
5	100.98	80.99	3070	1.40	20.0
6	100.98	79.66	3330	1.31	15.3

Calculated

Sec No	Q/A	$T_{w_{in}}$	ΔT	h	x_m
1	13,700	86.85	16.27	842	91.2
2	10,400	88.41	14.50	717	75.8
3	10,100	86.96	14.83	680	62.6
4	11,600	87.59	15.74	737	48.7
5	11,100	82.78	18.20	610	34.1
6	11,300	81.48	19.50	610	19.8

q_{cond} = 2,880 x 2.2 = 6,420 Btu/hr

q_{total} = 32,850 Btu/hr

$q_{total} = W(H_{in} - H_{out}) = 420(112.2 - 37.9) = 31,200$ Btu/hr

Heat Balance Error 5.5%

APPENDIX B

Details of Experimental Apparatus

B.1 Equipment

The basic closed-loop of condensation consists of a heating unit, a condensing unit, driving forces of fluid and regulators for stabilizing the system.

Boiler

In order to gererate the saturated vapor, a boiler was designed for maximum pressure 400 psia and rating 60,000 Btu/hr. A Chromalox Heating Element TM-6153 was placed in the lower part of a 24 in long, 20 in O.D. steel pipe. Six elements of the heating unit were separately connected to six Arrow-Heart and Hegemann Electric Nc 6808 switches. One of the six elements was connected to a General Radio V20H Variac and the other five directly to the power line. Heat input was controlled by the six switches and the Variac. All the connecting wire was 12/2 Type S 600 Volts. A high pressure (max 800 psia) Pyrex-glass 3/4 in. O.D. tube (Ernst Water Column & Gage, L-150) was used as a liquid level gage. The liquid level was always kept above the heating unit to avoid high surface temperature of the elements. The boiler shell was insulated with fiberglass to prevent heat loss to the atmosphere.

Pump

As the driving force of fluid for a closed circuit, one can use either a compressor or a pump. In general a reciprocating compressor is used in refrigeration systems as the fluid flow driving force and power input into the system. However, a pump was used for this experiment in order to avoid oil contamination of the refrigerant. A Flexi-liner

pump, which consists of a flexible liner between the liquid passage and an eccentric shaft, seemed to be ideal for this purpose, but the usual flexible liner, made of neoprene, is easily broken by the high system pressure and the initial attempt to use this kind of pump, Vanton XB-S90, failed.

A mechanical sealed-rotor pump, Blackmer X51 1/4 A C Max-flow rate 12 GPM, was substituted for the flexible liner pump. The new pump was driven by a General Electric 5KC 213AG601A 1 hp motor. Power input of the motor was fixed. A by-pass loop was provided for controlling the flow rate and the pressure level of the system. The manufacturer claims that this pump may be used for any kind of refrigerant with a 20 psi pressure rise across the pump, and 300 psia maximum system pressure.

After Condenser

A shell-and-tube type York Standard Condenser-Receiver was used for complete condensation and subcooling after the test section. The capacity was choosen for 70% of the vapor generator capacity (40,000 Btu/hr). The city water line was directly connected to the coolant passage. The condenser can be used safely up to 300 psia. The degree of subcooling was controlled with the cooling water flow rates.

B.2 Test Section

Since local values are to be measured, care must be taken to accurately determine the inlet fluid conditions and the tube length. It was shown that flow patterns depended not only on the local conditions but also on the past history, i.e. upstream conditions. [66] And in non-isothermal two-phase flow the flow pattern is also affected by heat flux. Particular pre-caution is necessary when a pre-condenser

is used to introduce low vapor quality mixtures. Use of a short test section should be avoided so that entrance effects will not interfere with measurement of local conditions.

In the present experiment, always the saturated vapor was introduced into the test section and the length of the test section, about 18 ft. was determined to give complete condensation for some inlet conditions. In order to measure local values the test section was divided into six 3 ft sections so that changes in wall temperature and vapor fraction along the test section are small, consistent with accurate measurement of the cooling water temperature rise.

In construction of the test section, six identical 3 ft sections were connected in series. Two 20 ft long, 1/4 in steel rods with seven pieces of plexi-glass block were fixed by U-bolts on a Dexion frame to provide a base on which the test section was placed horizontally. Copper is a common material for condenser tube in industry, but a lower conductivity material was required in order to use a heatmeter described by Rosson and Meyer [56], which measured the temperature drop across the tube wall to give the heat flux. Nickel was selected for its lower conductivity and the thickness of the tube was determined so that a simulation-variable $k\delta$, a measure of the peripheral conduction, was approximately the same in the nickel and copper tubes. But the initial attempt to use the Rosson and Meyer type heatmeter failed, because of the difficulties of locating the thermocouple junctions exactly at the inside tube wall and of obtaining precise measurements of small temperature drops (order of 0.1°F). The heat flux was subsequently determined by measuring cooling water flow rate and temperature rise.

Because of its low conductivity, plexi-glass was chosen as the outer annulus in order to provide insulation from the environment. The cooling water passage was sized so that flow velocity was high enough to make the water temperature uniform by turbulent mixing (2-5 ft/sec). Water temperature was varied from 60°F to 80°F by mixing hot and cold water in the main stream. The water flow rate was controlled separately for each 3 ft section by six gate valves at the outlet of each water passage.

Seven flange-type stainless steel connectors were made with special care to provide smooth connections between the 3 ft sections. Neopren O-rings were used to prevent leakage of refrigerant and cooling water.

Although a low conductivity material, plexi-glass, was used for the outer annulus, in order to ensure no heat loss to the environment, all test sections were completely insulated with fiberglass.

B.3 Instrumentation

Temperature All thermocouples were made of Thermo-Electric, 36 gage copper-constantan wire and the junctions were spot-welded by a Dynatech TIG Welder. The wire was insulated separately by nylon coating and the two wires were jacketed together with another nylon coating. Since a direct calibration scheme for each thermocouple was hardly available, calibration was done on three pieces of sample wire from the same spool, where all the thermocouples were taken. Emf was measured between a steam bath and ice and the deviation from the Leeds and Northrup Standard Conversion Table (National Bureau of Standard Circular 561) was interpolated between 32°F and 212°F.

A Leeds and Northrup K-2 Potentiometer, which is capable of reading to

± 2 microvolts, was also calibrated by a local company before data were taken. All emf were read with the potentiometer and a light-beam galvanometer.

Flow Rate Flow rate was measured at the nearest point to the test section inlet. Because of the large volume of the boiler and the after-condenser, there was a possibility of refrigerant accumulation at those two locations. In order to avoid the difficulties in measuring flow rate of two-phase mixture at the outlet of the test section, a Fischer and Poter 10A3565S Flowrator was placed at the test section inlet and vapor flow was measured. The flowrator has an accuracy of ± 2% of maximum flow.

Cooling water flow rates were measured by a weigh-tank and a stop watch. The time variation of water flow due to the pressure change in the main city water line was negligible (less than 1% for a 3 hour period).

Vapor Inlet The saturated condition was checked by a Frost-Line Refrigerant Pressure gage and a thermocouple at the tube axial position. The pressure was read to an accuracy of 1 psia. The vapor at the inlet was always kept slightly superheated (order of 0.4°F) within the accuracy of the pressure gage to ensure 100% vapor quality.

Bulk Vapor Temperature Each thermocouple was inserted to the tube axis through a 0.013 in O.D. hypotubing, which was soft-soldered to the tube wall and the bead of the thermocouple was exposed directly to the vapor stream. The thermocouple wire was continuous from the hot junction to the Leed and Northrup thermocouple switch which connected the cold junction (ice bath) and the potentiometer. The connections of wire and switch were insulated with fiber-glass.

Tube Wall Temperature The hot junction was soft-soldered to the outside tube wall. In order to prevent the thermocouple from being broken by the high speed water stream, the junction was covered by epoxi-resin. Although the cooling water was slightly disturbed by the junction, the insulation effect of epoxi-resin on the thermocouple was negligible (order of 0.01 °F).

Water Temperature Rise Two differential thermocouples were located at the inlet and the outlet of the cooling water circuit. The two thermocouples were easily movable to check the uniformity of the water temperature. The temperature rise was kept less than 3 °F. The potentiometer was read up to 0.1 micro-volts and the temperature was converted up to 0.01°F. However, the accuracy of the temperature measurement was of order 0.1°F.

Heat Balance At the exit of the after-condenser, a thermocouple measured the temperature of the subcooled liquid. Total enthalpy change between the inlet of the test section and the exit of the after-condenser was calculated from the temperature. The sum of the heat transfered in the test section and in the after condenser, (determined from the water flow rate and temperature rise) was compared with the enthalpy change. Except Run 1, the agreement was within 6%.

APPENDIX C

Review of Previous Work

A considerable amount of work has been done on in-tube condensation. At low vapor velocity, laminar film condensation occurs on the tube wall. The classical Nusselt analysis [49] and several modified correlations for a horizontal tube with consideration of the effect of accumulation of condensate at the bottom of a tube showed good agreement with empirical data [19], [20], [58].

As the flow rates increased, waves appeared in the liquid film and the bottom condensate inside a horizontal tube became thinner and thinner. These phenomena were dealt with by Rosson and Myer [54]. The variation of heat flux with time was measured. The Nusselt analysis was used to correlate data at the top of a tube and the von Karman analogy between heat and mass transfer was used to predict heat transfer rate at the bottom.

At sufficiently high vapor velocity, the liquid film and the vapor core are both turbulent and annular flow exists. There are three general approaches in this annular flow region. Since the scope of the present analysis is within this region, a more thorough literature survey on the annular flow model will follow.

C.1 Empirical Correlation of Non-Dimensional Group Type

Considering single-phase turbulent flow to be equivalent to the condensate flow, the single-phase flow McAdams equation was modified in various ways. The single-phase equation is

$$Nu = C\, Pr^{m}\, Re^{n} \tag{C1}$$

Akers et. al. [1] modified Reynolds number with an equivalent

liquid mass velocity which was defined as follows:

$$G_E = G_l + G_v \left(\frac{\rho_l}{\rho_v}\right)^{\frac{1}{2}} \tag{C2}$$

In terms of vapor quality defined by Eq. (7)

$$G_E = \left[1 - x + x\left(\frac{\rho_l}{\rho_v}\right)^{\frac{1}{2}}\right] G$$

$$G_E = \left[1 + x\left(\sqrt{\frac{\rho_l}{\rho_v}} - 1\right)\right] G \tag{C3}$$

Substituting Eq. (C3) into (C1)

$$h_z = h_o \left[1 + x\left(\sqrt{\frac{\rho_l}{\rho_v}} - 1\right)\right]^n \tag{C4}$$

where h_o is the heat transfer coefficient when only liquid flows at the same total mass flow rate. The term inside a square bracket is a modification factor. A similar approach appeared in a Russian paper by Boyko et. al. [14]. They made a direct modification on the heat transfer coefficient instead of Reynolds number [1].

$$h_z = h_o \left[1 + x\left(\frac{\rho_l}{\rho_v} - 1\right)\right] \tag{C5}$$

The constants of Eq. (C1) are as follows:

	c	m	n	Range
Akers et. al.	0.0265	1/3	0.8	$Re_E > 5 \times 10^4$
	5.03	1/3	1/3	$Re_E < 5 \times 10^4$
Boyko et. al.	0.024	0.43	0.8	

Those correction factors are compared in Fig C-1 for a particular case when Refrigerant 22 is condensed at the saturation temperature 90°F. A significant deviation appeared between those correction factors. If is interesting to note that the corrections are a function of vapor quality and density ratio, while the Nusselt analysis showed that the heat transfer coefficient is also a function of ΔT - temperature difference between vapor and condensing wall. However, this effect turned out to be very small.

Although those equations are very convenient to use in practice, because of their weak foundation on the physics of the phenomena itself, those constants which were determined empirically should be checked with data for every fluid and flow condition.

Later, Akers and Rosson [2] included the effect of ΔT. For $Re_\ell < 5000$. The following correlation was suggested.

$$Nu = C\, Pr^{\frac{1}{3}} \left(Re_v' \right)^n \left(\frac{h_{fg}}{C_p \Delta T} \right)^{\frac{1}{6}} \tag{C6}$$

where

$$Re_v' = \frac{DG_v}{\mu_\ell} \left(\frac{\rho_\ell}{\rho_v} \right)^{\frac{1}{2}}$$

is a modified vapor Reynolds number.

In order to compare with Eq. (C1) it is rearranged:

$$Nu = C\, Pr^{\frac{1}{3}}\, Re^n \left(\frac{h_{fg}}{C_p \Delta T} \right)^{\frac{1}{6}} \left(X \sqrt{\frac{\rho_\ell}{\rho_v}} \right)^n \tag{C7}$$

The terms in the square bracket of Eq. (C4) and (C7) are quite close to each other in the high quality region. However, the application of Eq. (C6) is limited because heat transfer data were correlated with the vapor Reynolds number alone inspite of the strong effect

of the liquid Reynolds number on heat transfer coefficients.

Equations of the same type with different constants and exponents are shown in Reference [16], [21], and [51]. Those equations should be verified with various data in a wide range of parameters.

Hilding and Coogan [33] reported that their attempt of using the Kutateladze [40] equation was not successful. The Kutateladze equation

$$\frac{hD}{\kappa} = C\,Pr^{a}\left(\frac{g_o D}{V_g^2}\right)^{b}\left(\frac{h_{fg}}{C_p \Delta T}\right)^{c}\left(\frac{f_i U_v^2 \rho_v}{g_o D \rho_g}\right)^{d} \tag{C8}$$

has liquid and vapor velocity terms explicitly. Hilding and Coogan's empirical correlation is the following:

$$\frac{h\Delta T}{\rho_v U_v \delta g_o} = 1.186\times10^{7}\left[\left(\frac{\mu_v}{\rho_v U_v D}\right)^{0.887}\left(\frac{\rho_g U_g \delta}{\mu_g}\right)^{0.374}\left(\frac{U_v}{U_g}\right)^{0.167}\left(\frac{D}{\delta}\right)^{1.446}\right] \tag{C9}$$

The above equation was reported to indicate that the tube diameter and vapor velocities play a stronger role in determining the rate of heat transfer than does the mean thickness of the annular liquid layer. The equation itself is not easily applicable because the relationship between given conditions and film thickness is difficult to calculate.

C.2 Semi-Empirical Correlations of Carpenter-Colburn

Carpenter and Colburn [17] assumed that the entire thermal resistance was offered by the laminar sublayer after sufficient condensate had been formed to produce turbulence.

As a resulting relationship for this laminar layer,

$$h_g = C\,Pr^{n}\,\frac{\kappa}{\nu}\sqrt{\frac{g_o \tau_o}{\rho_g}} \tag{C10}$$

This equation can be written as follows:

$$\frac{h_g}{\rho_g C_p U_\tau} = C\,Pr^{n-1} \tag{C11}$$

where

$$v_\tau = \sqrt{\frac{g_o \tau_o}{\rho_\ell}}$$

This equation has two main drawbacks:

1. Since only the resistance of the laminar layer is considered, it should result in greater than experimental heat transfer coefficients at the low vapor qualities.
2. For the high vapor quality region where film thickness is very small (liquid Reynolds number is less than around 120), Eq. (C10) itself predicts lower values unless it is modified.
3. There is no explicit Reynolds number effect. That is, for the same thickness of laminar sublayer, change in the upper layer flow produces different heat transfer rates. (Fig C-2)

With these inherent drawbacks, the constant and exponent of the Prandtl number were changed by later investigators [3], [61]. Also the shear stress term was modified. Even though the original investigators defined the shear stress τ_o as shear force acting on the unit surface area at the outer boundary of the laminar layer, τ_o should be interpreted as the wall shear stress. In single-phase studies of laminar sublayer boundary, y^+ is constant where the laminar and turbulent relations intersect and y^+ was non-dimensionalized by the wall shear stress τ_o. The same arguments were introduced in the Carpenter-Colburn analysis of the condensate flow.

Altman et. al. [3] calculated the shear force as follows:

$$\tau_o = \left(\frac{dP}{dz}\right)\frac{D}{4} \qquad \text{(C12)}$$

where (dP/dz) is the total static pressure gradient. Considering the momentum balance in a tube as in Eq. (D1) of Appendix D, it is clear that τ_o should be considered as

$$\tau_o = \left(\frac{dP}{dz}\right)_f \frac{D}{4}$$

instead of Eq. (C12).

Soliman et. al. [61] derived τ_o from the momentum balance equation. Lockhart-Martinelli's [44] results for isothermal two-phase flow were applied to the calculation of τ_v. Because of the effect of radial flow at the interface due to condensation, τ_v is not equal in isothermal flow and in non-isothermal flow with condensation [43], [60], and [67]. In terms of friction factor τ_v is

$$\tau_v = f_i^* \frac{\rho_v (U_v - U_i)^2}{2 g_o} \tag{C13}$$

where f_i^* is the friction factor for condensation at the interface. f_i^* may be divided into three terms.

$$f_i^* = (f_i)_{iso} + (f_i)_g + (f_i)_m$$

where $(f_i)_{iso}$ is the friction factor of isothermal horizontal flow, $(f_i)_g$ is the gravity effect on the friction factor and $(f_i)_m$ is the effect of momentum change on the friction factor. It is expected that $(f_i)_g$ and $(f_i)_m$ may be negligible compared with $(f_i)_{iso}$, but it has not yet been verified.

In the present analysis, Lockhart-Martinelli's results were used in the calculation of τ_c. The above argument is also applied to the calculation of τ_o; however, the effect of cross flow by condensation

is expected to be smaller at the wall than at the interface. Martinelli-Nelson [46] correlated data for isothermal flow and flow with boiling without distinguishing this effect and got a good result. That is, the effect of boiling or condensation on the friction factor may be negligible except in some extreme cases.

It is noticed that the momentum term and gravity term in the force balance equation (Eq. D1) should not be considered as the effect of momentum change and gravity on the wall shear stress as was done in the previous references.

Kunz and Yerazunis [39] modified Nikuradze's equation of mixing length for condensate flow as follows:

$$\frac{\epsilon_m}{\nu} = \frac{\left[0.14 - 0.08\left(\frac{\tau}{\tau_o}\right)^2 - 0.06\left(\frac{\tau}{\tau_o}\right)^4\right]^2}{\left(1 - \frac{\tau}{\tau_o}\right)^2} (y^+)^2 \left(1 - e^{-\frac{y^+}{A^+}}\right)^2 \frac{du^+}{dy^+}$$

where A^+ is the Van Driest turbulent damping constant. And

$$E = 1.5 \exp\left[\frac{-0.09}{\{\epsilon_m/(K\rho_\ell C_p)\}^{0.64}}\right]$$

was used to derive heat transfer coefficients. The results were present in the liquid Reynolds number versus Stanton number plot as shown in Fig. C-2. Since the effect of variations of D^+, gravitational force, and momentum pressure gradient terms were neglected, the discrepancy is significant when liquid Reynolds number is larger than 1000.

Not all the references are discussed here.

APPENDIX D

Local Pressure Gradients

The following postulates are made as in the analysis of isothermal two-phase flow [44]:

1. Static pressure drop for the liquid must equal the static pressure drop for the vapor phase regardless of the flow pattern, as long as an appreciable radial static pressure difference does not exist.
2. The volume occupied by the liquid plus the volume occupied by the gas at any instant must equal the volume of the pipe.

With the above assumptions, consider a cross element of a tube shown in Fig. D-1 as a control volume.

$$-\left(\frac{dP}{dz}\right)A - \tau_o S + A\,\frac{a}{g_o}[\alpha\rho_v + (1-\alpha)\rho_\ell\,] = \frac{1}{g_o}\frac{d}{dz}(U_v W_v + U_\ell W_\ell) \quad \text{(D1)}$$

where a is external acceleration force field. Rearranging Eq. (D1) yields

$$-\left(\frac{dP}{dz}\right) = \tau_o\,\frac{S}{A} - \frac{a}{g_o}[\alpha\rho_v + (1-\alpha)\rho_\ell\,] + \frac{1}{g_o A}\frac{d}{dz}(U_v W_v + U_\ell W_\ell) \quad \text{(D2)}$$

The above equation shows that total static pressure gradient is the sum of pressure gradients due to friction, gravity and momentum change.

$$\left(\frac{dP}{dz}\right) = \left(\frac{dP}{dz}\right)_f + \left(\frac{dP}{dz}\right)_g + \left(\frac{dP}{dz}\right)_m \quad \text{(D3)}$$

Comparing Eq. (D2) and (D3).

$$\left(\frac{dP}{dz}\right)_f = -\tau_o\,\frac{S}{A} \quad \text{(D4)}$$

$$\left(\frac{dP}{dz}\right)_g = \frac{a}{g_o}\,[\,\alpha\rho_v + (1-\alpha)\,\rho_\ell\,] \quad \text{(D5)}$$

$$\left(\frac{dP}{dz}\right)_m = -\frac{1}{g_o A}\frac{d}{dz}\left(U_v W_v + U_\ell W_\ell\right) \tag{D6}$$

D.1 Evaluation of Pressure Gradients

Friction Assuming that the pressure drop due to friction does not change by condensation, the correlation of isothermal data will be used directly. The same assumption was made in Reference [46] and resulted in a good agreement with boiling data.

$$\left(\frac{dP}{dz}\right)_f = \left(\frac{dP}{dz}\right)_{TPF} \tag{D7}$$

where $(dP/dz)_{TPF}$ is the pressure gradient due to friction for isothermal two-phase flow. The Lockhart-Martinelli [44] method seemed to be regarded as the best available to predict the friction pressure drop. The correlation of Reference [44] in the present notation is

$$\left(\frac{dP}{dz}\right)_{TPF} = \phi_v^2 \left(\frac{dP}{dz}\right)_v \tag{D8}$$

where

$$\phi_v = f(X_{tt})$$

$$X_{tt} = \frac{\left(\frac{dP}{dz}\right)_\ell}{\left(\frac{dP}{dz}\right)_v}$$

According to Reference [44], the pressure drop in vapor flow and parameter ϕ_v are given as follows:

$$X_{tt} = \left(\frac{\mu_\ell}{\mu_v}\right)^{0.1} \left(\frac{W_\ell}{W_v}\right)^{0.9} \left(\frac{\rho_v}{\rho_\ell}\right)^{0.5} \tag{D9}$$

$$\left(\frac{dP}{dz}\right)_v = -0.143 \frac{\mu_v^{0.2} W_v^{1.8}}{g_o \rho_v D^{4.8}} \tag{D10}$$

And the Lockhart-Martinelli data of ϕ_v were given in an approximate curve by Soliman et. al. [61] as follows:

$$\phi_v = 1 + 2.85 X_{tt}^{0.523} \tag{D11}$$

The agreement with data is within 5% for $X_{tt} < 1$ as shown in Fig. D-4. Combining Eq. (D7), (D8), (D9),(D10) and (D11) yields

$$\left(\frac{dP}{dz}\right)_f \frac{g_o D}{G^2/\rho_v} = -0.09 \left(\frac{GD}{\mu_v}\right)^{-0.2} \left[x^{1.8} + \right.$$

$$+ 5.7 \left(\frac{\mu_\ell}{\mu_v}\right)^{0.0523} (1-x)^{0.470} x^{1.33} \left(\frac{\rho_v}{\rho_\ell}\right)^{0.261}$$

$$\left. + 8.11 \left(\frac{\mu_\ell}{\mu_v}\right)^{0.105} (1-x)^{0.94} x^{0.86} \left(\frac{\rho_v}{\rho_\ell}\right)^{0.522} \right] \tag{D12}$$

Gravity

$$\left(\frac{dP}{dz}\right)_g = \frac{a}{g_o} [\alpha \rho_v + (1-\alpha) \rho_\ell] \tag{D5}$$

or

$$\left(\frac{dP}{dz}\right)_g = \frac{a}{g_o} [\rho_\ell - \alpha(\rho_\ell - \rho_v)] \tag{D13}$$

In the same form as Eq. (D12)

$$\left(\frac{dP}{dz}\right)_g \frac{g_o D}{G^2/\rho_v} = \frac{1}{Fr} \left[\left(\frac{\rho_\ell}{\rho_v}\right) + B\alpha \right] \tag{D14}$$

where

$$Fr = \frac{(G/\rho_v)^2}{a/D} \tag{D15}$$

is the Froude number based on the total flow rate and

$$B = \frac{\rho_\ell - \rho_v}{\rho_v} \tag{D16}$$

is the buoyancy modulus. In the gravity field

$$a = g \sin\theta \tag{D17}$$

where θ is the angle of inclination from the horizontal position.

The Zivi equation for local void fraction [71] is recommended to use in Eq. (D14) as done in Reference [61].

$$\alpha = \frac{1}{1 + \left(\frac{1-x}{x}\right)\left(\frac{\rho_v}{\rho_\ell}\right)^{2/3}} \tag{D18}$$

The discussion of local void fractions will be followed in Appendix E.

Momentum

$$\left(\frac{dP}{dz}\right)_m = -\frac{1}{g_o A}\frac{d}{dz}\left(\int \rho v^2 dA\right)$$

In order to avoid the complexity of evaluating local velocity, momentum changes will be estimated for the ideal annular flow. For one-dimensional flow models using average velocities in the liquid and in the vapor region

$$g_o\left(\frac{dP}{dz}\right)_m A = -\eta \frac{d}{dz}(UW)$$

where

$$\eta = \frac{\int v^2 dA}{\left(\int v\, dA\right)^2}$$

for a constant density.

Previous detailed investigations [43] show that in most cases of turbulent flow the value of η becomes unity. In the following it will be assumed $\eta = 1$.

The pressure drop due to momentum change during condensation may be separated into two terms: momentum change in the liquid film and in the vapor core.

$$\left(\frac{dP}{dz}\right)_m = \left(\frac{dP}{dz}\right)_{m\ell} + \left(\frac{dP}{dz}\right)_{mv} \tag{D19}$$

From Eq. (D2)

$$\left(\frac{dP}{dz}\right)_{mv} = -\frac{1}{g_o A}\frac{d}{dz}(V_v W_v) \tag{D20}$$

$$\left(\frac{dP}{dz}\right)_{m\ell} = -\frac{1}{g_o A}\frac{d}{dz}(V_\ell W_\ell) \tag{D21}$$

The average velocities of vapor and liquid at any location along the tube may be written in terms of the local vapor quality x and void fraction α as follows:

$$V_v = \frac{xW}{\rho_v \alpha A} \tag{D22}$$

$$V_\ell = \frac{(1-x)W}{\rho_\ell (1-\alpha) A} \tag{D23}$$

Substituting Eq. (D22) and (D23) into Eq.(D20) and (D21) respectively gives

$$\left(\frac{dP}{dz}\right)_{mv} = -\frac{1}{g_o A}\frac{W^2}{\rho_v A}\frac{d}{dz}\left(\frac{x^2}{\alpha}\right) \tag{D24}$$

$$\left(\frac{dP}{dz}\right)_{m\ell} = -\frac{1}{g_o A}\frac{W^2}{\rho_\ell A}\frac{d}{dz}\left[\frac{(1-x)^2}{1-\alpha}\right] \tag{D25}$$

And with Eq. (D18)

$$\left(\frac{dP}{dz}\right)_{mv} = -\frac{G^2}{g_o \rho_v}\frac{dx}{dz}\left[2x + (1-2x)\left(\frac{\rho_v}{\rho_\ell}\right)^{\frac{2}{3}}\right] \tag{D26}$$

$$\left(\frac{dP}{dz}\right)_{m\ell} = -\frac{G^2}{g_o D}\frac{dx}{dz}\left[2(x-1)\left(\frac{\rho_v}{\rho_\ell}\right) + (1-2x)\left(\frac{\rho_v}{\rho_\ell}\right)^{\frac{1}{3}}\right] \tag{D27}$$

Adding Eq. (D26) and (D27) results

$$\left(\frac{dP}{dz}\right)_m \frac{g_o D}{G^2/\rho_v} = -D\left(\frac{dx}{dz}\right)\left[2x + (1-2x)\left(\frac{\rho_v}{\rho_\ell}\right)^{\frac{1}{3}} + \right.$$

$$\left. + (1-2x)\left(\frac{\rho_v}{\rho_\ell}\right)^{\frac{2}{3}} + 2(1-x)\left(\frac{\rho_v}{\rho_\ell}\right)\right] \tag{D28}$$

D.2 Evaluation of F_o in Eq. (1)

Considering a liquid film element (Fig. D-2),

$$-\left(\frac{dP}{dz}\right)A_\ell + \tau_v S_v - \tau_o S + \frac{a}{g_o}\rho_\ell A_\ell = \frac{1}{g_o}\left[\frac{d}{dz}(U_\ell W_\ell) - U_i \frac{dW_\ell}{dz}\right] \tag{D29}$$

or

$$\tau_o S = -\left(\frac{dP}{dz}\right)A_\ell + \frac{a}{g_o}A_\ell \rho_\ell - \frac{1}{g_o}\frac{d}{dz}(U_\ell W_\ell) + \frac{1}{g_o}U_i \frac{dW_\ell}{dz} + \tau_v S_v \tag{D30}$$

Let

$$\tau_o = F_o \frac{A}{S} + \tau_v \frac{S_v}{S} \tag{D31}$$

where

$$F_o = -\frac{dP}{dz} + \frac{a}{g_o}\rho_\ell - \frac{1}{g_o A_\ell}\left[\frac{d}{dz}(U_\ell W_\ell) - U_i \frac{dW_\ell}{dz}\right] \tag{D32}$$

When condensation occurs on a flat plate. Eq. (D31) becomes:

$$\tau_o = F_o \delta + \tau_v \tag{D33}$$

The momentum term in Eq. (D32) will be calculated by the same method as used in the calculation of $(dP/dz)_m$.

$$(F_o)_m = -\frac{1}{g_o A_\ell}\left[\frac{d}{dz}(U_\ell W_\ell) - U_i \frac{dW_\ell}{dz}\right] \tag{D34}$$

The interfacial velocity U_i depends on the velocity distribution within the liquid layer and may be written in the following form

$$U_i = \beta U_\ell \tag{D35}$$

where β is a constant. From the universal velocity distribution β can be estimated as follows:

$$\beta = \frac{U_i}{U_\ell} = \frac{U_{y=\delta}}{\frac{1}{\delta}\int_0^\delta v\, dy} \tag{D36}$$

For $\delta^+ < 5$

$$\beta = 2 \tag{D37}$$

For $5 < \delta^+ < 30$

$$\beta = \frac{-3.05\delta^+ + 5\delta^+ \ln \delta^+}{12.5 - 8.05\delta^+ + 5\delta^+ \ln \delta^+} \tag{D38}$$

For $\delta^+ > 30$

$$\beta = \frac{5.5 + 2.5 \ln \delta^+}{-64 + 3\delta^+ + 2.5\delta^+ \ln \delta^+} \tag{D39}$$

Fig. D-5 shows that values of β decrease with increasing δ^+. Combining Eq. (D18), (D23), (D34) and (D35) yields

$$(F_o)_m = -\frac{G^2/\rho_v}{g_o D} D\left(\frac{dx}{dz}\right)\left[\frac{1}{1-\alpha}\left\{2(x-1)\left(\frac{\rho_v}{\rho_\ell}\right) + (1-2x)\left(\frac{\rho_v}{\rho_\ell}\right)^{\frac{1}{3}} + \frac{\beta(1-x)}{(1-\alpha)^2}\left(\frac{\rho_v}{\rho_\ell}\right)\right] \tag{D40}$$

Therefore

$$F_o = -\left(\frac{dP}{dz}\right) + \frac{a}{g_o}\rho_\ell - \frac{G^2/\rho_v}{g_o D}\left[D\left(\frac{dx}{dz}\right)\frac{1-2x}{1-\alpha}\left(\frac{\rho_v}{\rho_\ell}\right)^{\frac{1}{3}} + \left\{\frac{\beta(1-x)}{(1-\alpha)^2} - \frac{2(1-x)}{1-\alpha}\right\}\left(\frac{\rho_v}{\rho_\ell}\right)\right] \quad \text{(D41)}$$

D.3 Evaluation of τ_v in Eq. (1)

Considering an element of vapor core (Fig. D-3),

$$-\left(\frac{dP}{dz}\right)A_v - \tau_v S_v + \frac{a}{g_o}\rho_v A_v = \frac{1}{g_o}\frac{d}{dz}(U_v W_v) + U_i\frac{dW_v}{dz}$$

or

$$\tau_v S_v = -\frac{dP}{dz}A_v + \frac{a}{g_o}\rho_v A_v - \frac{1}{g_o}\frac{d}{dz}(U_v W_v) + U_i\frac{dW_v}{dz} \quad \text{(D42)}$$

Considering the curvature of the condenser tube wall, the term τ_v of Eq. (1) may be modified as $\tau_v \frac{S_v}{S}$. Then from Eq. (D42),

$$\tau_v = \left[-\frac{dP}{dz} + \frac{a}{g_o}\rho_v - \frac{1}{g_o A_v}\left\{\frac{d}{dz}(U_v W_v) + U_i\frac{dW_v}{dz}\right\}\right]\frac{A_v}{S}$$

Substituting Eq. (D18), (D22) and (D35) yields

$$\tau_v \frac{4}{\alpha D} = -\frac{dP}{dz} + \frac{a}{g_o}\rho_v - \frac{G^2/\rho_v}{g_o D} D\frac{dx}{dz}\left[2\frac{x}{\alpha} + \frac{1-2x}{\alpha}\left(\frac{\rho_v}{\rho_\ell}\right)^{\frac{2}{3}} + \frac{\beta(1-x)}{\alpha(1-\alpha)}\left(\frac{\rho_v}{\rho_\ell}\right)\right] \quad \text{(D43)}$$

APPENDIX E

Derivation of Heat Transfer Coefficient

It was thought that the condensate flow in a tube is quite different from the single-phase turbulent flow because of the strong effect of vapor shear stress at the interface of vapor and liquid. However, since the von Karman formulations of the universal velocity distribution are non-dimensionalized such that the distribution is affected by the force field of flow by using the friction velocity $v_\tau = \sqrt{g_o \tau_o / \rho_\ell}$, it is a reasonable assumption to apply the formulations to the condensate flow substituting actual τ_o of the flow. For flow of thin films with little interfacial shear ($\delta^+ < 30$ and $\tau_v = 0$), or for highly turbulent flow near the liquid-vapor interface ($\delta^+ > 30$ and $\tau_v >> 0$), this assumption is quite likely to be in error. But for the practical ranges of flow rates where the annular flow regime occurs, vapor shear stress τ_v is of the same order of magnitude as wall shear stress τ_o for thin films, i.e. the high quality region. With a no slip condition at the interface, the order of magnitude of τ_v/τ_o may be obtained from Eq. (D31) for the small change of momentum in the flow.

$$\frac{\tau_v}{\tau_o} \cong \sqrt{\alpha} \tag{E1}$$

For $\delta^+ < 30$, the void fraction α is larger than 0.95 for most fluids condensed in about 0.5 in I.D. tubes at mass velocities from 60,000 to 600,000 lbm/ft^2 hr, which is in the range of the present experiments. Therefore, practically $\tau_v/\tau_o = 1$ * and the universal velocity

---

* $\tau/\tau_o = 1$ is an assumption which is implicitly implied in von Karman's equation for the range of $\delta^+ < 5$ [26]

distribution of this range is quite adequate for the condensate flow. For the highly turbulent region of thick films ($\delta^+ > 30$), even though vapor shear is decreased as the film thickness is increased at the same conditions, the strong effect of vapor shear still remains and deviations may be expected in this region. However, realizing that the region of expected error is also a region of very small resistance to heat flow when compared to that of the buffer layer and the laminar sublayer, it is felt that deviations in this area will have but little effect on the predicted values of heat transfer coefficients for the entire film.

D.1 Laminar Sublayer ($0 < \delta^+ < 5$)

In this region the turbulent motion is very small compared to viscous motion.

$$\epsilon_m / \nu_\ell << 1, \qquad \epsilon_h << 1 \tag{E2}$$

From Eq. (3) of Chapter II

$$\frac{(q/A)}{\rho_\ell c_p} = \alpha \frac{dT}{dy} \tag{E3}$$

Integrating from 0 to δ,

$$\frac{q/A}{T_\delta - T_o} = \rho_\ell c_p \alpha_\ell \frac{1}{\delta} \tag{E4}$$

$$h_\ell = \rho_\ell c_p \alpha_\ell \frac{1}{\delta} \tag{E5}$$

Let

$$F_2 \equiv Pr\, \delta^+ \tag{22a}$$

$$h = \frac{\rho_\ell c_p}{F_2} \sqrt{\frac{g_o \tau_o}{\rho_\ell}} \tag{E6}$$

In a dimensionless form

$$h_z^* \equiv \frac{h}{\kappa}\left(\frac{\nu_\ell u_\ell}{g_o F_o}\right)^{1/3} \tag{19}$$

$$h_z^* = \frac{Pr}{F_2}\left(\frac{\delta^+}{M}\right)^{1/3} \tag{17}$$

where

$$M \equiv \frac{F_o \delta}{\tau_o} \tag{E7}$$

or from Eq. (1),

$$M = \frac{1}{1 + \frac{\tau_v}{F_o \delta}}$$

In a dimensionless form

$$M = \frac{1}{1 + \tau_v^* / \delta^*} \tag{18}$$

The Reynolds number can be obtained by substituting Eq. (14a) into Eq. (13).

$$Re_\ell = \frac{4}{\nu_\ell}\int_o^\delta v_z \, dy \tag{E8}$$

In a dimensionless form

$$Re_\ell = 4\int_o^{\delta^+} v_z^+ \, dy^+ \tag{E9}$$

or

$$Re_\ell = 2(\delta^+)^2 \tag{16a}$$

D.2 Buffer Layer ($5 < \delta^+ < 30$)

Both the turbulent and the viscous motion have an important effect in this region. However it is still valid to assume $\tau/\tau_o = 1$.

Substituting Eq. (14b) into Eq. (3) with $\tau/\tau_o = 1$,

$$\epsilon_m = \nu \left(\frac{y^+}{5} - 1 \right) \tag{E10}$$

Since $\epsilon_m/\epsilon_h = 1$ was assumed,

$$\epsilon_h = \nu \left(\frac{y^+}{5} - 1 \right) \tag{E11}$$

Substituting Eq. (E11) into Eq. (3) and integrating from $\delta^+ = 0$ to δ^+,

$$h_2 = \frac{q/A}{T_\delta - T_o} = \frac{\rho_\ell C_p}{F_2} \sqrt{\frac{g_o \tau_o}{\rho_\ell}} \tag{E12}$$

where

$$F_2 = 5 Pr + 5 \ln \left[1 + Pr \left(\frac{\delta^+}{5} - 1 \right) \right] \tag{22b}$$

And substituting Eq. (14b) into Eq. (E3),

$$Re_\ell = 4 \int_5^{\delta^+} (-3.05 + 5.0 \ln y^+) \, dy^+ + 50 \tag{E13}$$

$$Re_\ell = 50 - 32.2\delta^+ + 20\delta^+ \ln \delta^+ \tag{16b}$$

Without assuming $\tau/\tau_o = 1$, a quite complicated solution can be obtained for this region

From Eq. (1)

$$\frac{\tau}{\tau_o} = \frac{F_o}{\tau_o}(\delta - y) + \frac{\tau_v}{\tau_o} \tag{E14}$$

and

$$\epsilon_m = \frac{\nu}{5} \left[-5 + y^+ - \frac{M}{\delta^+} (y^+)^2 \right] = \epsilon_h \tag{E15}$$

Following the same procedure as before

$$F_2 = 5\,Pr + \frac{5}{\sqrt{1 + 20\,(1/Pr - 1)\frac{M}{\delta^+}}} \times$$

$$\times \ln \left[\frac{2M - 1 + \sqrt{1 + 20\left(\frac{1}{Pr} - 1\right)\frac{M}{\delta^+}}}{2M - 1 - \sqrt{1 + 20\left(\frac{1}{Pr} - 1\right)\frac{M}{\delta^+}}} \quad \frac{\frac{10}{\delta^+}M - 1 - \sqrt{1 + 20\left(\frac{1}{Pr} - 1\right)\frac{M}{\delta^+}}}{\frac{10}{\delta^+}M - 1 + \sqrt{1 + 20\left(\frac{1}{Pr} - 1\right)\frac{M}{\delta^+}}} \right]$$

Numerical values of Eq. (21c) and (E15) are not significantly different.

D.3 Turbulent layer ($\delta^+ > 30$)

The only significant motion is the turbulent motion in this region. $\varepsilon_m/\nu \gg 1$ and ν is neglected.

$$\epsilon_m = \frac{\tau_v}{\left(\frac{dv}{dy}\right)} \tag{E16}$$

Substituting Eq. (14c)

$$\epsilon_m = \frac{\nu}{2.5}\,\frac{\tau}{\tau_o}\,y^+ \tag{E17}$$

Because of the considerable thickness of the liquid film in this region, the assumption of uniform stress ($\tau/\tau_o = 1$) is no longer valid. Combining Eq. (1) and (E17),

$$\epsilon_m = \frac{\nu}{2.5}\left[y^+ - \frac{M}{\delta^+}(y^+)^2 \right] = \epsilon_h \tag{E18}$$

Substituting this into Eq. (3),

$$h_z = \frac{\rho_\ell C_P}{F_2}\sqrt{\frac{g_o \tau_o}{\rho_\ell}}$$

where

$$F_2 = 5Pr + 5\ln(1+5Pr) + \frac{2.5}{\sqrt{1+\frac{10}{Pr}\frac{M}{\delta^+}}} \times$$

$$\times \ln\left[\frac{2M-1+\sqrt{1+\frac{10}{Pr}\frac{M}{\delta^+}}}{2M-1-\sqrt{1+\frac{10}{Pr}\frac{M}{\delta^+}}} \quad \frac{\frac{60}{\delta^+}M-1-\sqrt{1+\frac{10}{Pr}\frac{M}{\delta^+}}}{\frac{60}{\delta^+}M-1+\sqrt{1+\frac{10}{Pr}\frac{M}{\delta^+}}}\right] \tag{22c}$$

and substituting Eq. (14c) into Eq. (E8),

$$Re_\ell = -256 + 12\delta^+ + 10\,\delta^+ \ln \delta^+ \tag{16c}$$

APPENDIX F

Discussion of Void Fraction

Void Fraction α is defined as follows:

$$\alpha = \frac{A_v}{A} \tag{F1}$$

For the annular flow model without entrainment of liquid into the vapor core, α becomes

$$\alpha = \left(1 - \frac{2\delta}{D}\right)^2 \tag{F2}$$

or

$$\alpha = \left(1 - 2\frac{\delta^+}{D^+}\right)^2 \tag{F3}$$

where δ^+ and D^+ are non-dimensionalized length by friction velocity $v_\tau = \sqrt{g_o \tau_c / \rho_\ell}$. Since τ_o may be obtained from Eq. (33) of Chapter II, the void fraction was already determined by assuming the velocity distribution in the liquid film. However, Zivi's correlation [71] was used in the calculation of momentum changes

$$\alpha = \frac{1}{1 + \frac{1-x}{x}\left(\frac{\rho_v}{\rho_\ell}\right)^{\frac{2}{3}}} \tag{38}$$

Although it seemed to be inconsistant in the theory to use other information for void fraction, it is suggested that Zivi's equation be used in the calculation of pressure gradients as in Reference [61]. Zivi's equation has been proved successful in correlating experimental data [6]. It is believed that the universal velocity distribution gives a good approximation of the eddy diffusivities for the condensate flow. But the velocity distribution itself is still to be proved. Comparison of Eq. (F3) and Eq. (38) is shown in Fig. F-1. The wall shear stress τ_o was obtained from Eq. (33) as follows:

$$\tau_o = \left(\frac{dP}{dz}\right)_f \frac{D}{4} \qquad \text{(F4)}$$

The small discrepancy between those two equations indicates that momentum changes of the flow have small effects on the total static pressure gradients.

APPENDIX G

List of Computer Programs

```
PAGE    1

// FOR
*IOCS(CARD,1132 PRINTER)
      REAL L(19),M
      DIMENSION X(19),DPF(19),DPM(19),DPG(19),DPT(19),TV(19),
     1REZ(19),HST(19),HZ(19),DST(30),REX(19,15),HSTT(19,15),
     2HV(19),RH(19),GX(19),AGX(19),BGX(19),XL(19),SH(19)
      DATA G,TSAT,D,DET/2.50E5,86.,0.0411,10./,
     1DST/0.5,0.7,0.9,2.,4.,6.,8.,10.,20.,30.,40.,50.,60.,
     280.,100./,AGX/19*0.001/
      K=1
      DO 1 I=1,19
1     GX(I)=-AGX(I)
      GO TO 4
2     DO 3 I=1,19
3     GX(I)=-BGX(I)
4     GR=4.17E8
C     GRAVITY FORCE
      A=0
      BT=1.25
C     PHYSICAL PROPERTIES OF FREON 22 (80F TO 120F)
C     VISCOSITY
      UL=0.673-(0.00135*TSAT)
      UV=0.028+((0.5*TSAT)/10000)
C     LIQUID CONDUCTIVITY
      RK=0.0699-((0.235*TSAT)/1000)
C     DENSITY,LATENT HEAT, SPECIFIC HEAT
      DL=86.056-(0.149*TSAT)
      IF(TSAT-100) 5,5,6
5     DV=(0.05*TSAT)-1.1115
      HFG=98.363-(0.255*TSAT)
      CP=0.255+((0.6*TSAT)/1000)
      GO TO 7
6     DV=(0.0665*TSAT)-2.6593
      HFG=101.6-(0.288*TSAT)
      CP=0.24+((0.75*TSAT)/1000)
7     RVS=UL/UV
      RDE=DV/DL
C     LOCAL PRESSURE GRADIENTS
      DO 21 I=1,19
      XL(I)=0.05*I
      X(I)=1-XL(I)
      A1=G*G/(GR*DV*D)
      A2=0.09*((UV/(G*D))**0.2)
      A3=X(I)**1.8
      A4=5.7*(RVS**0.0523)*(XL(I)**0.47)*(X(I)**1.33)
     1*(RDE**0.261)
      A5=8.11*(RVS**0.105)*(XL(I)**0.94)*(X(I)**0.86)
     1*(RDE**0.522)
      DPF(I)=-(A1*A2*(A3+A4+A5))
```

PAGE 2

```
      B1=2*X(I)
      B2=(1-2*X(I))*(RDE**0.333)
      B3=(1-2*X(I))*(RDE**0.667)
      B4=2*XL(I)*RDE
      DPM(I)=-(A1*GX(I)*(B1+B2+B3+B4))
      V=(XL(I)*(RDE**0.667))/X(I)
      R=1/(1+V)
      DPG(I)=((R*DV)+((1-R)*DL))*(A/GR)
      DPT(I)=DPF(I)+DPM(I)+DPG(I)
      G1=(1-2*X(I))*(RDE**0.333)/(1-R)
      G2=BT*XL(I)*RDE/((1-R)*(1-R))
      G3=-2*XL(I)*RDE/(1-R)
      FO=-DPT(I)+((A/GR)*DL)-(A1*GX(I)*(G1+G2+G3))
      E1=2*X(I)/R
      E2=(1-2*X(I))*(RDE**0.667)/R
      E3=BT*XL(I)*RDE/(R*(1-R))
      T1=((A/GR)*DV)-DPT(I)-(A1*GX(I)*(E1+E2+E3))
      TV(I)=T1*R*D/4
      COR=((UL*UL)/(GR*DL*FO))**0.333
      TVST=TV(I)/(FO*COR)
      REZ(I)=G*D*XL(I)/UL
C     LOCAL HEAT TRANSFER COEFFICIENTS
      PR=UL*CP/RK
      J=0
8     J=J+1
      DP=DST(J)*SQRT(DST(J)+TVST)
      M=DST(J)/(DST(J)+TVST)
      IF(DP-5) 12,12,9
9     IF(DP-30) 11,11,10
10    C1=SQRT(1+(10*M/(PR*DP)))
      C2=2*M-1+C1
      C3=2*M-1-C1
      C4=(60/DP)*M-1-C1
      C5=(60/DP)*M-1+C1
      F2=5*PR+5*ALOG(1+5*PR)+(2.5/C1)*ALOG((C2*C4)/(C3*C5))
      REX(I,J)=-256+12*DP+10*DP*ALOG(DP)
      GO TO 13
11    F2=5*PR+5*ALOG(1+PR*((DP/5)-1))
      REX(I,J)=50-32.2*DP+20*DP*ALOG(DP)
      GO TO 13
12    F2=PR*DP
      REX(I,J)=2*DP*DP
13    HSTT(I,J)=PR*((DP/M)**0.333)/F2
      IF(REX(I,J)-REZ(I)) 14,15,15
14    IF(J-14) 8,15,15
15    JR=J
      IF(JR-1) 16,16,17
16    HST(I)=HSTT(I,JR)
      GO TO 18
```

```
PAGE   3

17      JQ=JR-1
        D1=HSTT(I,JR)-HSTT(I,JQ)
        D2=REX(I,JR)-REX(I,JQ)
        D3=REZ(I)-REX(I,JQ)
        HST(I)=HSTT(I,JQ)+((D1*D3)/D2)
18      HZ(I)=(HST(I)*RK)/COR
        L(I)=0.05*HFG*G*D/(4*HZ(I)*DET)
        RGX(I)=0.025*D/L(I)
        IF(I-1) 19,19,20
19      HM(I)=HZ(I)
        SH(I)=1/HZ(I)
        GO TO 21
20      IR=I-1
        RH(I)=1/HZ(I)
        SH(I)=RH(I)+SH(IR)
        HM(I)=I/SH(I)
21      CONTINUE
        WRITE(3,22) TSAT,G,D,DET
22      FORMAT(1H1,5X'FREON 22 AT ',F5.1,5X'G= ',F9.1,5X'D= ',
       1F6.4,5X'DET= ',F4.1//2X'THERMAL AND PHYSICAL
       2 PROPERTIES'/)
        WRITE(3,23) UV,UL
23      FORMAT(5X'VAPOR VISCOSITY',F8.4,5X'LIQUID VISCOSITY',
       1F7.3/)
        WRITE(3,24) DV,DL
24      FORMAT(5X'VAPOR DENSITY',F10.4,5X'LIQUID DENSITY',F9.3/)
        WRITE(3,25) RK,CP,HFG,PR
25      FORMAT(5X'CONDUCTIVITY',F8.4,3X'SPECIFIC HEAT',F7.3,
       13X'LATENT HEAT',F8.3,3X'PR',F6.2//2X'X',5X'DPF',
       211X'DPM',6X'DPT',9X'TV',9X'REZ',9X'HST',6X'HZ',
       37X'HM',8X'L'/)
        WRITE(3,26) (X(I),DPF(I),DPM(I),DPT(I),TV(I),
       1REZ(I),HST(I),HZ(I),HM(I),L(I),I=1,19)
26      FORMAT(19(F4.2,F9.3,E14.3,F9.3,E12.3,E14.5,F8.3,
       12F9.1,E14.5/))
        IF(K-1) 27,27,28
27      K=K+1
        GO TO 2
28      CONTINUE
        CALL EXIT
        END
```

Appendix H

Sample Calculation

Given conditions

$G = 250{,}000 \quad lbm/ft^2\ hr$

$T_{sat} = 86°F$

$T_o = 76°F$

physical properties (from Du Pont Table of F-22)

Viscosity	$\mu_\ell = 0.557$	lbm/hr ft
	$\mu_v = 0.0322$	lbm/hr ft
Conductivity	$K_\ell = 0.0495$	Btu/hr ft°F
Specific heat	$C_p = 0.305$	Btu/lbm °F
Latent heat	$h_{fg} = 76.470$	Btu/lbm
Density	$\rho_\ell = 73.278$	lbm/ft^3
	$\rho_v = 3.1622$	lbm/ft^3

$Pr = 3.43$

$D = 0.493$ in

Assuming that complete condensation occurs in the tube, the quality change is divided into 20 steps. A sample calculation will be done for the quality change from 72.5% to 67.5%. The local heat transfer coefficient at x = 0.7 will be considered as the average value in this quality change. The calculation procedure is outlined in Sect. 2.5.

Eq. (33)

$$-\left(\frac{dP}{dz}\right)_f = \frac{(250{,}000)^2/3.1622}{4.17 \times 10^8 \times (0.493/12)} \times 0.09 \times \left(\frac{250{,}000 \times 0.493}{0.0322 \times 12}\right)^{-0.2} \times$$

$$\times \left[0.7^{1.8} + 5.7\left(\frac{0.557}{0.0322}\right)^{0.0523} (1-0.7)^{0.47}\ 0.7^{1.33}\left(\frac{3.162}{73.278}\right)^{0.261}\right.$$

$$+ 8.11 \left(\frac{0.557}{0.0322}\right)^{0.0523} (1-0.7)^{0.94} \; 0.7^{0.86} \left(\frac{3.162}{73.278}\right)^{0.522} \Bigg]$$

$$\left(\frac{dP}{dz}\right)_f = -16.849 \quad \text{lbf/ft}^2\text{/ft}$$

Taking -0.001 as the first trial value of $D\left(\frac{dx}{dz}\right)$

Eq. (34)

$$\left(\frac{dP}{dz}\right)_m = \frac{(250{,}000)^2/3.1622}{4.17 \times 10^8 \times (0.493/12)} \times 0.001 \times \Big[2 \times 0.7$$

$$+(1 - 2 \times 0.7) \left(\frac{3.162}{73.278}\right)^{1/3} + (1 - 2 \times 0.7) \left(\frac{3.162}{73.278}\right)^{2/3}$$

$$+2(1 - 0.7) \left(\frac{3.162}{73.278}\right) \Big]$$

$$\left(\frac{dP}{dz}\right)_m = 1.41 \quad \text{lbf/ft}^2\text{/ft}$$

For a horizontal tube $\left(\frac{dP}{dz}\right)_g = 0$

Eq. (32)

$$\frac{dP}{dz} = -16.849 + 1.41 = -15.44 \quad \text{lbf/ft}^2\text{/ft}$$

Eq. (38)

$$\alpha = \frac{1}{1 + \frac{1 - 0.7}{0.7} \left(\frac{3.162}{73.278}\right)^{2/3}}$$

$$= 0.95$$

Eq. (39)

$$F_o = 15.44 + \frac{(250{,}000)^2/3.162}{4.17 \times 10^8 \times (0.493/12)} \times 0.001 \times$$

$$\times\left[\frac{1-1.4}{1-0.95}\left(\frac{3.162}{73.278}\right)^{1/3}+\left\{\frac{1.25(1-0.7)}{(1-0.95)^2}-\frac{2(1-0.7)}{1-0.95}\right\}\left(\frac{3.162}{73.278}\right)\right]$$

$$F_o = 18.5 \quad \text{lbf/ft}^2/\text{ft}$$

Eq. (40)

$$\tau_v = \frac{0.95 \times 0.493}{4 \times 12}\left[15.44+\frac{(250{,}000)^2/3.162}{4.17 \times 10^8 \times (0.493/12)} \times 0.001 \times\right.$$

$$\left.\times\left\{\frac{2 \times 0.7}{0.95}+\frac{1-1.4}{0.95}\left(\frac{3.162}{73.278}\right)^{2/3}+\frac{1.25(1-0.7)}{0.95(1-0.95)}\left(\frac{3.162}{73.278}\right)\right\}\right]$$

$$\tau_v = 0.17 \quad \text{lbf/ft}^2$$

Eq. (20)

$$\left(\frac{\mu_\ell \nu_\ell}{g_o F_o}\right)^{1/3} = \left(\frac{0.557^2/73.278}{4.17 \times 10^8 \times 18.5}\right)^{1/3} = 0.819 \times 10^{-4}$$

$$\tau_v^* = \frac{0.17}{18.5} \times \frac{1}{0.819 \times 10^{-4}}$$

$$= 112.3$$

Eq. (5) and (9)

$$Re_\ell = \frac{250{,}000 \times 0.7 \times 0.493}{0.557 \times 12}$$

$$= 55{,}350$$

Eq. (16)

$$55{,}350 = -256 + 12\delta^+ + 10\delta^+ \ln\delta^+$$

By a trial and error calculation $\delta^+ = 716$

Eq. (23)

$$716 = \delta^* \sqrt{\delta^* + 112.3}$$

Again by a trial and error calculation $\delta^* = 55.2$

Eq. (18)

$$M = \frac{1}{1 + (112.3/55.2)}$$

$$= 0.33$$

Eq. (22c)

$$1 + \frac{10 \times 0.33}{3.43 \times 716} \doteq 1$$

$$F_2 = 5 \times 3.43 + 5 \ln(1 + 5 \times 3.43)$$

$$+2.5 \ln\left[\frac{(2 \times 0.33)}{(2 \times 0.33) - 2} \; \frac{(60 \times 0.33/716) - 2}{(60 \times 0.33/716)}\right]$$

$$= 40.6$$

Eq. (17)

$$h_z^* = \frac{3.43}{40.6} \left(\frac{716}{0.33}\right)^{1/2}$$

$$= 1.09$$

Eq. (19)

$$h_z = \frac{1.09 \times 0.0495}{0.819 \times 10^{-4}}$$

$$= 662 \quad \text{Btu/hr ft}^2 \text{ °F}$$

$$\Delta T = T_{sat} - T_o = 86 - 76 = 10 \quad \text{°F}$$

$$D\left(\frac{\Delta x}{\Delta z}\right) = \frac{4 \times 662 \times 10}{76.470 \times 250{,}000}$$

$$= 0.00139$$

Comparing with the initial trial value, 0.001, $\left(\frac{dP}{dz}\right)_m$ should be re-calculated with $D\left(\frac{\Delta x}{\Delta z}\right) = 0.00139$. Following the same procedure gives

$$h_z = 673$$

And again

$$D\left(\frac{\Delta x}{\Delta z}\right) = \frac{4 \times 673 \times 10}{76.470 \times 250{,}000}$$

$$= 0.00141$$

Comparing with the second trial value 0.00139, no further iteration is necessary. The final results are as follows:

$$h_z = 673$$

$$\Delta z = \frac{0.05 \times 0.493}{0.00141 \times 12}$$

$$= 1.46 \text{ ft}$$

where Δz is the condensation length for the vapor quality change from 72.5% to 67.5%.

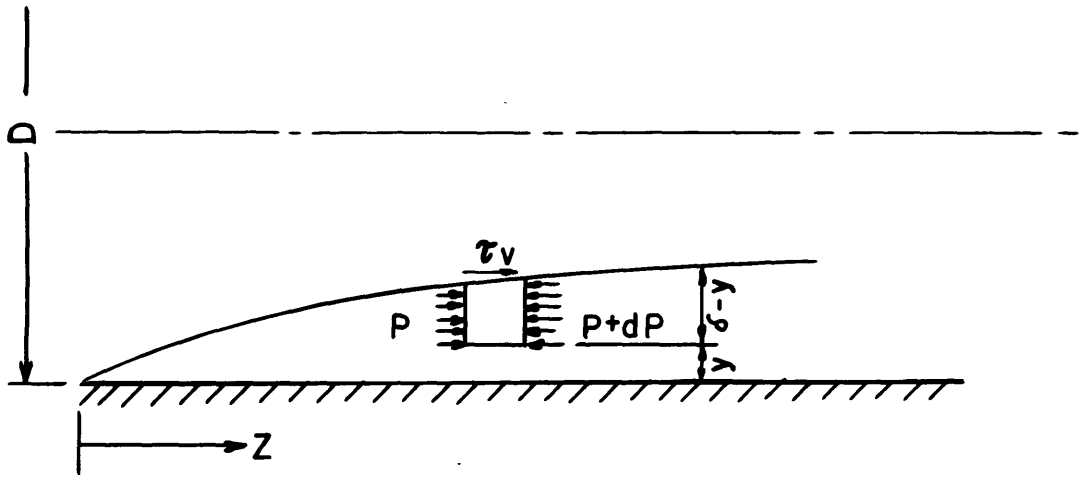

FIGURE 1 ELEMENTAL VOLUME IN CONDENSATE FILM

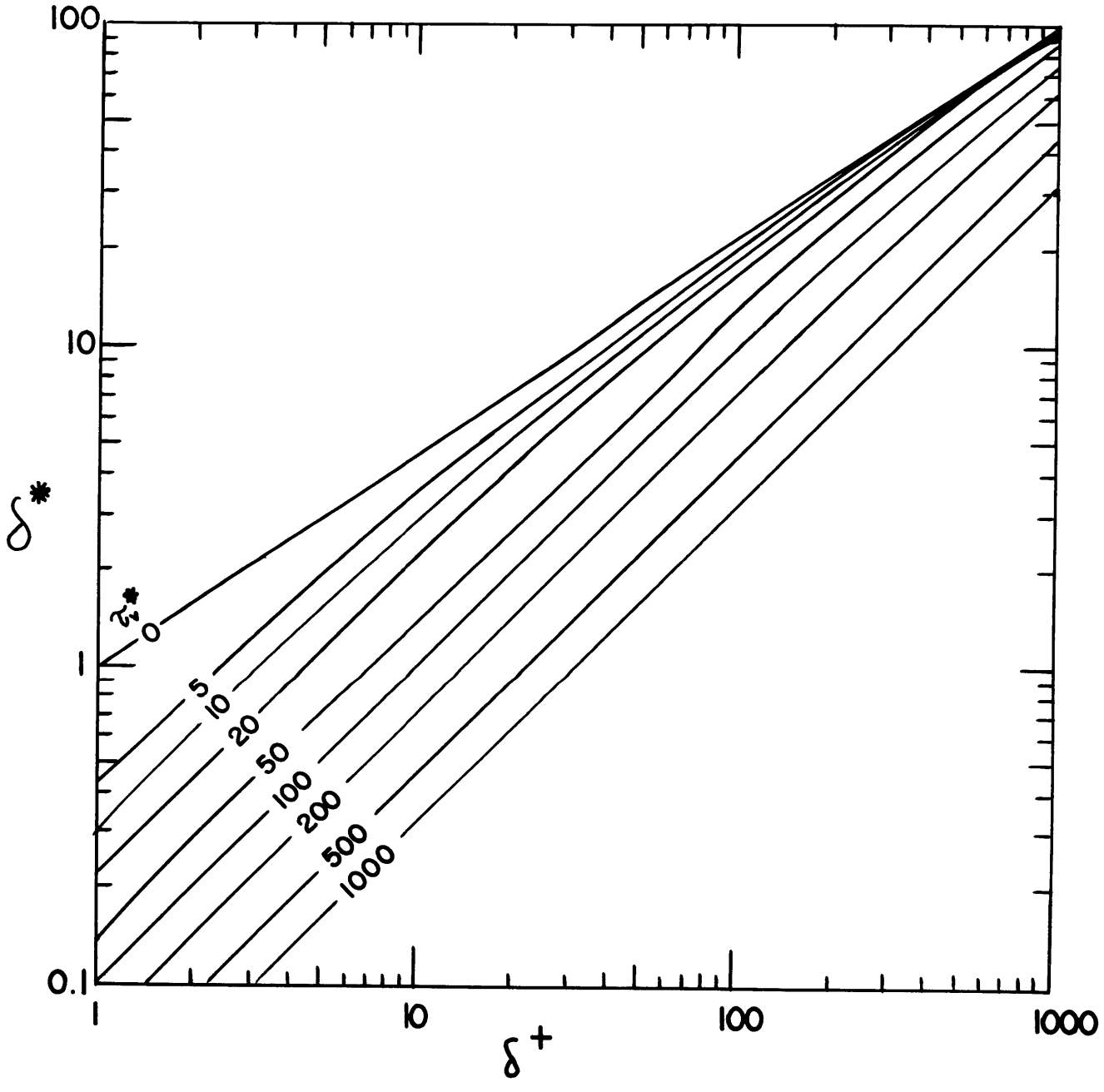

FIGURE 2 δ^* vs. δ^+ FOR VALUES OF $\tau_v{}^*$

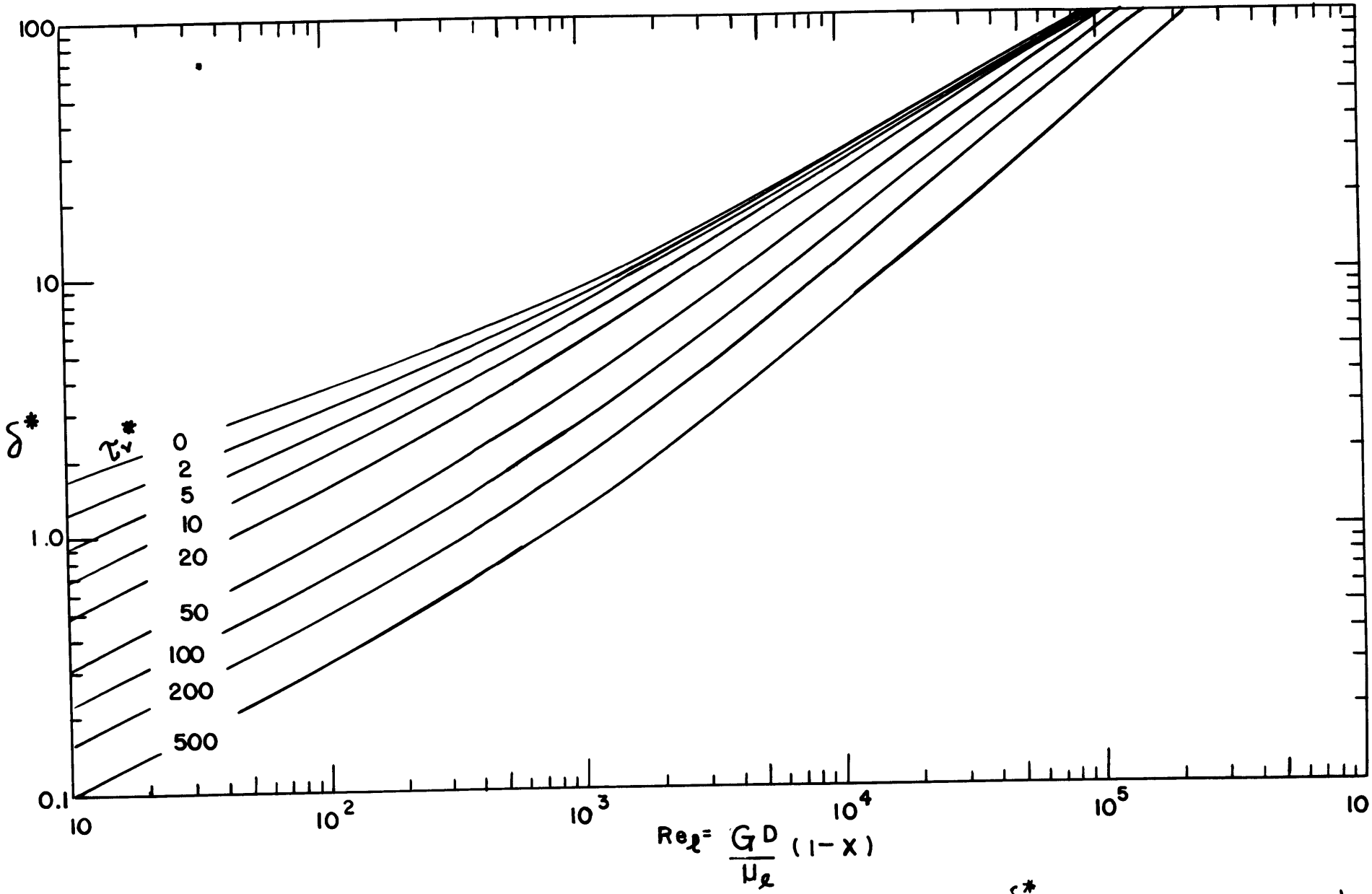

FIGURE 3 DIMENSIONLESS FILM THICKNESS δ^* FOR VALUES OF τ_v^*

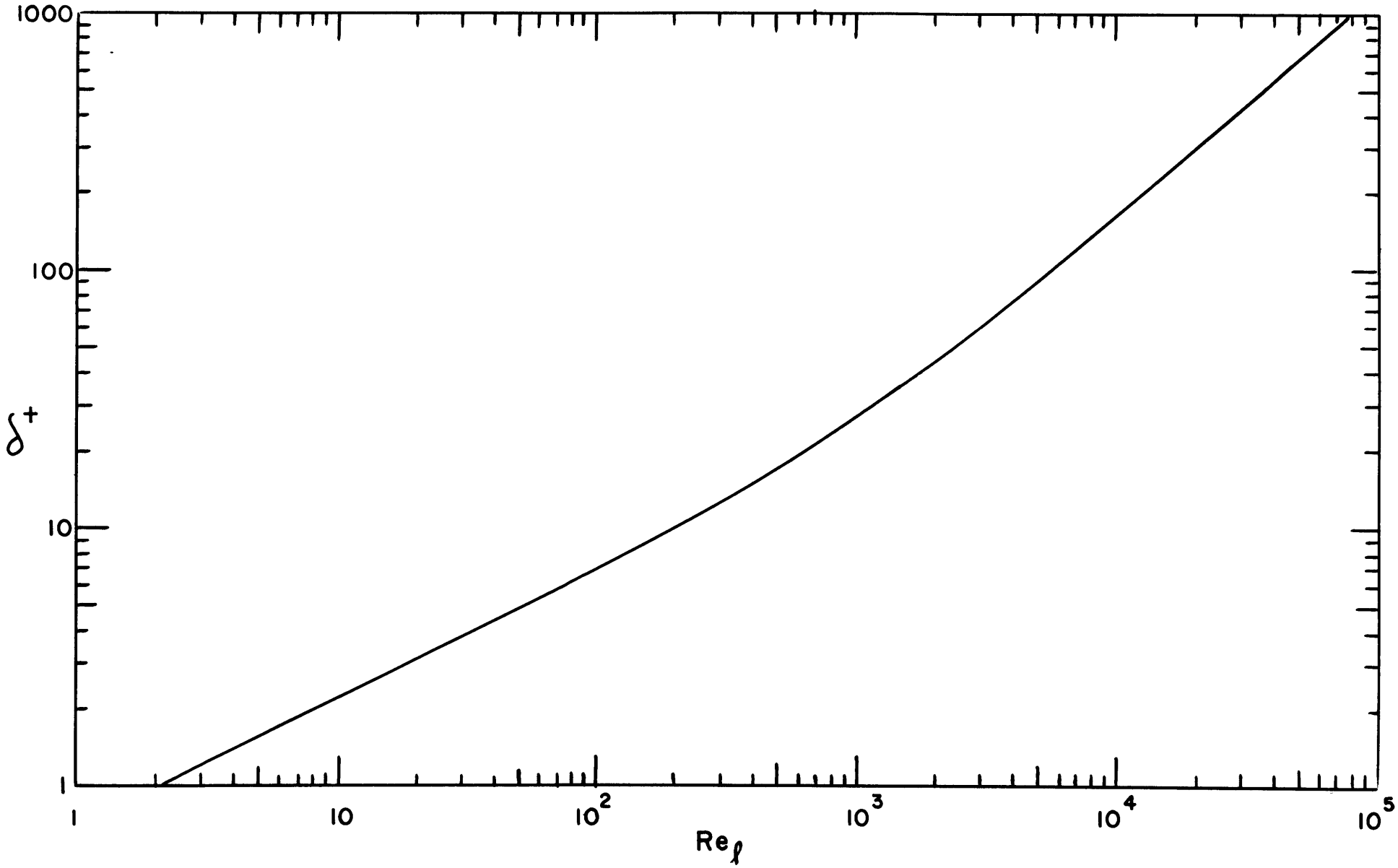

FIGURE 4 DIMENSIONLESS FILM THICKNESS δ^+

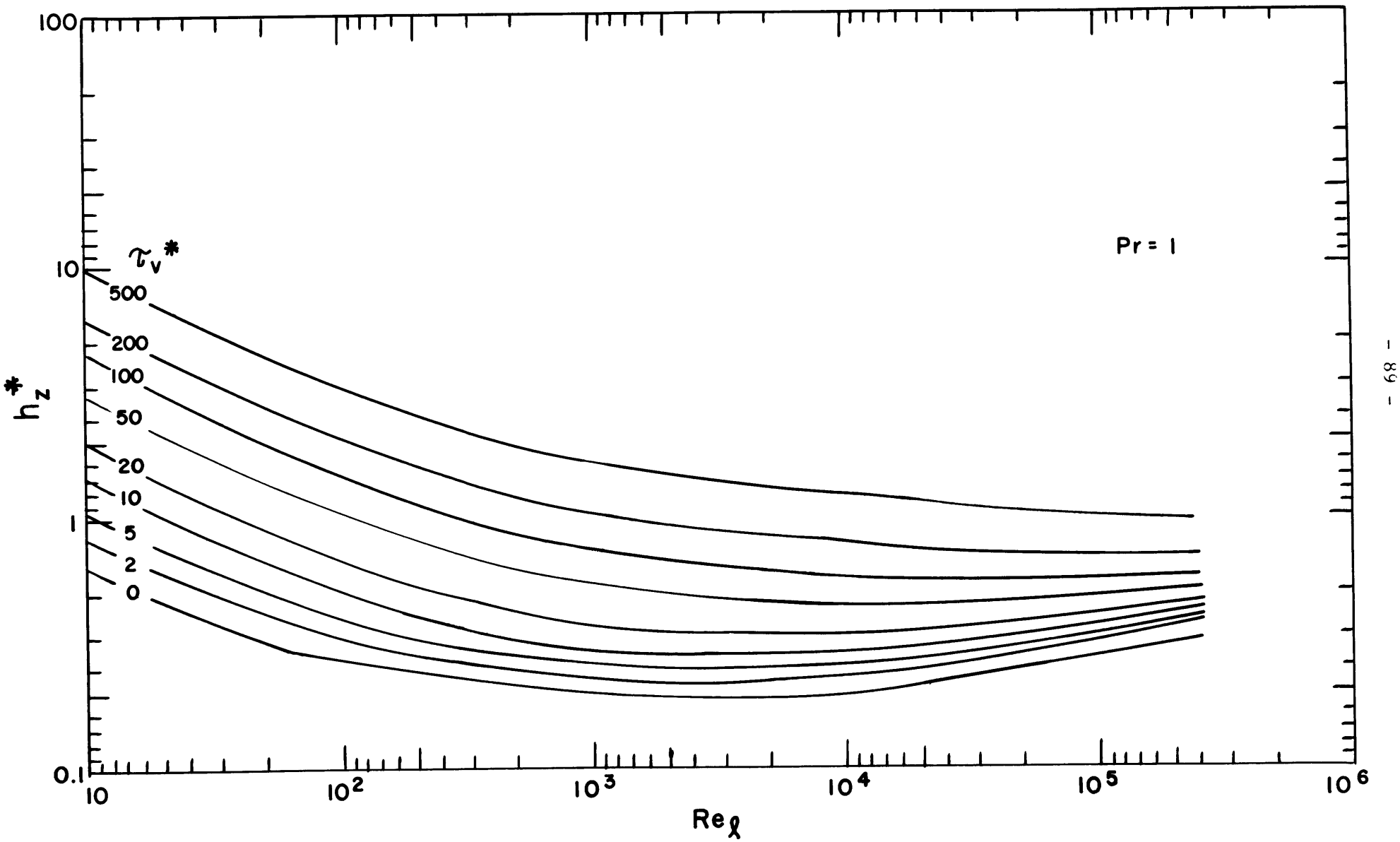

FIGURE 5 DIMENSIONLESS LOCAL HEAT TRANSFER COEFFICIENTS (Pr=1)

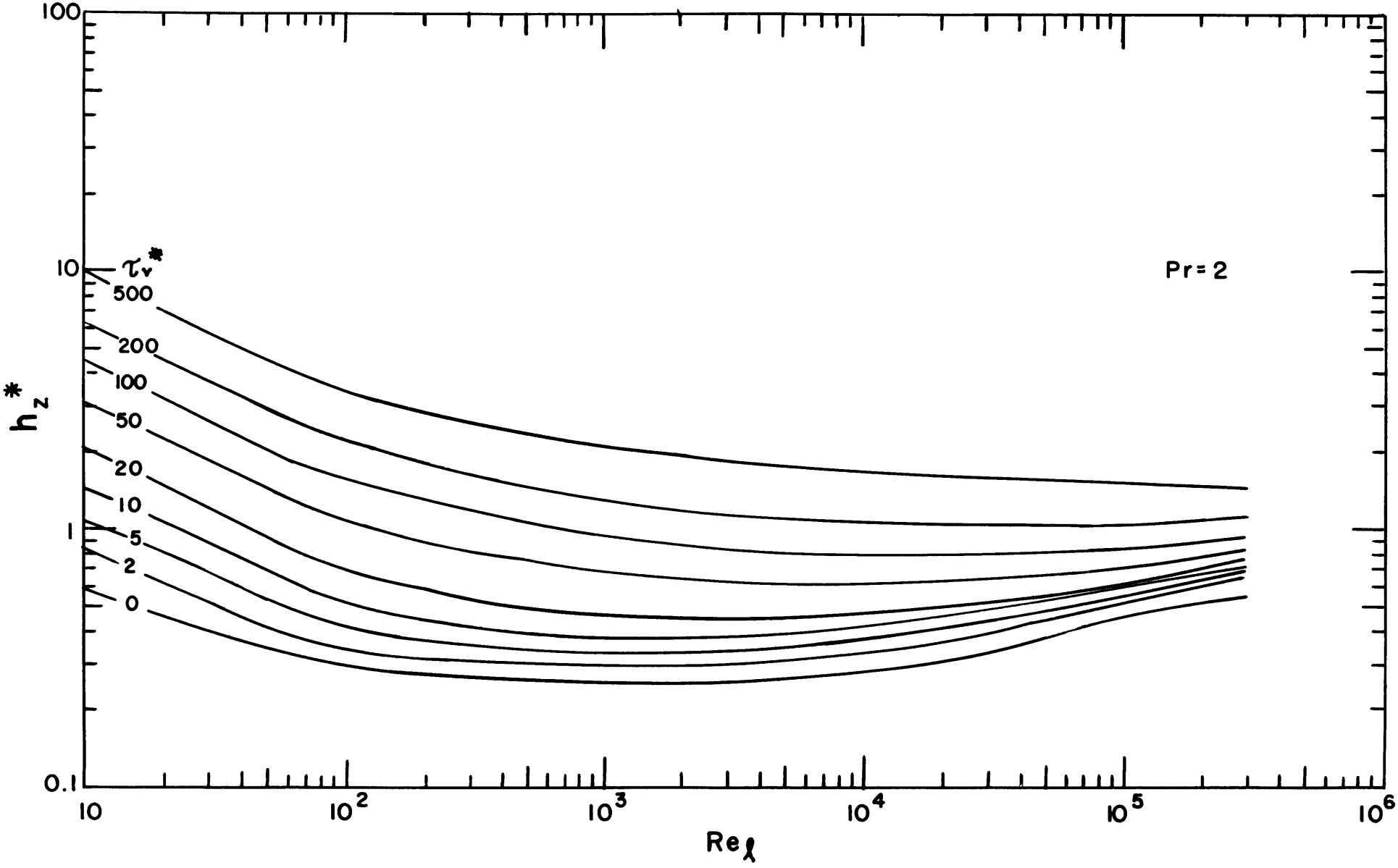

FIGURE 6 DIMENSIONLESS LOCAL HEAT TRANSFER COEFFICIENTS (Pr=2)

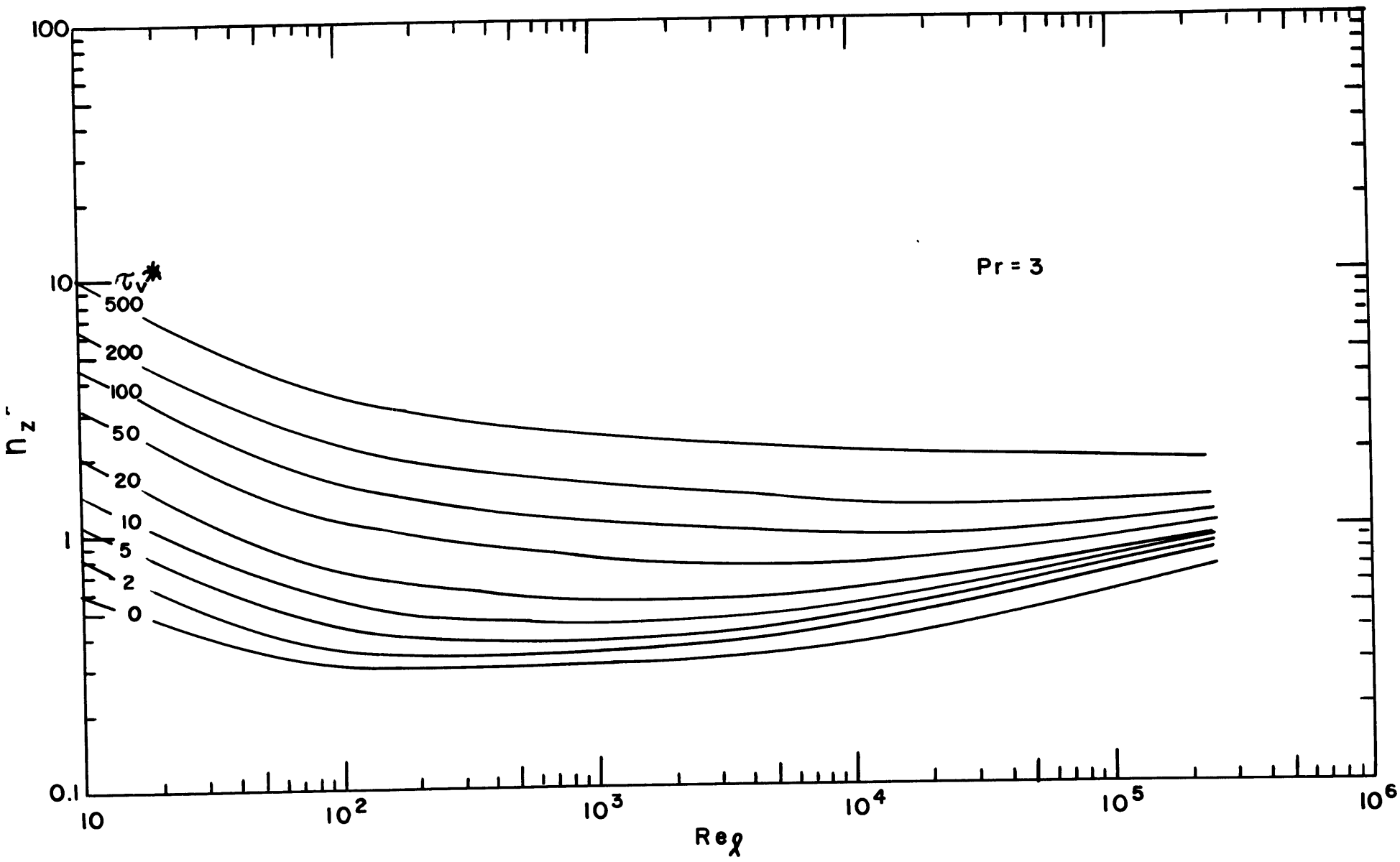

FIGURE 7 DIMENSIONLESS LOCAL HEAT TRANSFER COEFFICIENTS (Pr=3)

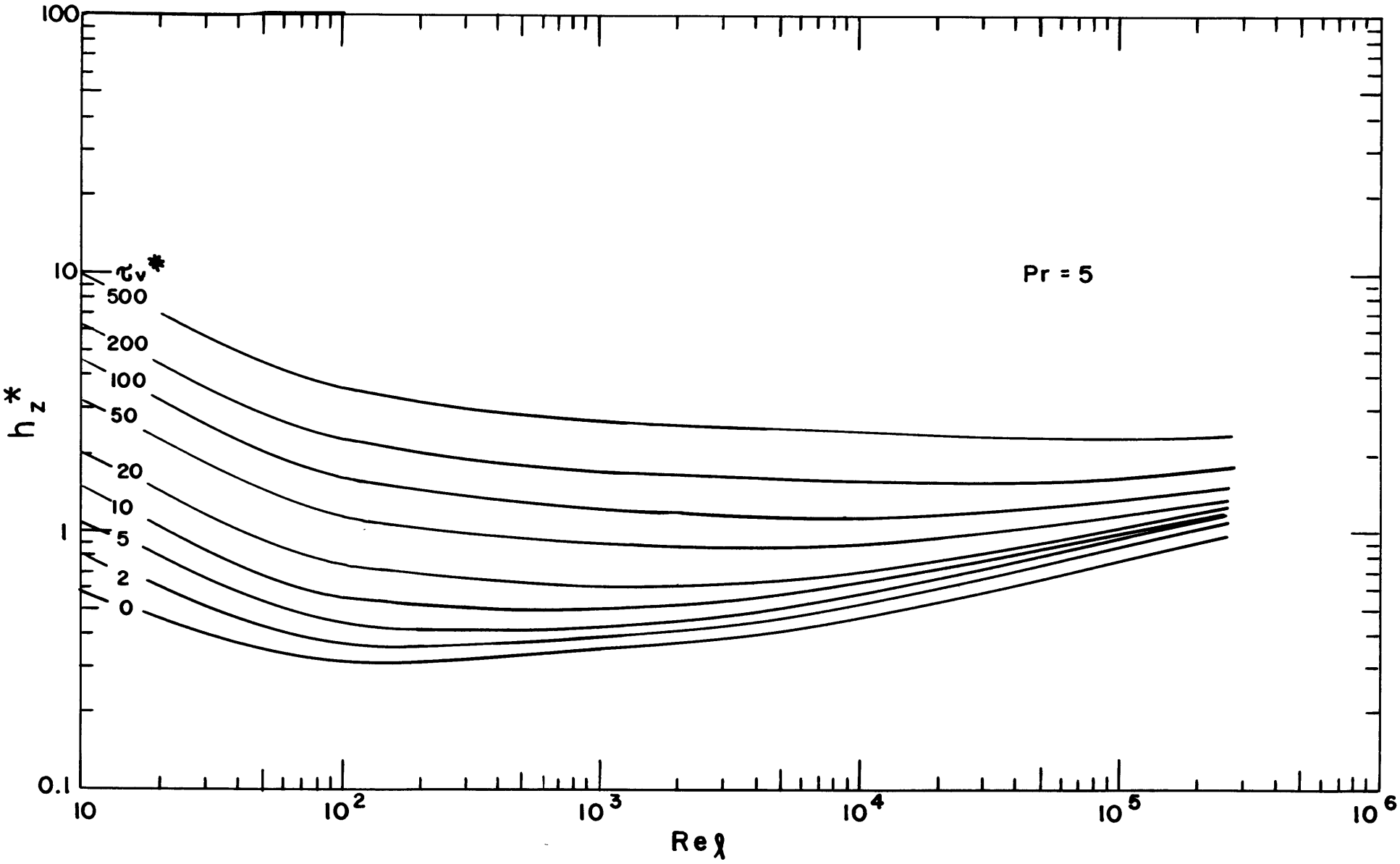

FIGURE 8 DIMENSIONLESS LOCAL HEAT TRANSFER COEFFICIENTS (Pr=5)

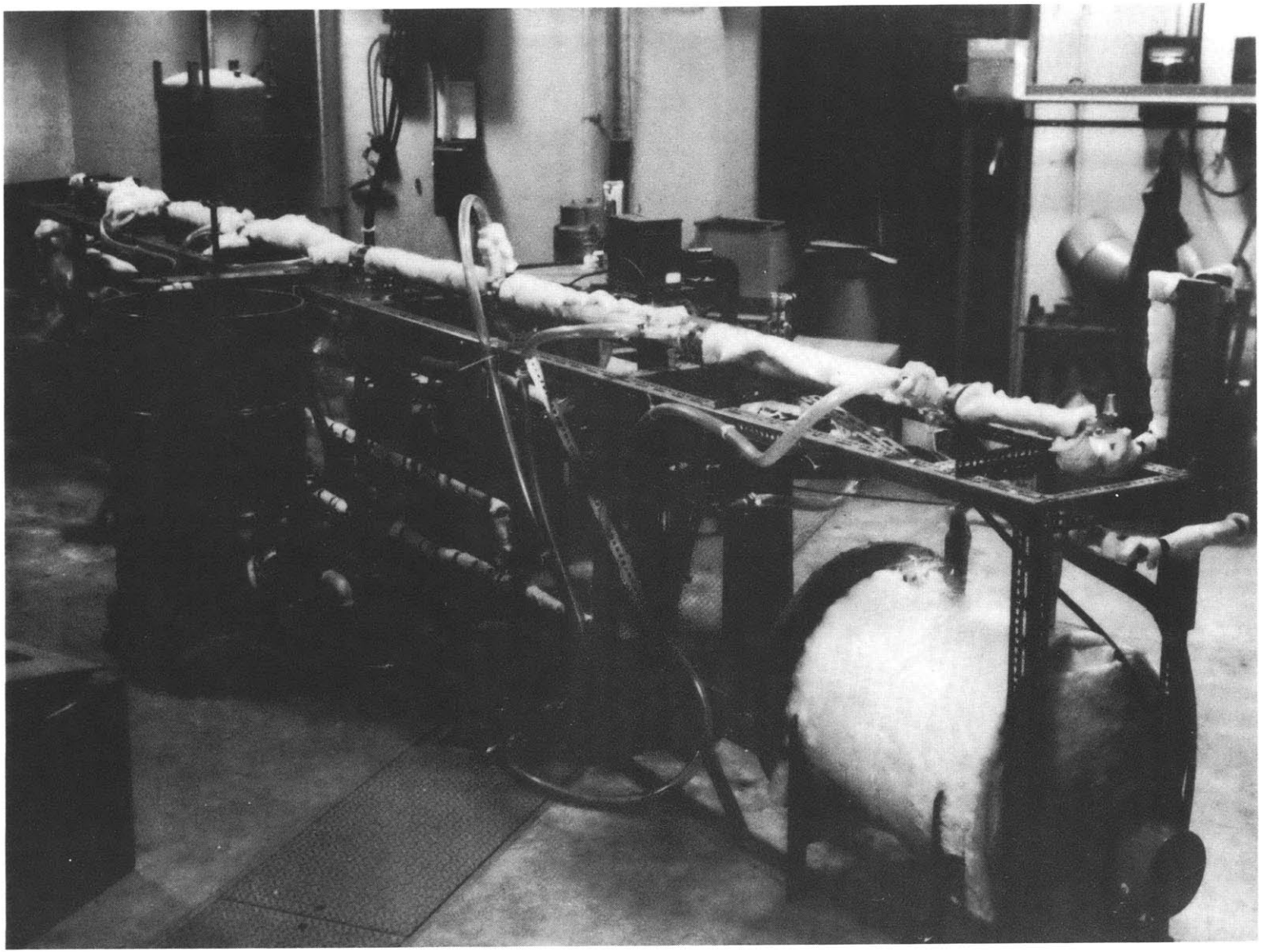

FIGURE 9 PHOTOGRAPH OF THE EXPERIMENTAL APPARATUS

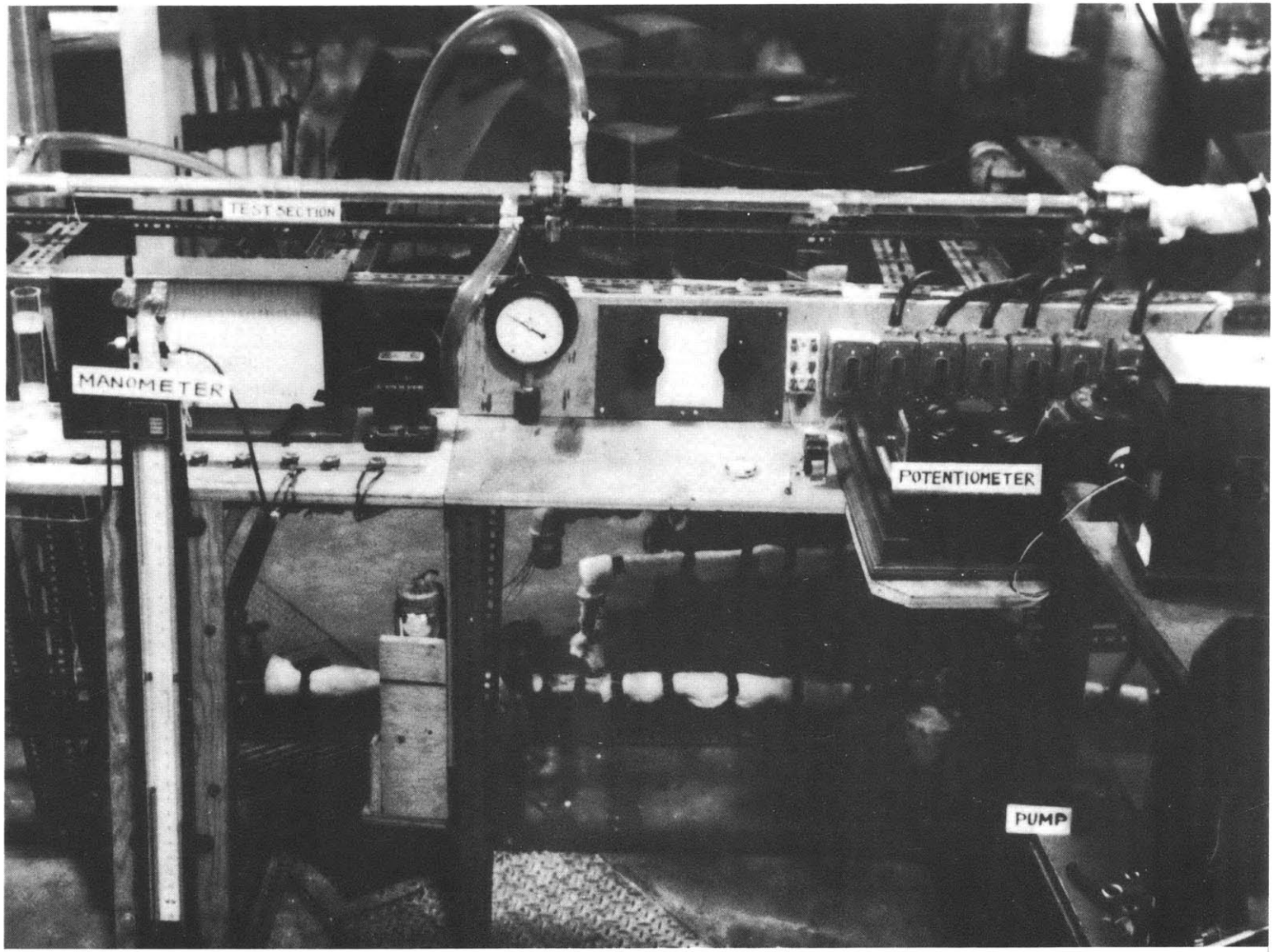

FIGURE 10 PHOTOGRAPH OF THE INSTRUMENTATION

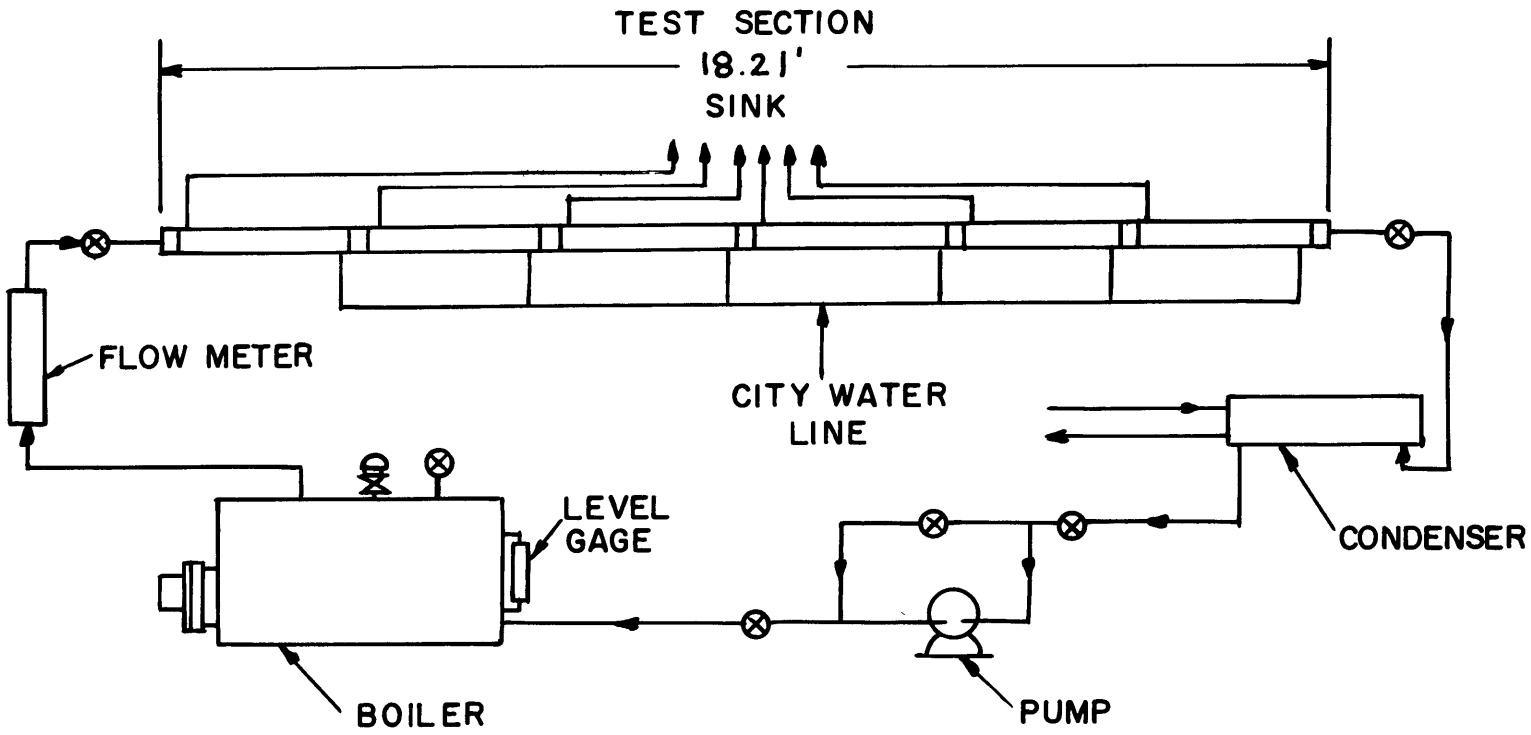

FIGURE 11 SCHEMATIC DIAGRAM OF APPARATUS

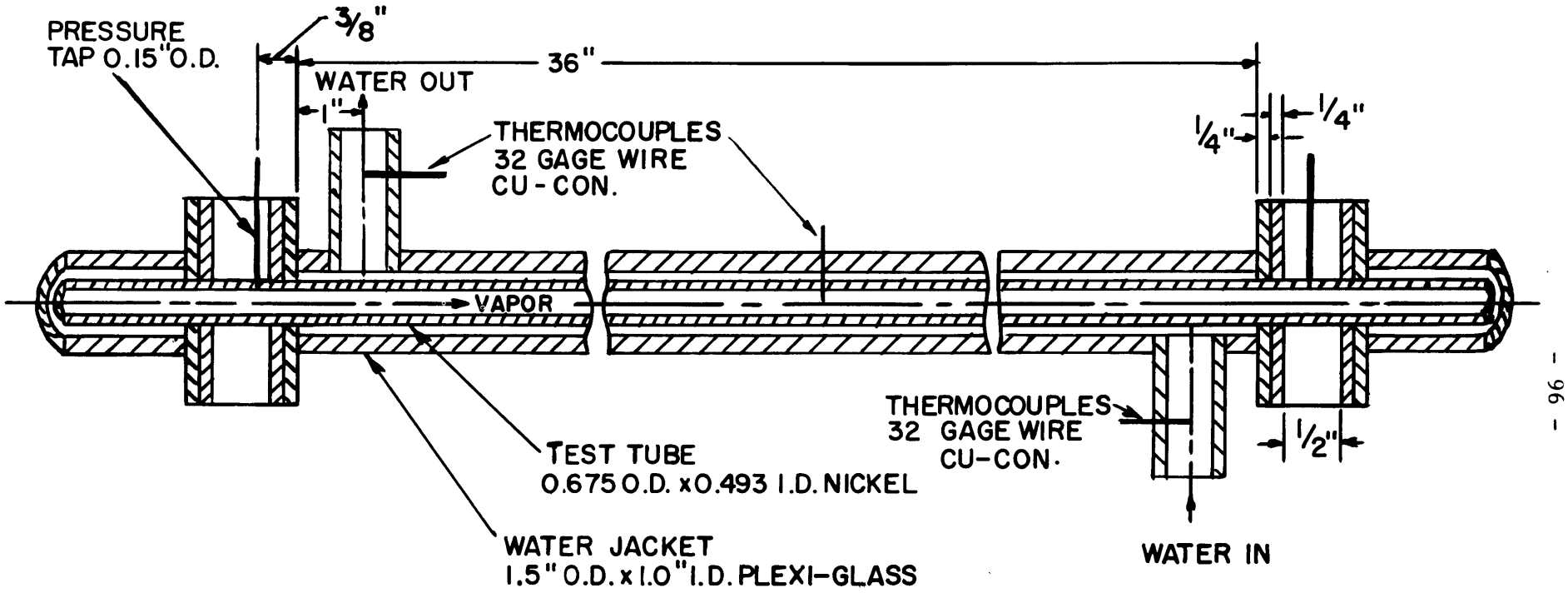

FIGURE 12 SCHEMATIC DRAWING OF ONE SECTION OF THE TEST SECTION

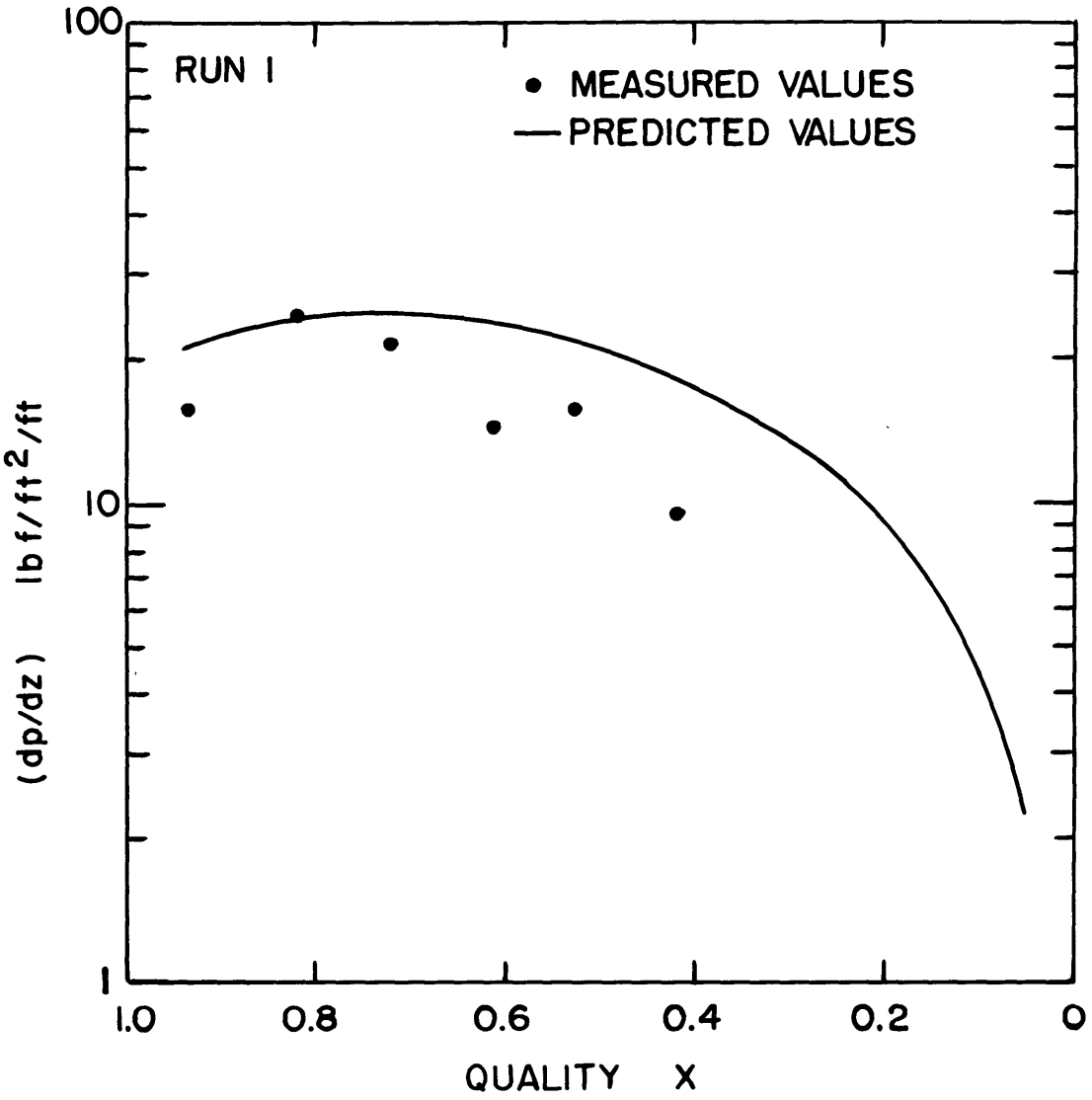

FIGURE 13-1 TOTAL STATIC PRESSURE GRADIENTS

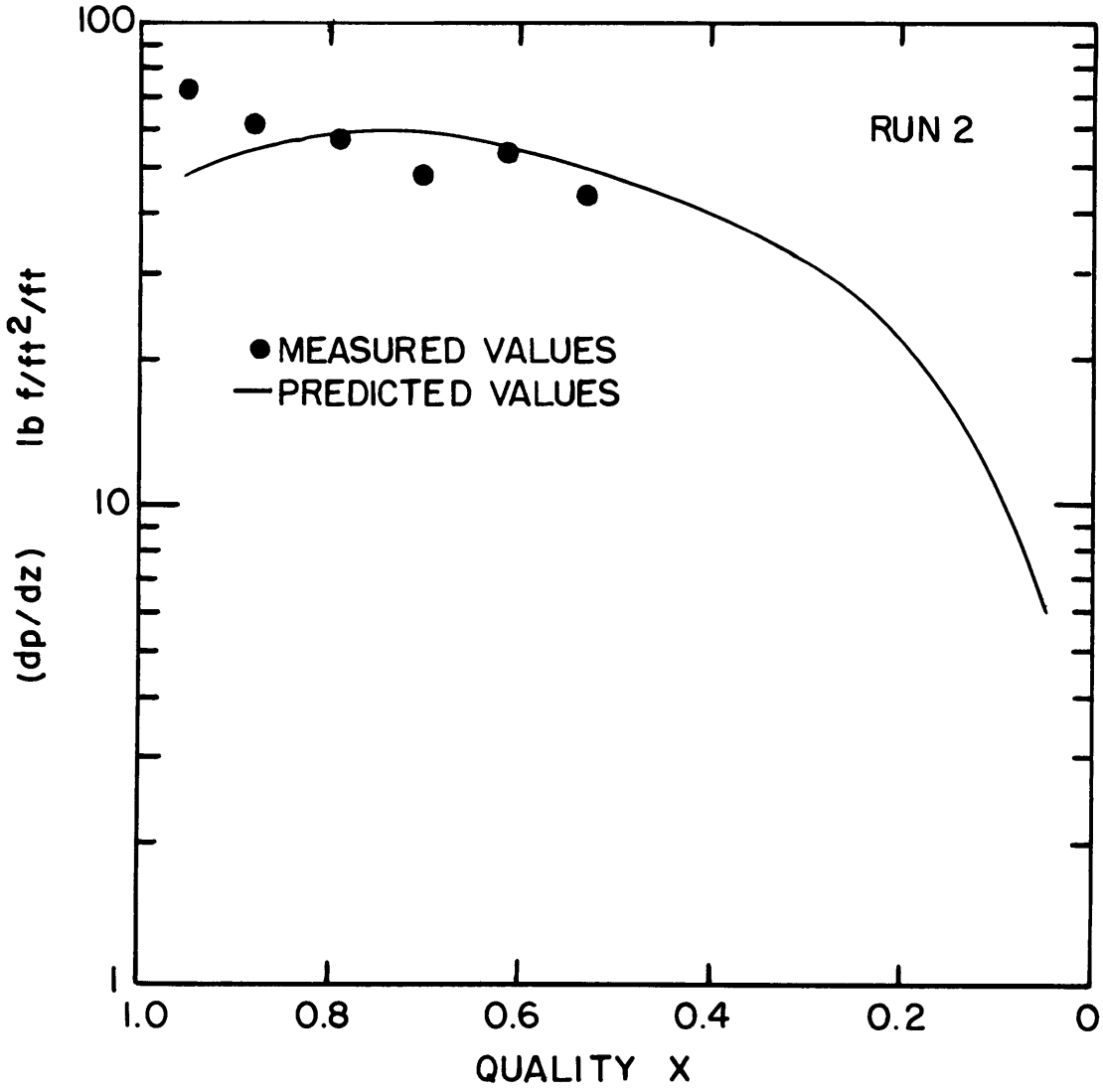

FIGURE 13-2 TOTAL STATIC PRESSURE GRADIENTS

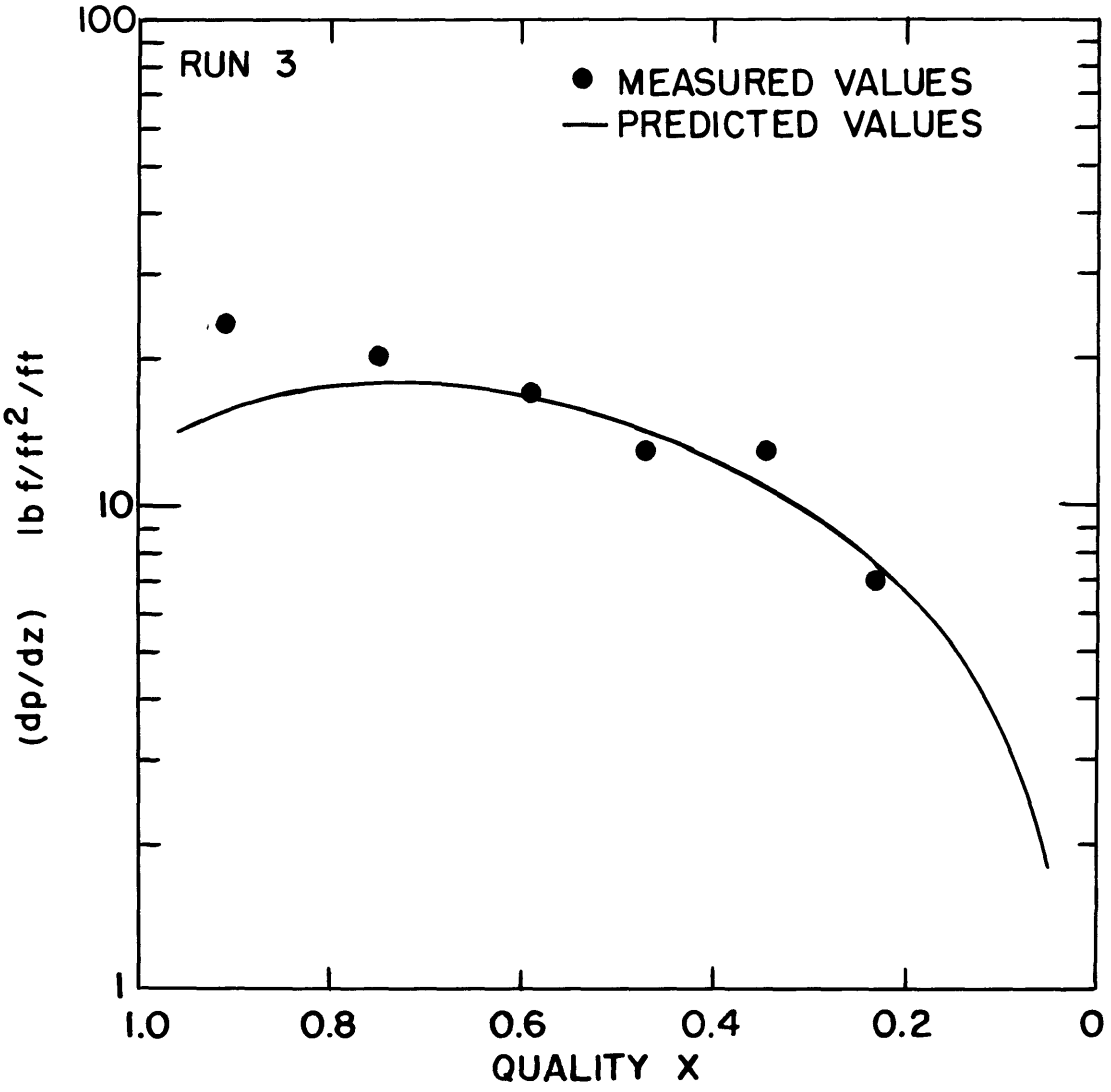

FIGURE 13-3 TOTAL STATIC PRESSURE GRADIENTS

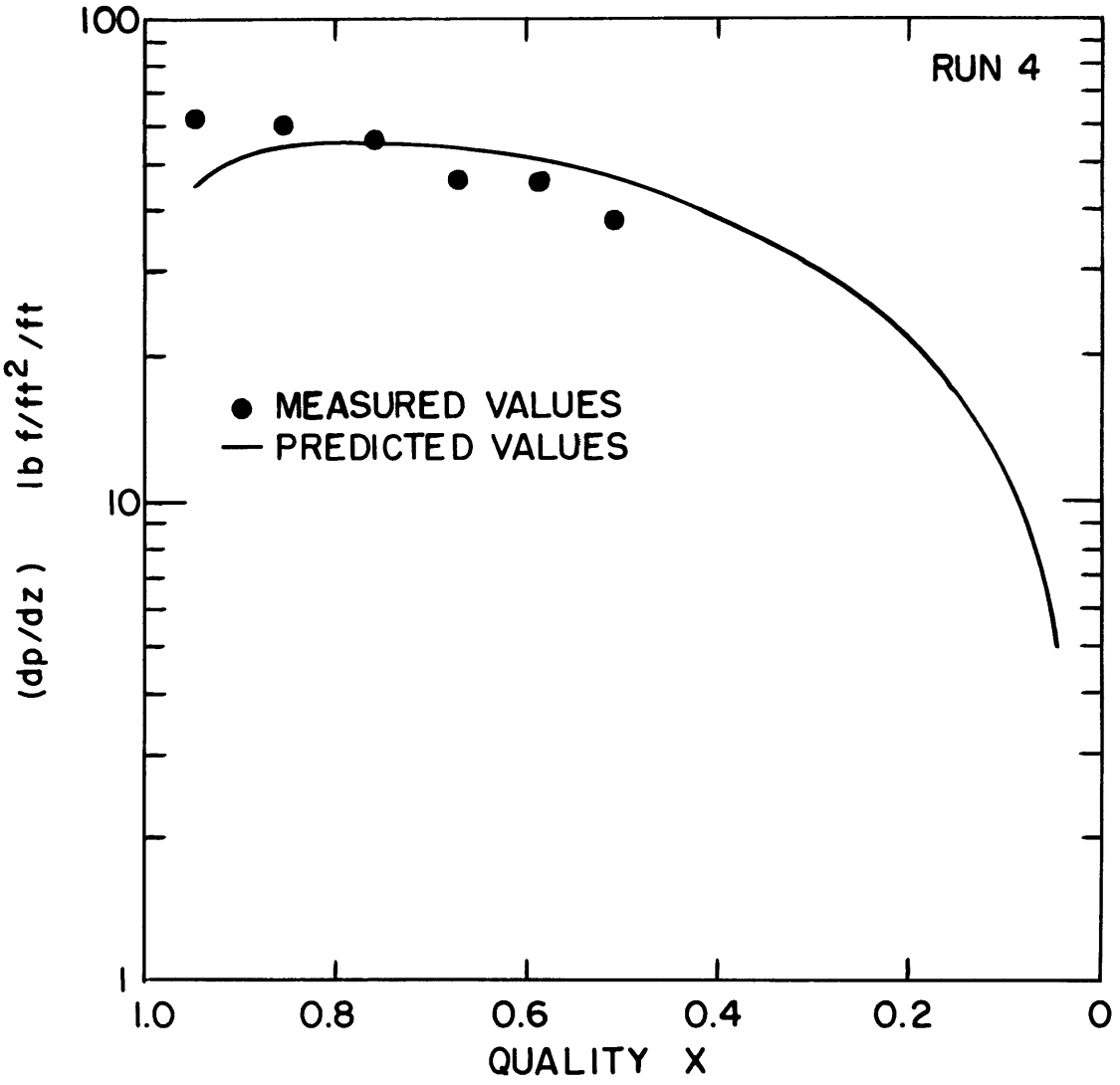

FIGURE 13-4 TOTAL STATIC PRESSURE GRADIENTS

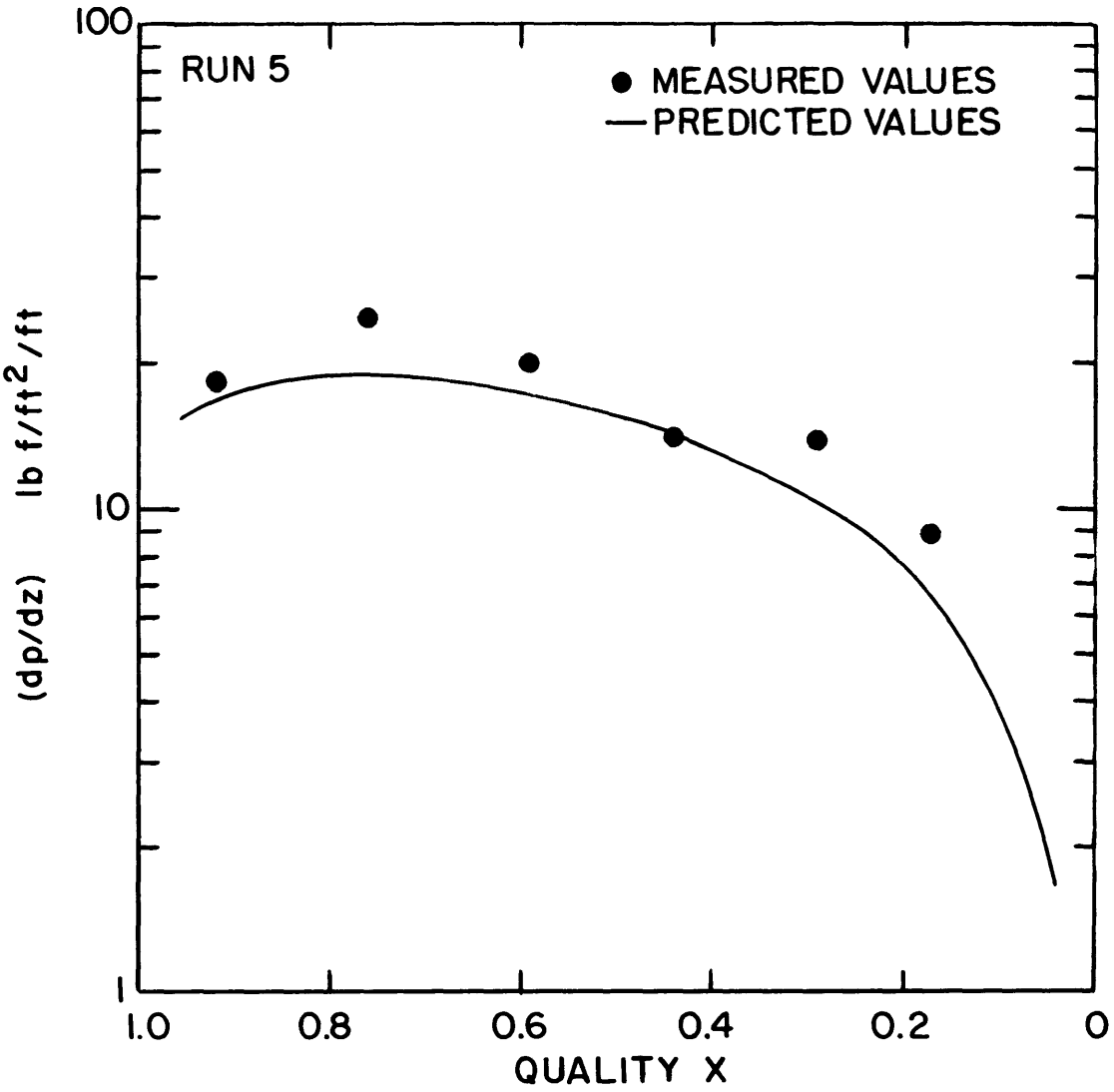

FIGURE 13-5 TOTAL STATIC PRESSURE GRADIENTS

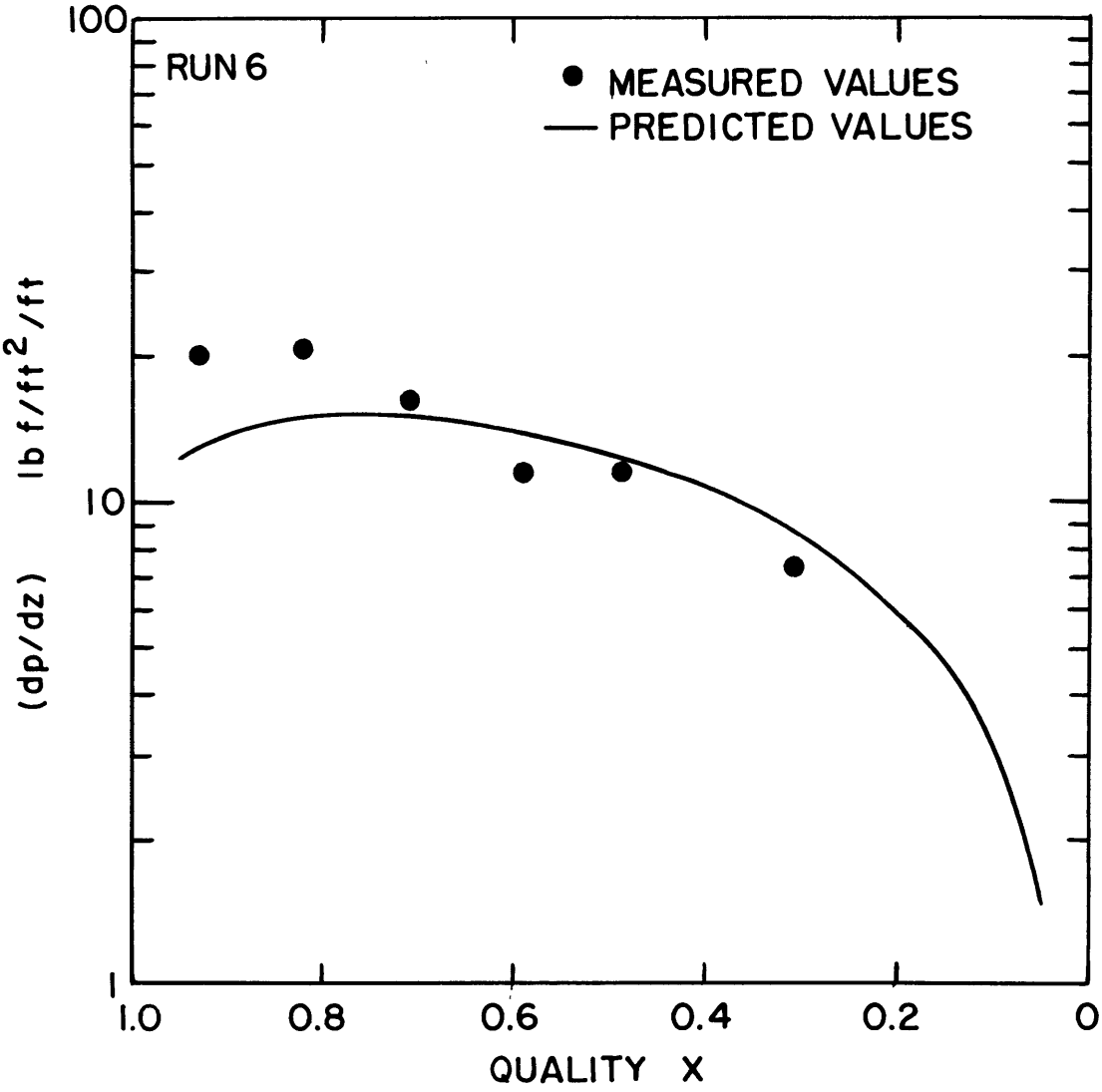

FIGURE 13-6 TOTAL STATIC PRESSURE GRADIENTS

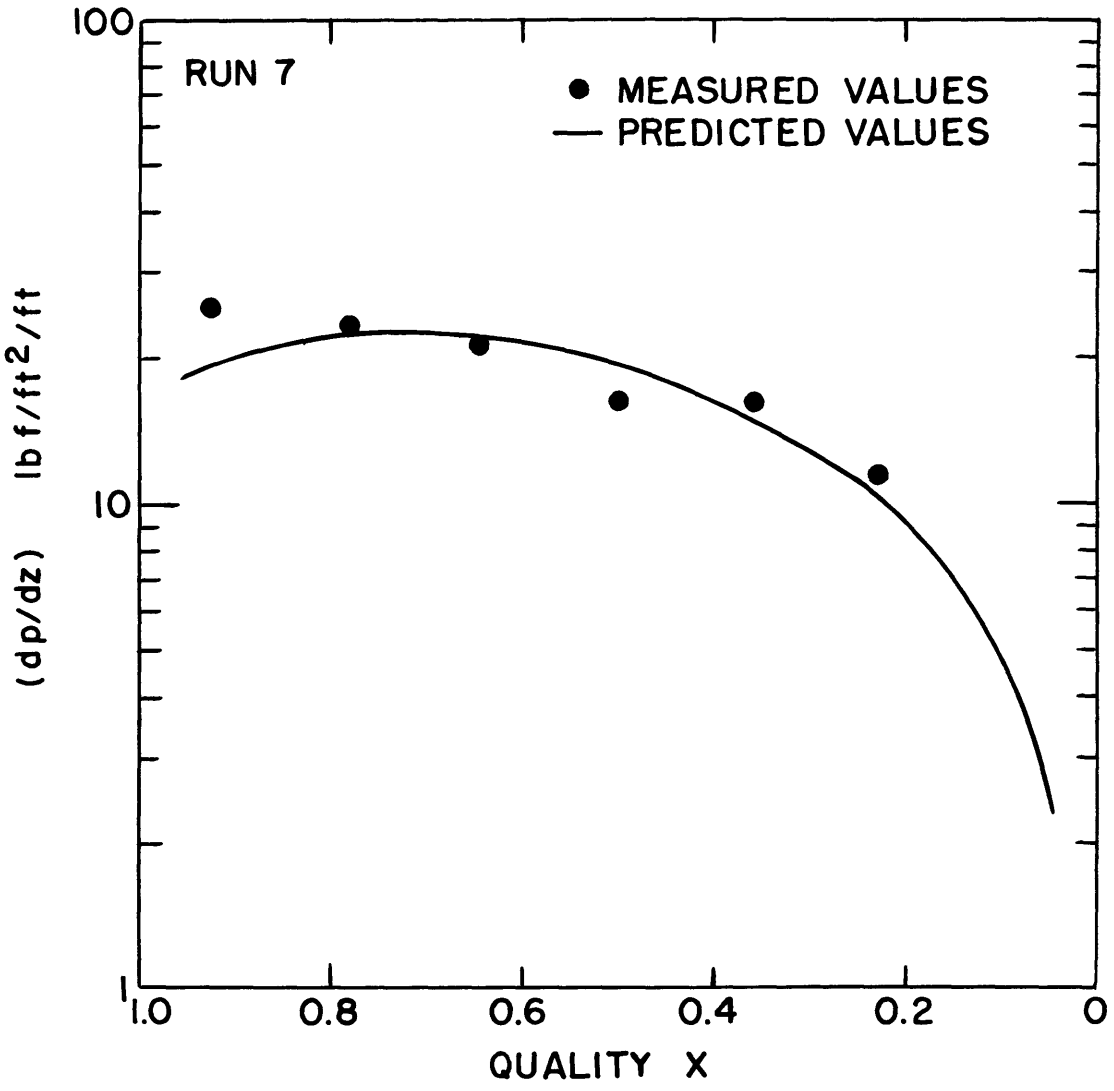

FIGURE 13-7 TOTAL STATIC PRESSURE GRADIENTS

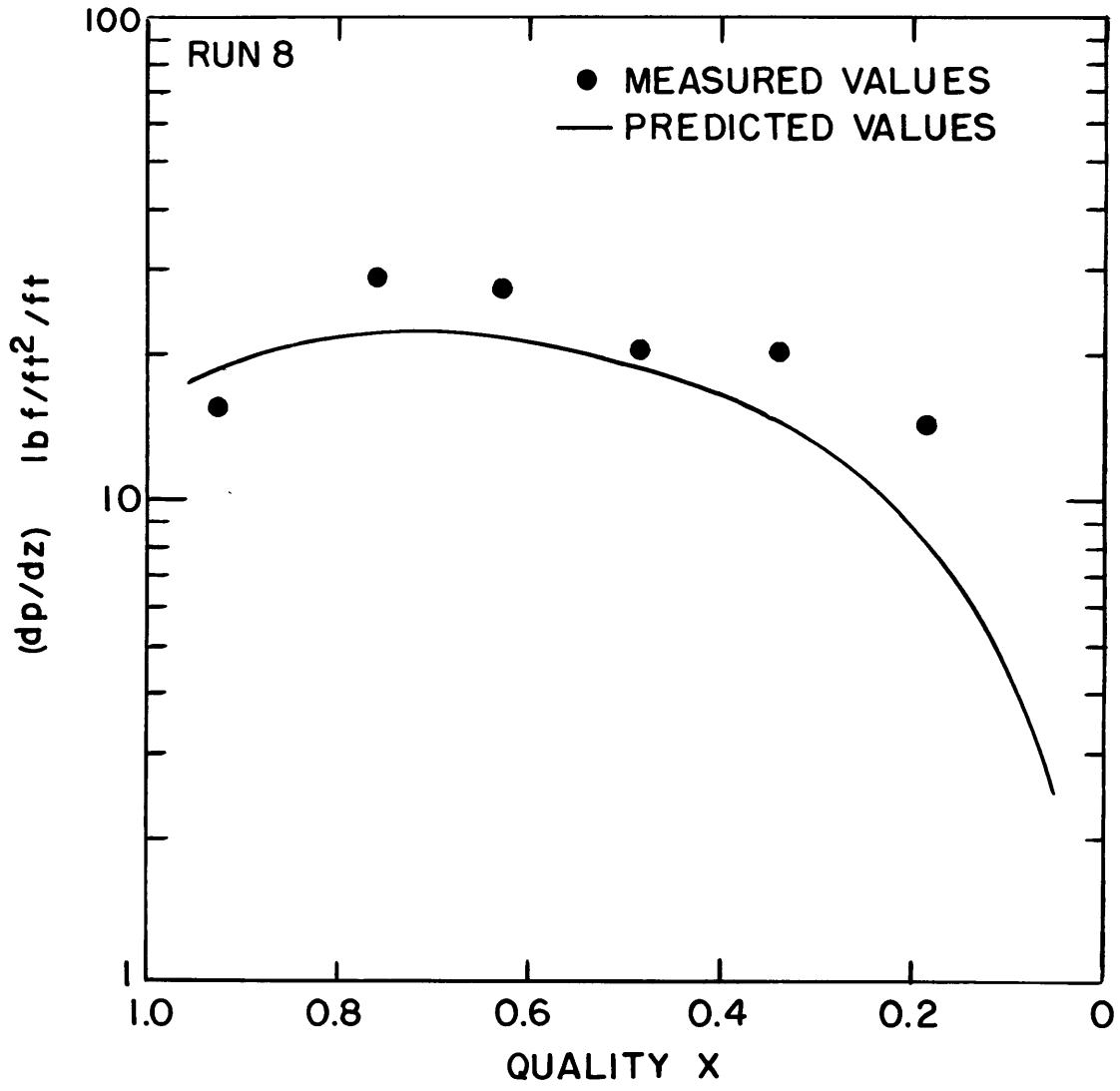

FIGURE 13-8 TOTAL STATIC PRESSURE GRADIENTS

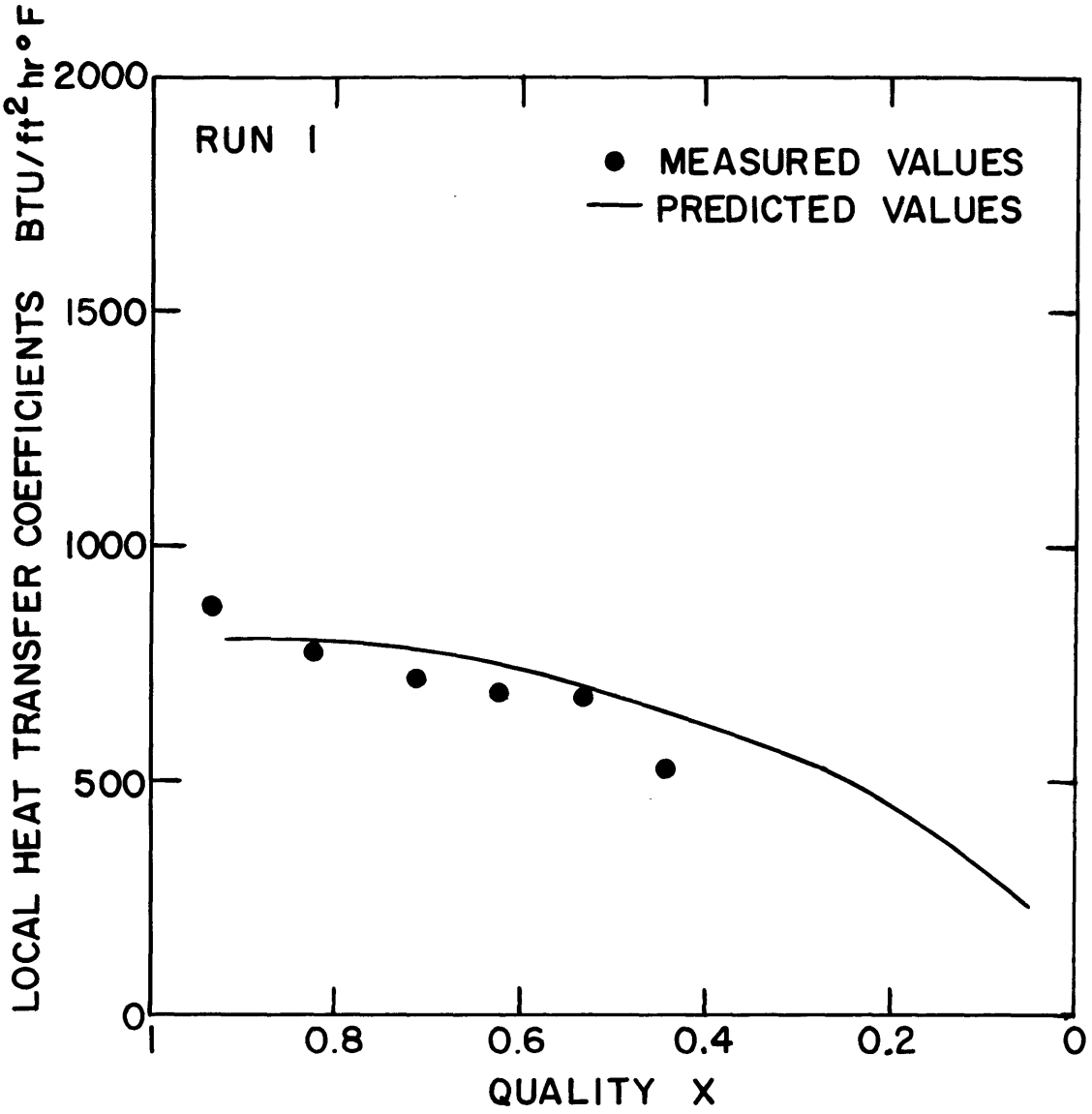

FIGURE 14-1 LOCAL HEAT TRANSFER COEFFICIENTS

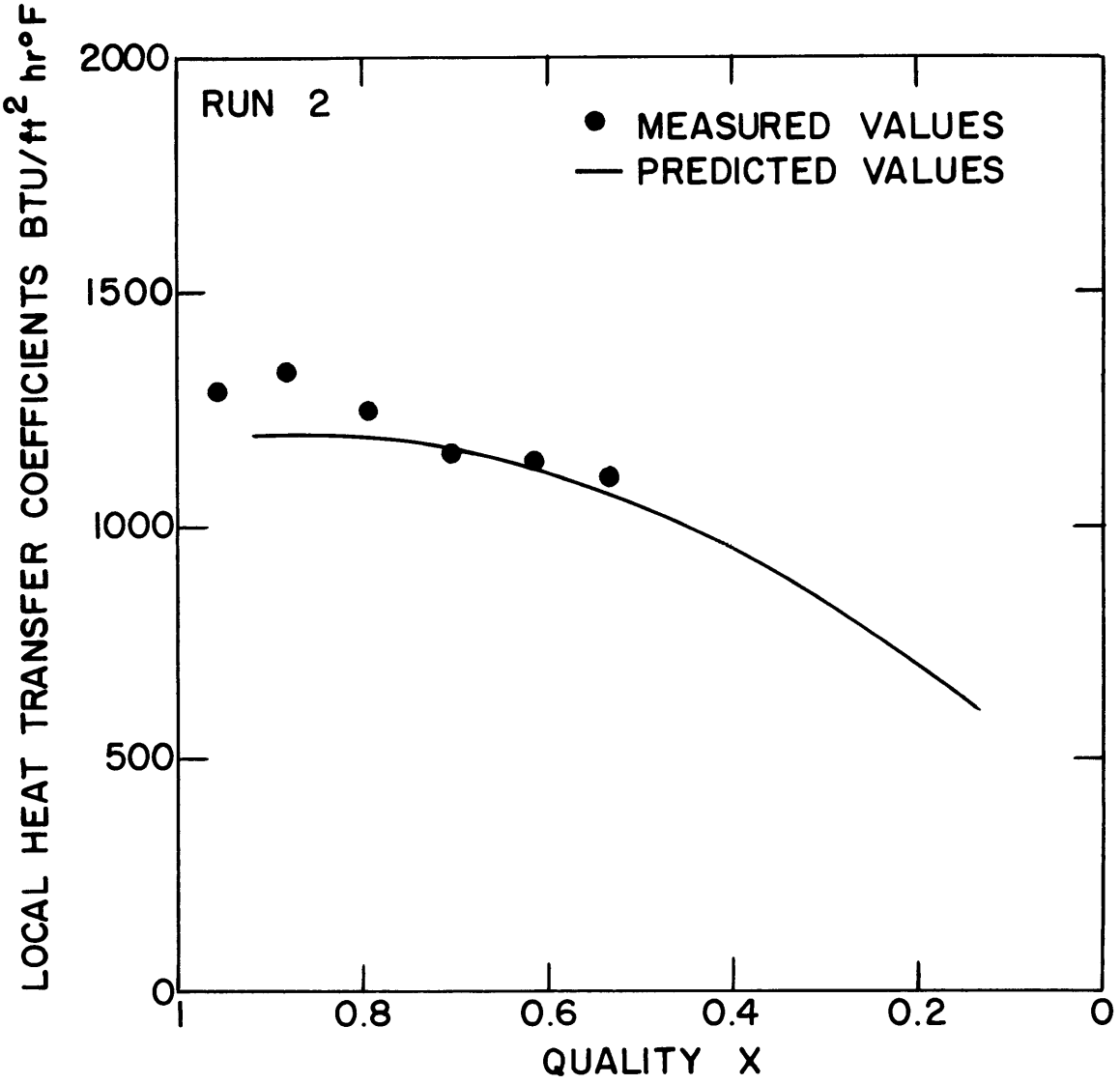

FIGURE 14-2 LOCAL HEAT TRANSFER COEFFICTENTS

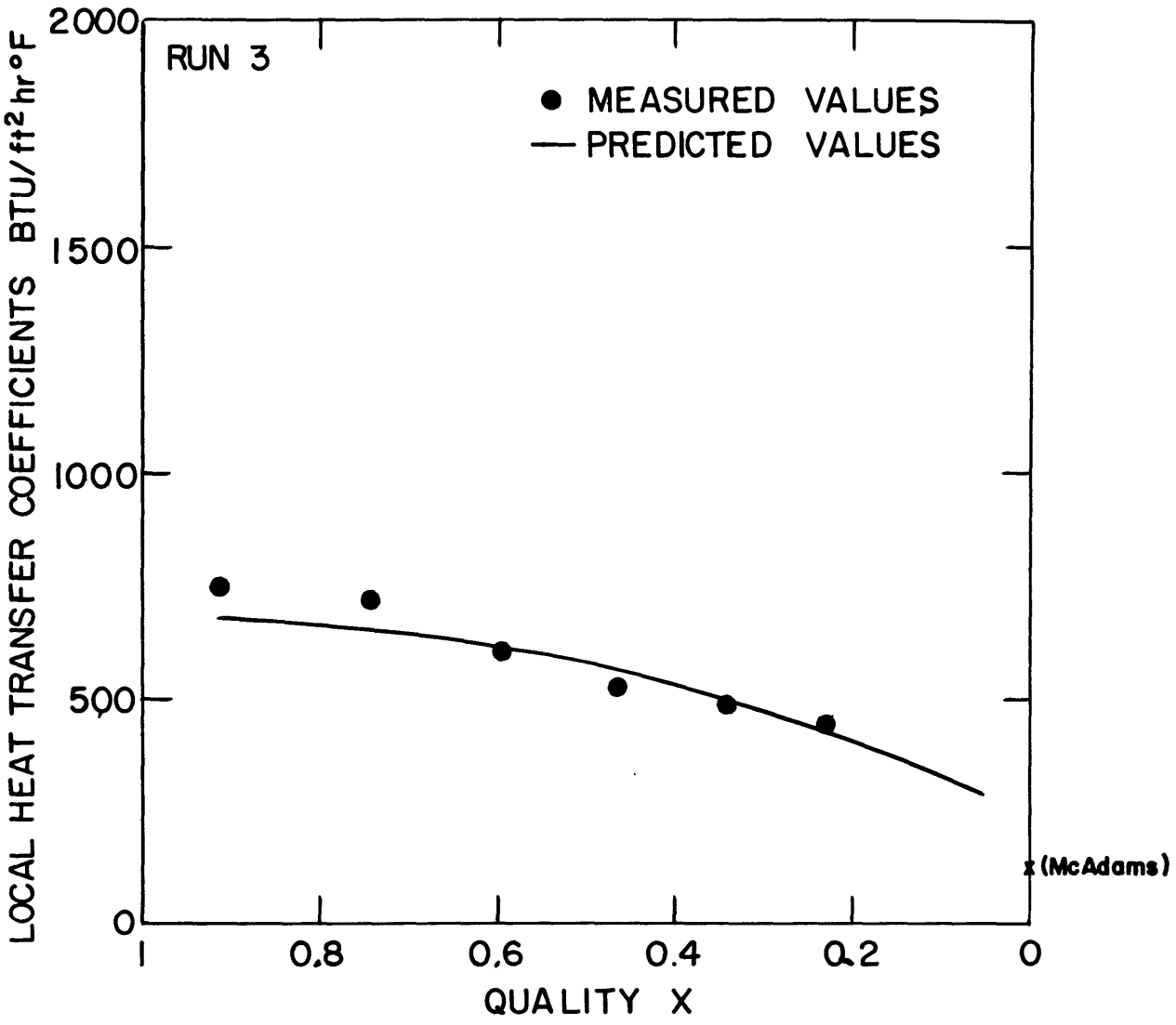

FIGURE 14-3 LOCAL HEAT TRANSFER COEFFICIENTS

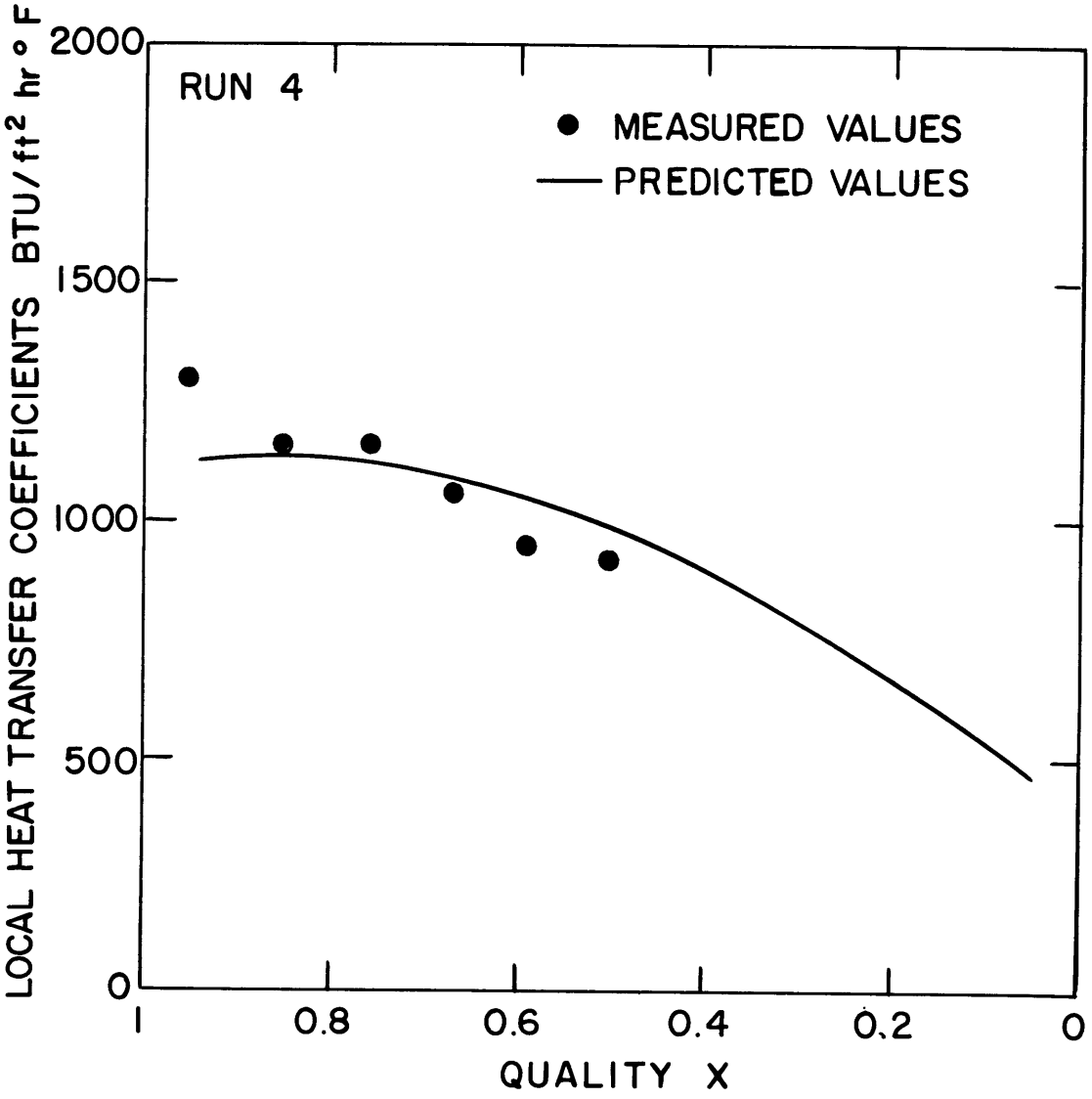

FIGURE 14-4 LOCAL HEAT TRANSFER COEFFICIENTS

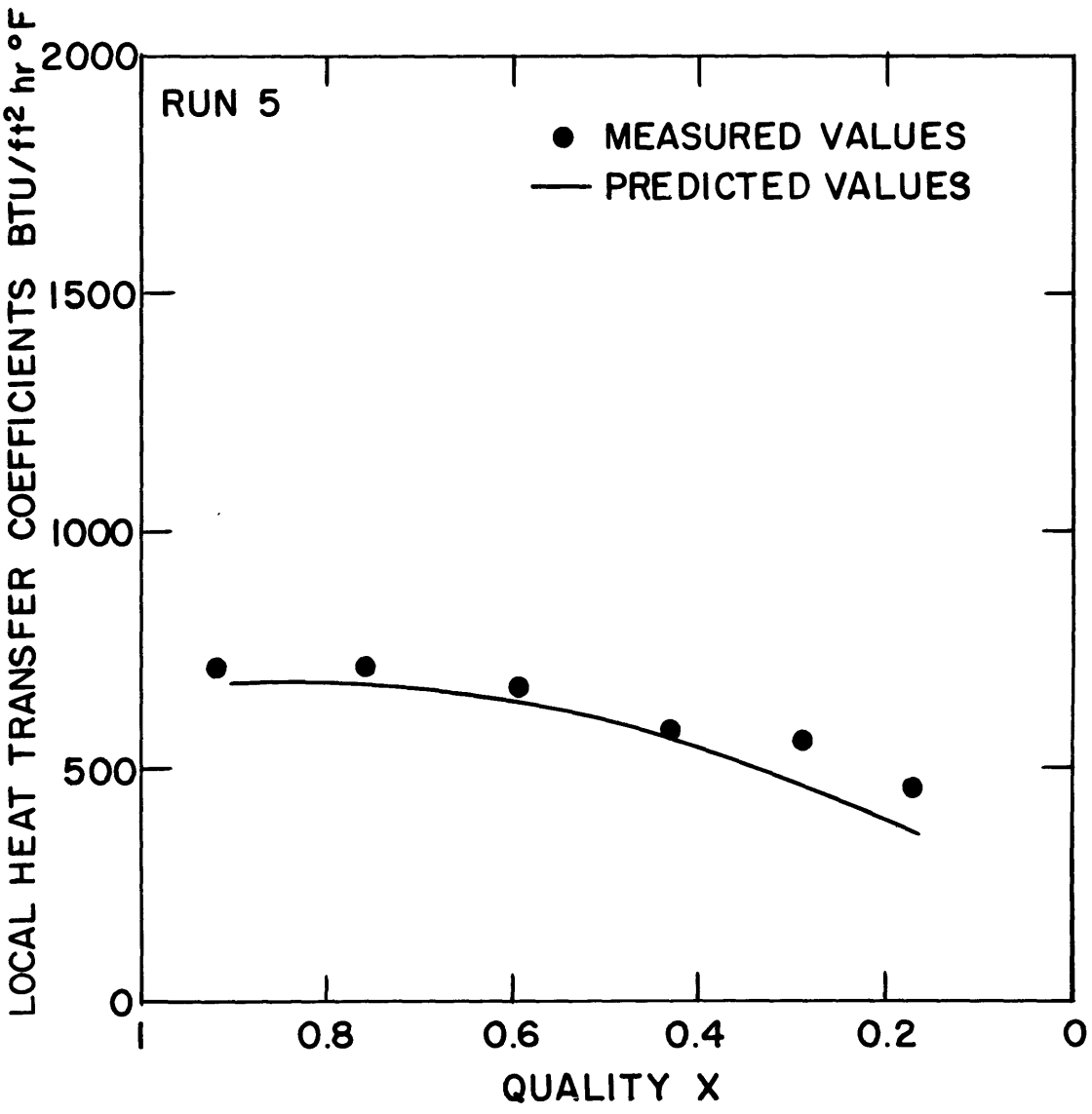

FIGURE 14-5 LOCAL HEAT TRANSFER COEFFICIENTS

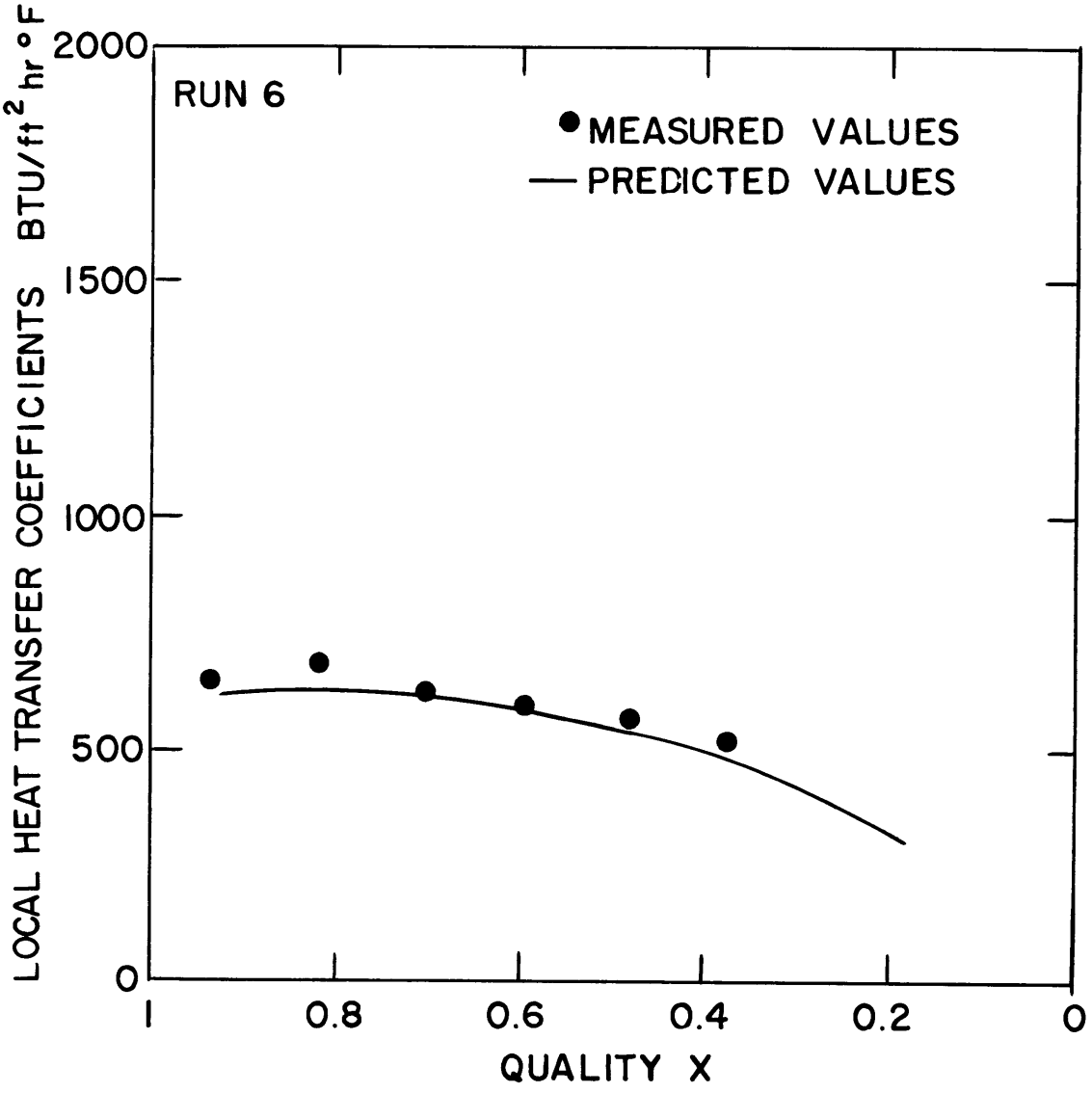

FIGURE 14-6 LOCAL HEAT TRANSFER COEFFICIENTS

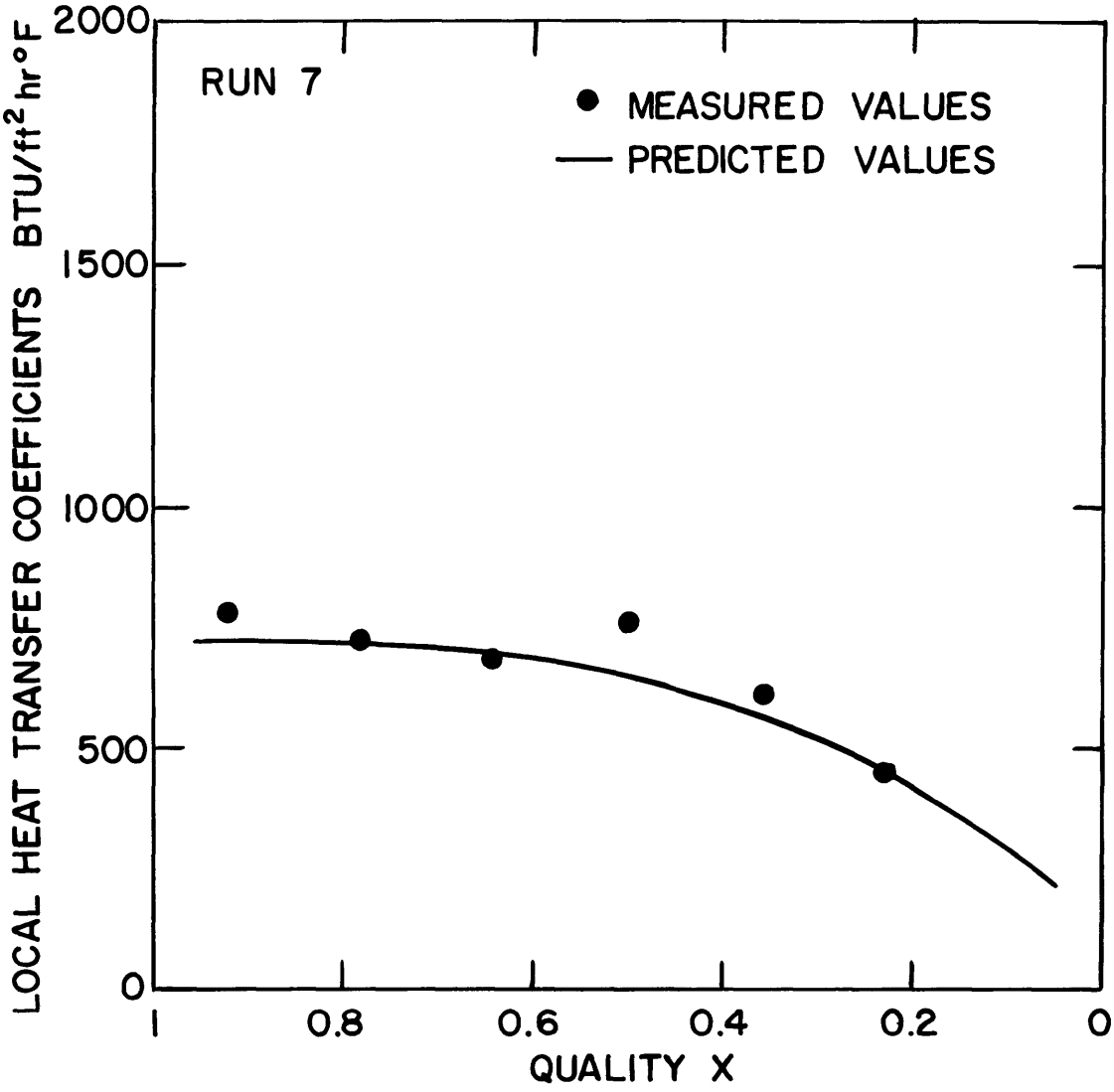

FIGURE 14-7 LOCAL HEAT TRANSFER COEFFICIENTS

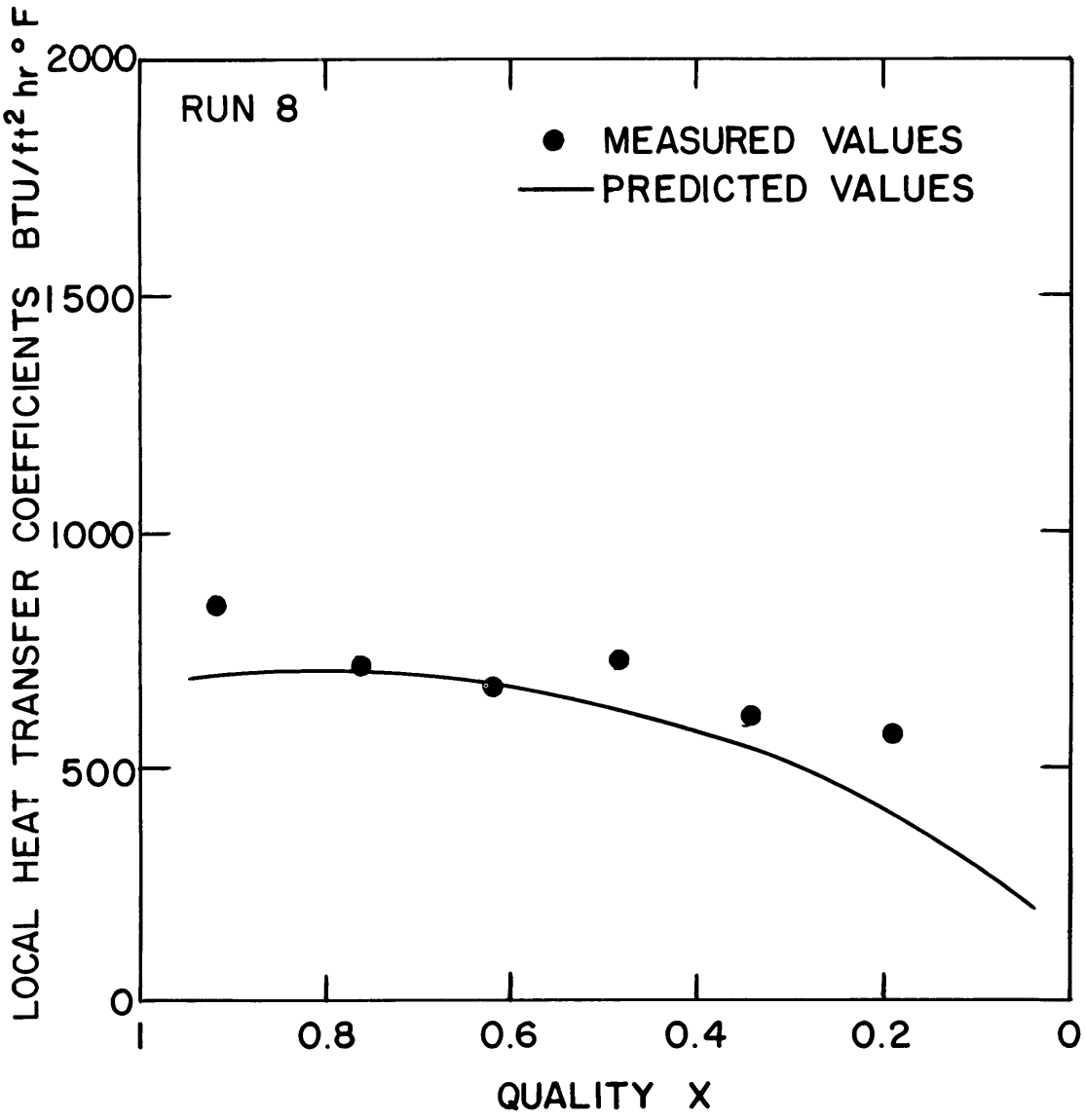

FIGURE 14-8 LOCAL HEAT TRANSFER COEFFICIENTS

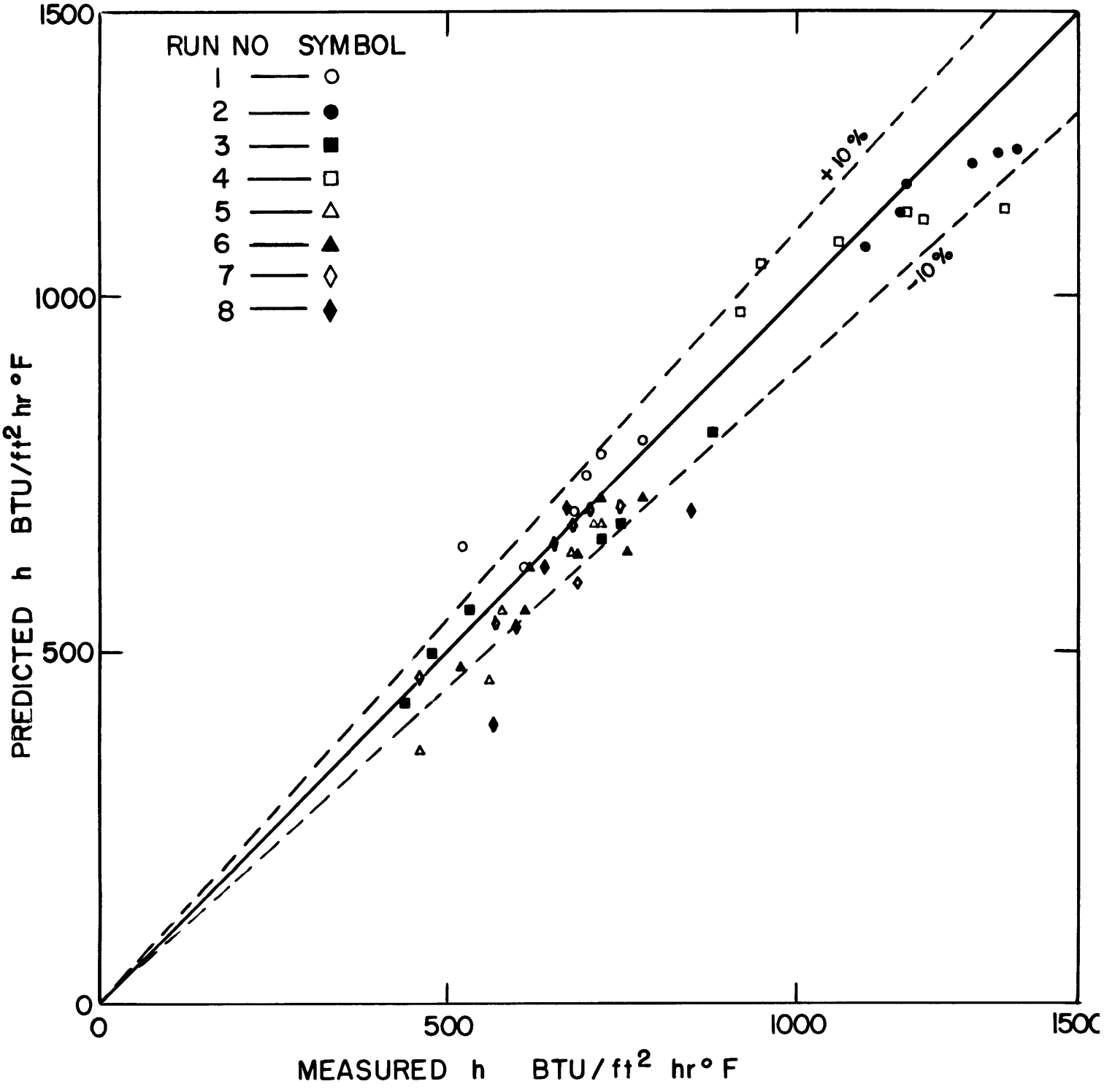

FIGURE 15 DATA COMPARED WITH PRESENT ANALYSIS

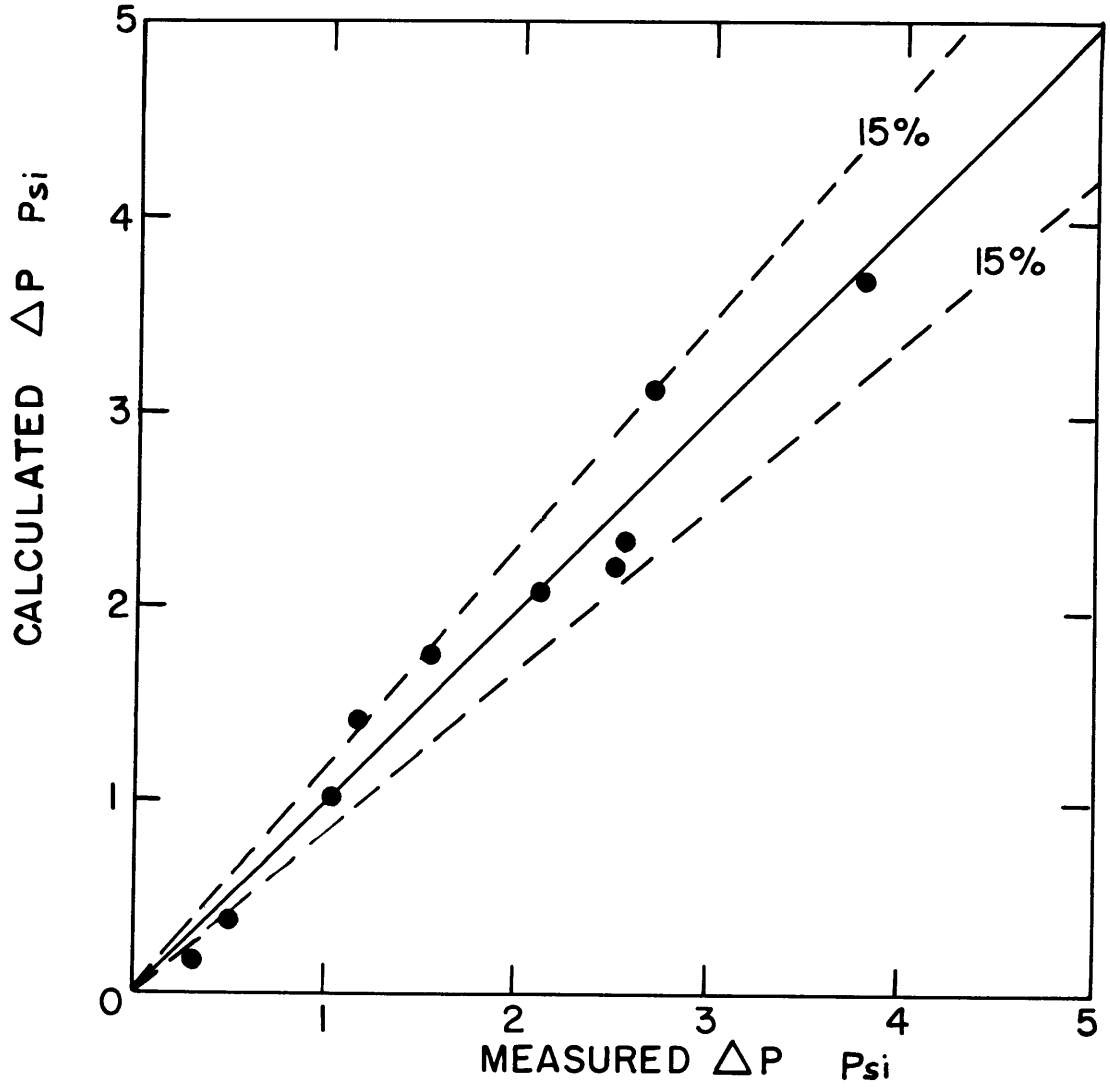

FIGURE 16 COMPAIRSON WITH ALTMAN et al DATA [3] PRESSURE DROP

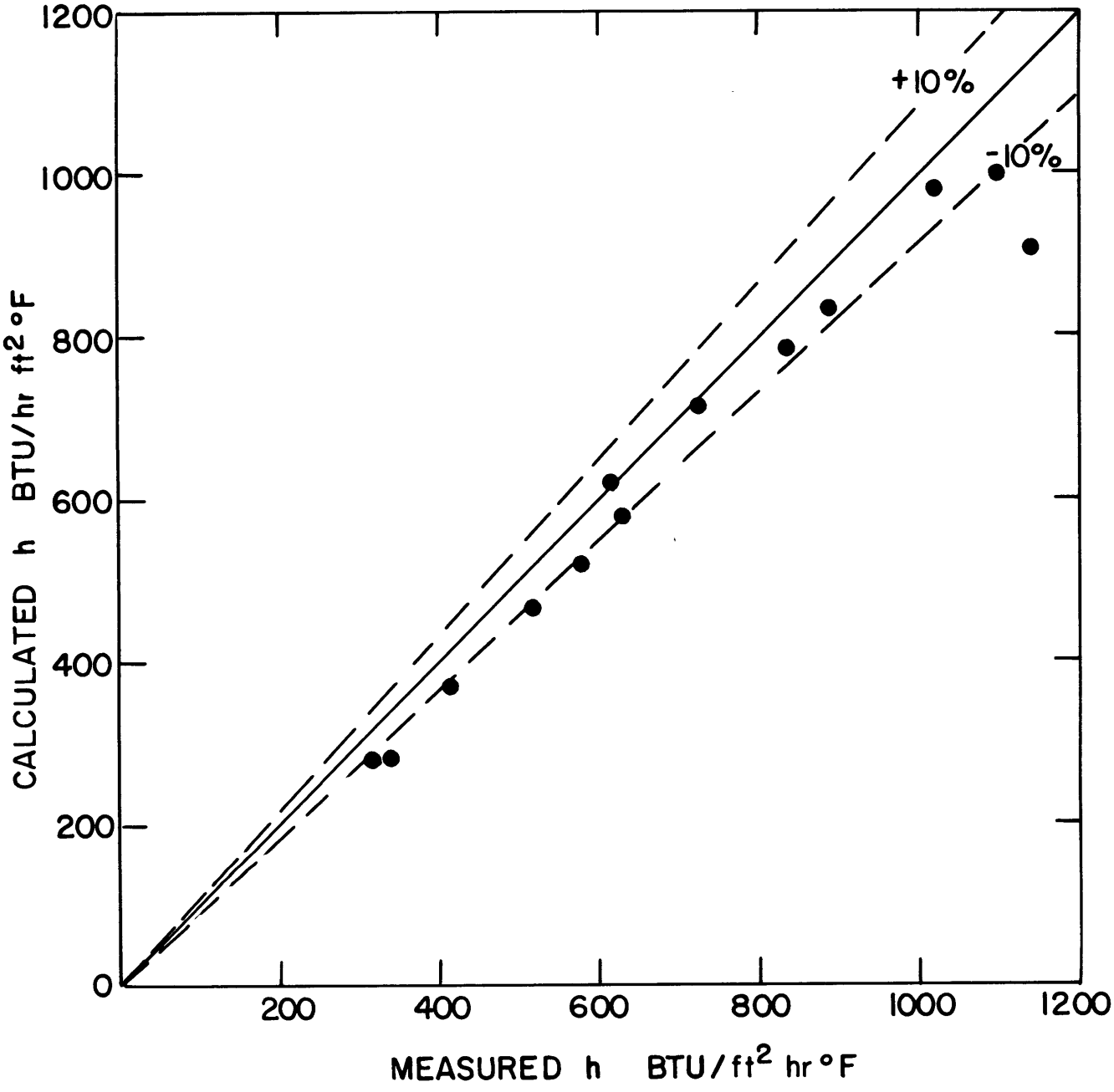

FIGURE 17 COMPARISON WITH ALTMAN et. al. DATA [3] HEAT TRANSFER COEFFICIENTS

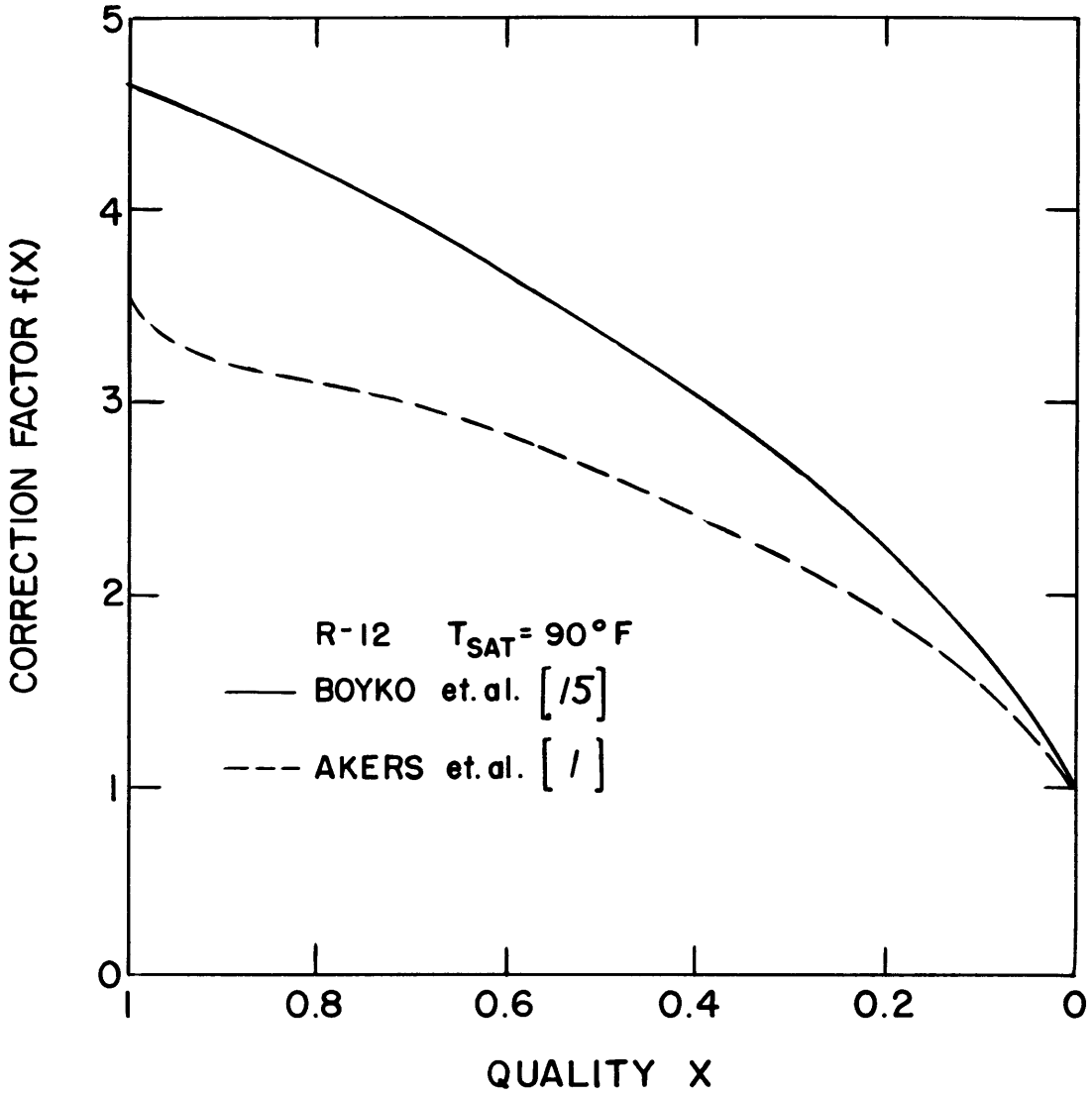

FIGURE C-1 CORRECTION FACTORS

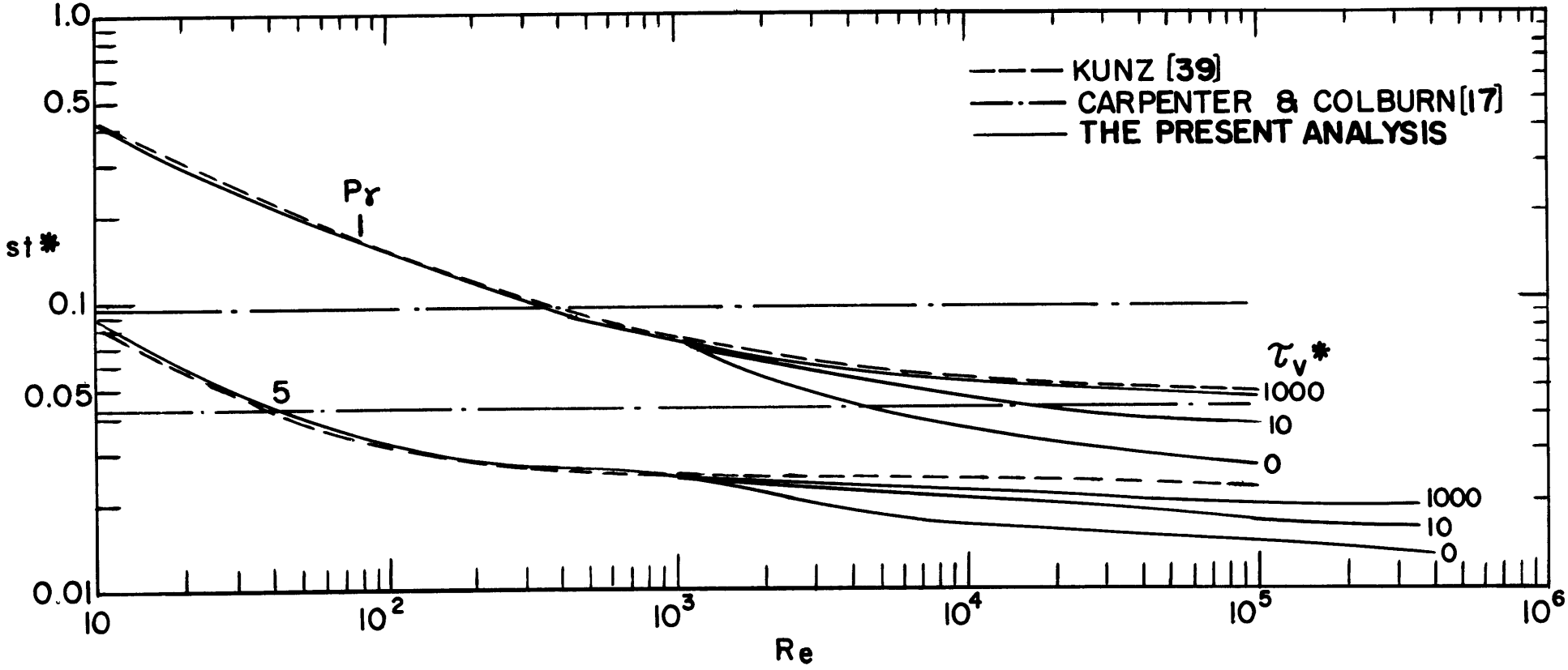

FIGURE C-2 COMPARISON OF CORRELATIONS

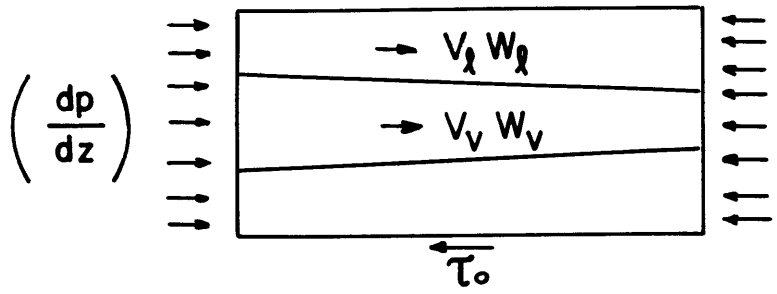

FIG. D-1 CONTROL VOLUME OF A TUBE ELEMENT

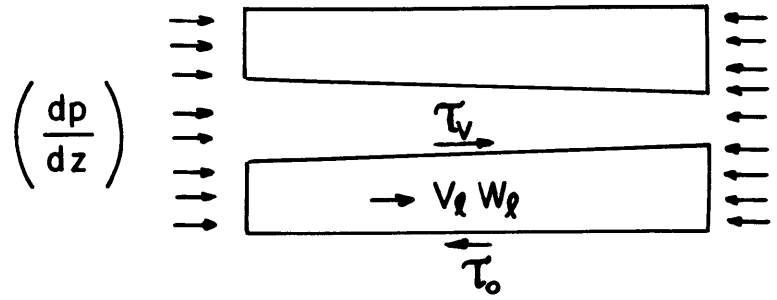

FIG. D-2 CONTROL VOLUME OF LIQUID FILM

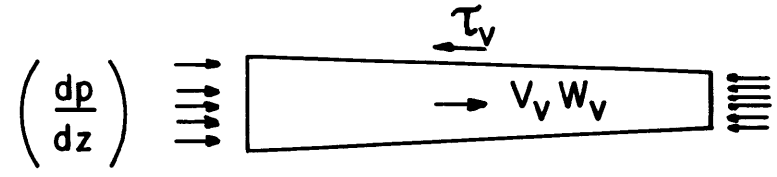

FIG. D-3 CONTROL VOLUME OF VAPOR CORE

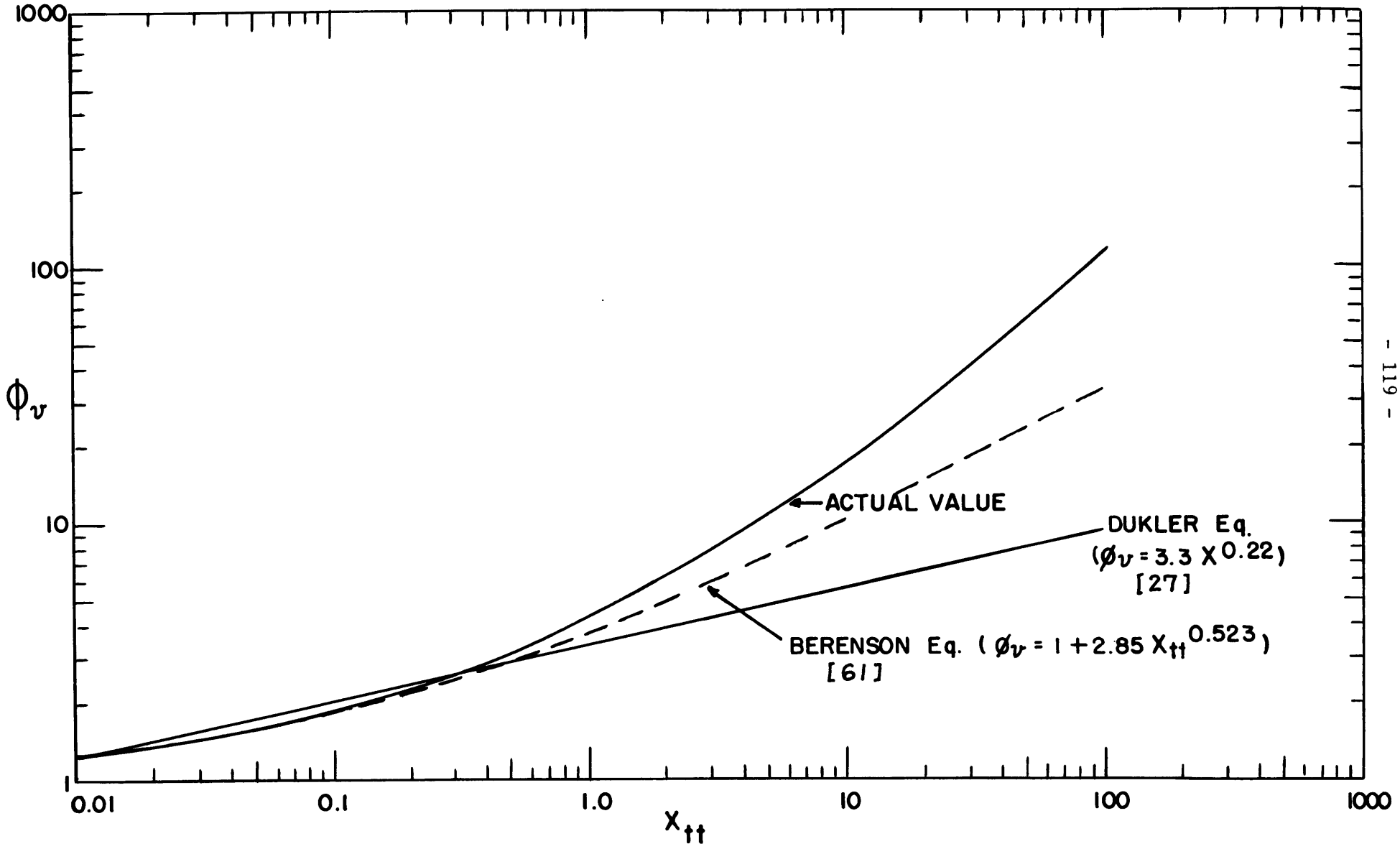

FIGURE D-4 LOCKHART — MARTINELLI PARAMETERS

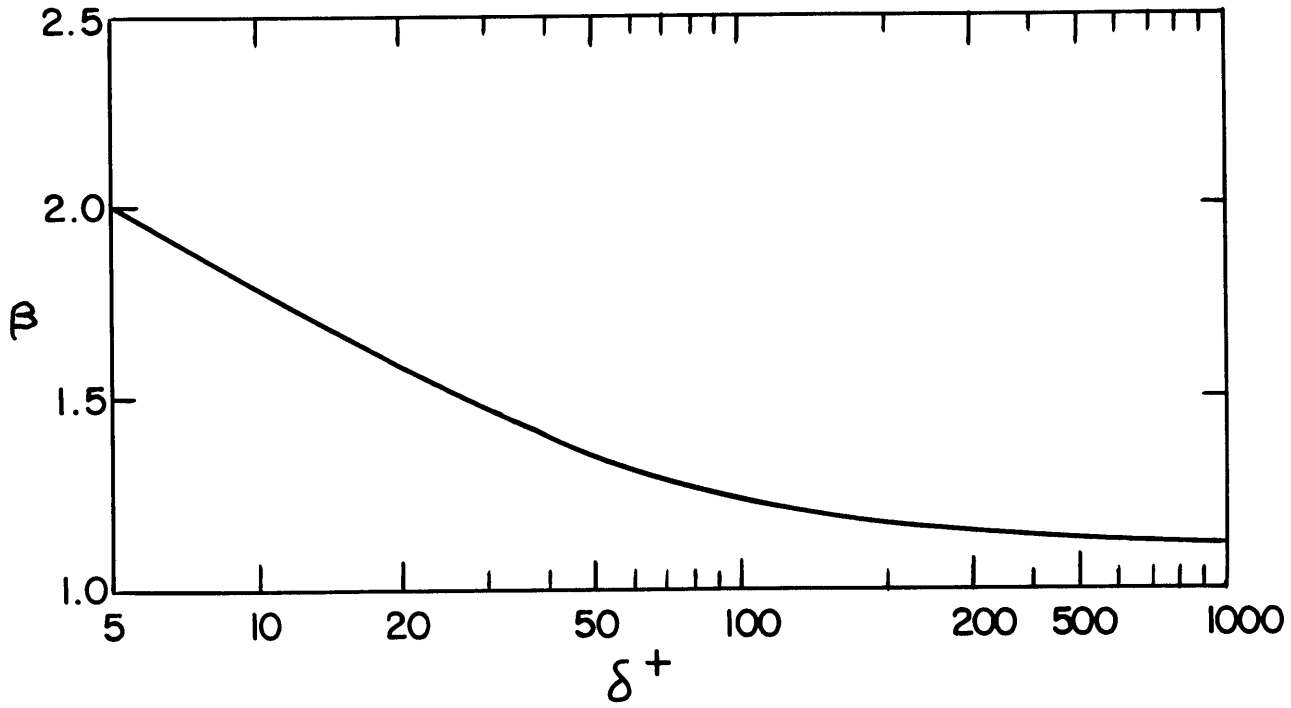

FIGURE D-5 δ^+ vs. β

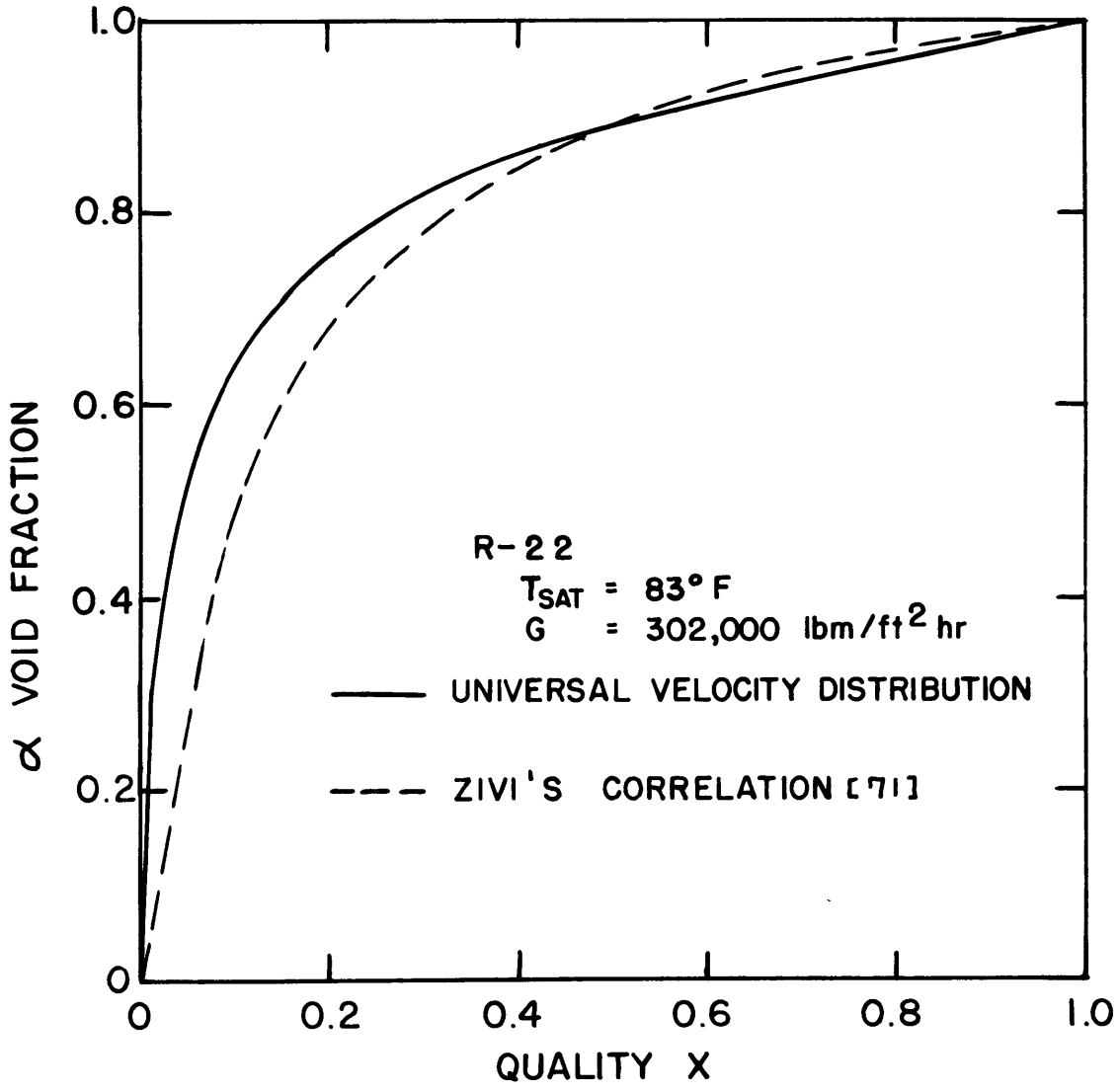

FIGURE F-1 VOID FRACTION vs. QUALITY